

September 26, 2019

RE: Submission acp-2019-429

Dear Handing Editor,

Please find below our response to the Reviewer Comments on our manuscript, "Importance of Dry Deposition Parameterization Choice in Global Simulations of Surface Ozone". We are grateful for the reviewer comments, and feel that the changes made in response to these comments have strengthened the quality of our manuscript.

We follow the response to the reviewer comments with a Tracked Changes version of our manuscript.

We would like to note that, in response to comments from Reviewer 1, we have uploaded a new Supplement to accompany our manuscript. Given that we have added a Supplement, we moved Tables A1, A2, and A3 (which were included as Appendices in our original submission) into this new Supplement. The new supplement is also attached here following the Tracked Changes manuscript.

As always, we are very grateful for your time and effort as handling editor for our manuscript, and we look forward to your decision.

All the best,

Jeffrey Geddes (Corresponding Author)  
Assistant Professor  
Department of Earth & Environment  
Boston University  
[jgeddes@bu.edu](mailto:jgeddes@bu.edu)

We thank the referee for their positive and constructive comments on our manuscript. We provide our response to each individual reviewer comment (shown in italics) below, including detailed changes to the manuscript (additions in red).

### Major issues:

- 1) The linearity of response of surface ozone concentration to ozone deposition velocity is uncertain, but a major assumption in this study. I'm not convinced that the results from Wong et al. 2018 are sufficient to warrant confidence in this assumption. one reason being that they were testing the response to surface ozone to LAI, which involves changes in several processes.*

### Response:

We agree with the reviewer that our assumption of linearity is important. Our objective with this experiment was to use this first order approach to identify “hotspots” globally where uncertainty/variability in dry deposition velocity could have large impacts on simulated ozone, and then use the assumption of linearity to approximate those impacts. Our approach helps identify regions where more rigorous observations and modeling could be targeted for future work. Still, we address this assumption further. The reviewer notes in particular that the response involves changes in several processes (e.g. non-linearity in chemistry, transport and changes in background ozone).

In response to the reviewer’s comment, we have made two changes:

- (1) We have changed the manuscript to be more clear about our intentions with using the assumption linearity between perturbations in dry deposition velocity and ozone concentrations, and include a stronger caveat in this interpretation:

~~Nevertheless, we use this sensitivity to estimate the potential impact of  $v_d$  simulation on surface  $O_3$  concentration to a first order in subsequent sections. This approach is based on the reasonably linear response of surface  $O_3$  to  $v_d$  over comparable range of  $v_d$  change (Wong et al., 2018).~~ We use this sensitivity to identify areas where local uncertainty and variability in  $v_d$  is expected to affect local surface  $O_3$  concentration, and we use the assumption of linearity to estimate those impacts to a first order (e.g. Wong et al. 2018). [...] However, we note this first-order assumption may not be able to capture the effects of chemical transport, changes in background ozone and non-linearity in chemistry, which can contribute a non-linear response of  $O_3$  concentration to  $v_d$ . Our experiment helps identify regions where more rigorous observation and modeling efforts could be targeted for future work.

- (2) To provide an estimate of the error introduced by assuming linearity, we further investigated this assumption in two ways:

- (a) We have mathematically derived an argument for our first-order approximation to calculate  $\Delta O_3$  under small  $\Delta v_d$ , and included this in a new Supplemental Information section.
- (b) We ran another GC sensitivity simulation with 15% increase (instead of the 30% increase) in  $v_d$  and to test a second-order approximation to calculate July  $\Delta O_3$  with the

ZO3\_BB deposition parameterization. This approach is compared with our original approach in the new Supplemental Information section.

Based on our analysis, the uncertainty introduced by first-order approximation is within 30%. We have added the following to the manuscript:

In the Methods Section of the manuscript:

We use this sensitivity to identify areas where local uncertainty and variability in  $v_d$  is expected to affect local surface O<sub>3</sub> concentration, and we use the assumption of linearity to estimate those impacts to a first order (e.g. Wong et al. 2018). **In the Supplemental Methods, we justify this first order assumption mathematically, as well as demonstrate the impact of using a second order approximation, and estimate the uncertainty using an assumption of linearity to be within 30%.** However, we note this first-order assumption may not be able to capture the effects of chemical transport, changes in background ozone and non-linearity in chemistry, which can contribute to response of O<sub>3</sub> concentration to  $v_d$ . Our experiment could help identify regions where more rigorous modelling efforts could be targeted in future work.

Supplementary Information, Section 1:

Mathematical analysis for sensitivity of O<sub>3</sub> to  $\Delta v_d/v_d$ :

Assume that  $\Delta O_3$  is due to changes in dry deposition flux (with proportionality constant  $k_d$ ) and other first-order processes (e.g. NO titration, loss to HO<sub>2</sub> and OH, having total reaction rate  $k_c$ ):

$$dO_3 = d(-k_c O_3 - k_d v_d O_3) \quad (S1)$$

Here,  $k_c$  and  $k_d$  (which are related to meteorology and concentration of other relevant chemical species), are assumed to be relatively constant, so that that the perturbation in  $v_d$  does not trigger significant non-linearity. Expanding the differential and rearranging the terms yields:

$$\frac{dO_3}{O_3} = \frac{-k_d dv_d}{1 + k_c + k_d v_d} \quad (S2)$$

Integrating S2 between perturbed ( $O_3 + \Delta O_3$ ,  $v + \Delta v_d$ ) and unperturbed ( $O_3$  and  $v_d$ ) values yields:

$$\ln\left(1 + \frac{\Delta O_3}{O_3}\right) = -\ln\left(1 + \frac{k_d \Delta v_d}{1 + k_c + k_d v_d}\right) \quad (S3)$$

Since  $\Delta O_3$  is small compared to  $O_{3,0}$ , first-order expansion is valid. When  $\Delta v_d$  is small enough relative to  $v_d$  for first-order approximation, Taylor's expansion of S4 yield:

$$\frac{\Delta O_3}{O_3} = -\frac{k_d}{1 + k_c + k_d v_d} \Delta v_d \quad (S4)$$

S5 can be rearranged to yield:

$$\Delta O_3 = -\frac{k_d v_d O_3}{1 + k_c + k_d v_d} \frac{\Delta v_d}{v_d} = \beta \frac{\Delta v_d}{v_d}, \text{ where } \beta = -\frac{k_d v_d O_3}{1 + k_c + k_d v_d} < 0 \quad (S5)$$

This shows that when the  $\Delta v_d/v_d$  is small enough ( $\ln(1+x) \approx x$ ) and does not cause non-linearity ( $k_c$  and  $k_d = \text{constant}$ ) in chemistry,  $\Delta O_3$  is linearly proportional to  $\Delta v_d/v_d$ . The error of linearizing the natural logarithms equals to the difference between  $\ln(1+x)$  and  $x$ . This analysis gives the

conditions for when the first-order approximation is reasonable, and allowing us to estimate the error when deviating from these condition. Assuming  $\beta$  is correctly estimated by chemical transport model, the error of linearization at  $\Delta v_d/v_d = \pm 50\%$  (the upper bound of  $\Delta v_d/v_d$  consistent with our analysis), is on the order of 25%. For more typical value of  $\Delta v_d/v_d$  (20%), the error is around 10%.

As  $\Delta v_d/v_d$  gets larger, we can expand R.H.S of S3 to the second order and investigate sensitivity of  $\Delta O_3$  to  $\Delta v_d/v_d$ :

$$\Delta O_3 = \beta \frac{\Delta v_d}{v_d} - \frac{\beta^2}{2O_3} \left( \frac{\Delta v_d}{v_d} \right)^2 = \left( \beta - \frac{\beta^2}{2O_3} \frac{\Delta v_d}{v_d} \right) \left( \frac{\Delta v_d}{v_d} \right) = \beta' \frac{\Delta v_d}{v_d} \quad (S6)$$

Where  $\beta'$  is the “corrected  $\beta$ ”, which is a function of  $\Delta v_d/v_d$ .

To illustrate the potential impact of such non-linearity on  $\Delta O_3$ , we compare July  $\Delta O_{3,Z03\_BB}$  estimated using first-order estimation with  $\beta$  derived from  $\Delta v_d/v_d = +15\%$  and  $+30\%$ , and second-order approximation, and the result is shown in figure S1. The three different methods produce very similar  $\Delta O_3$ , and their differences have little impact on our conclusion. For simplicity, we only show the result using  $\beta$  derived from  $\Delta v_d/v_d = +30\%$  in the main manuscript.

As noted above and in the main manuscript, our approach is limited by the assumption that chemistry and transport do not introduce non-linear terms which may not be realistic. Rather, our approach is intended to identify hotspots of impact, and quantify these potential impacts to a first order. More rigorous modeling efforts could then be targeted in future work.

Supplemental figure 1:

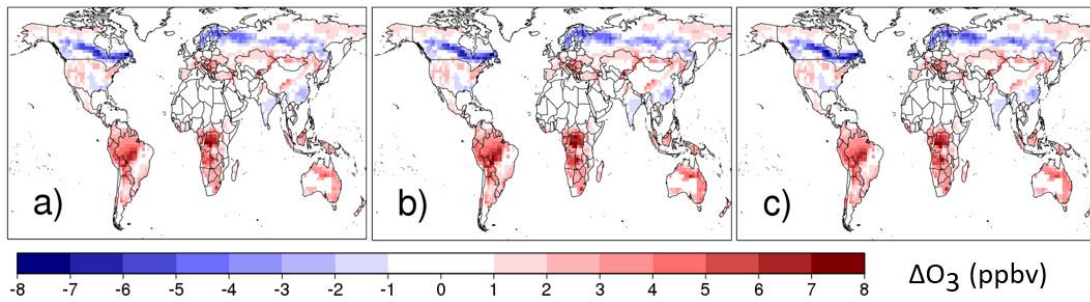


Figure S1. July  $\Delta O_{3,Z03\_BB}$  calculated using a) first-order method where  $\beta$  is derived from  $\Delta v_d/v_d = +30\%$  GC sensitivity run, b) first-order method where  $\beta$  is derived from  $\Delta v_d/v_d = +15\%$  GC sensitivity run, and c) second-order method with  $\beta$  derived from  $\Delta v_d/v_d = +15\%$ .

- 2) *The authors' attribution of biases and intermodel differences are entirely speculative. there is no rigorous evaluation of the processes/aspects leading to differences. I tend to not be in favor of such speculation and I think it masks the strength of the model evaluation (that not any one parameterization is best or worst) and model intercomparison.*

## Response:

We appreciate the reviewer's caution, and do not want to detract from other strengths of the manuscript. We have identified several speculative statements in our model evaluation, and have removed them from the manuscript.

We have removed the following statements from the manuscript:

~~...The simple linear VPD response function in Z03 may overestimate the sensitivity of  $g_s$  to VPD under the high temperature in tropical rainforest...~~

~~...The higher cuticular uptake may explain the better performance of Z03 over W98 over coniferous forests, where strong non-stomatal (though not necessarily cuticular) ozone sinks are often observed (e.g. Gerosa et al., 2005; Wolfe et al., 2011)...~~

~~...This may be attributed to the lack of response to VPD over all crop and grass land types in Z03...~~

We believe additional cases are addressed in response to the Reviewer's minor comments below.

## Minor issues:

10: *I tend to think the sinks of ozone are chemistry and dry deposition so "second largest sink" doesn't say much to me:*

Response: We agree with the reviewer that this wording is unnecessary. In response, we have changed our manuscript to:

**Dry deposition is the second largest a major sink of tropospheric ozone.**

15-16: *"to drive four ozone dry deposition parameterizations"*

Response: We have made the suggested changes:

**We use consistent assimilated meteorology and satellite-derived leaf area index (LAI) to drive four ozone dry deposition parametrizations simulate  $v_d$  over 1982-2011 driven by four sets of ozone dry deposition parametrization that are representative of the current approaches of global ozone dry deposition modelling over 1982-2011 ...**

62: *I wouldn't say Silva & Heald 2018 is a review*

Response: We have made the suggested correction:

**A recent review study (Silva and Heald, 2018)...**

66: “account for” is vague; in general this sentence implies canopy column models are better than big-leaf ones, which has yet to be shown in the literature, and

67: the authors said previously that reaction with BVOCs is a nonstomatal pathway so here saying that it is in addition to surface sinks is a little confusing

Response: We agree that “account for” is vague. Our intention was to discuss the additional processes and details that canopy column model simulates comparing to big-leaf model, rather than commenting which one is better (in terms of more accurate simulation of  $v_d$ ). In response to the reviewer comment we have reworded this:

**...which are able to ~~account for~~ simulate the effects vertical gradients inside the canopy environment, and gas-phase reaction with BVOCs ~~in addition to surface sinks~~...**

67-71: canopy column models still use resistance networks ...

Response: We agree that the main difference between canopy column model and general CTM parameterizations is multi-layer vs big-leaf representation, rather than the use of resistance network. In response to the reviewer comment we have reworded this.

**...and horizontal resolution for resolving the plant canopy in such detail, ~~instead represent plant canopy foliage as 1 to 2 big leaves, and rely on parameterization~~  $v_d$  is parameterized as a network of resistance...**

77-80: this has yet to be shown... these formulations can be variable across models ...

Response: We acknowledge the formulations can be variable across model. Wu et al. (2018) show that out of the 4 big-leaf parameterizations that are considered in their work, all of them shares very similar formulae for  $r_b$ .  $r_a$  is mostly based using Monin-Obukhov similarity theory and the difference in universal function is not found to affect  $v_d$  significantly. Other parameterizations that are not included in that study (e.g. Simpson et al., 2012) often use very similar formulae for  $r_b$  and Monin-Obukhov similarity theory for  $r_a$ . In response to the reviewer comment, we have reworded this:

**The calculation of  $R_a$  (mostly based on Monin-Obukhov similarity theory) and  $R_b$ ...**

80-88: the connection between these paragraphs (last sentence of previous one and first sentence of next one) could be articulated better

Response: We agree with this suggestion. In response, we have added the following wording:

**Such formalism is empirical in nature and does not adequately represent the underlying ecophysiological processes affecting  $R_s$  (e.g. temperature acclimation). An advance of these efforts includes harmonizing  $R_s$  with that computed by land surface models...**

101: Hardacre et al. show factor of 2-3 differences across models - so are all models' seasonal cycles well represented? also I suggest changing "demonstrating" to "suggesting".

Response: We agree with the reviewer. In response to the reviewer comment, we have reworded this sentence:

**This work found that the seasonal cycle is well-simulated across models, while demonstrating suggests that the difference in land cover classification is the main source of discrepancy between models...**

125: "unable" seems harsh; it doesn't seem Clifton et al. even tried to do this

Response: We have reworded this:

**...although they were unable to conclude do not show how the IAV of  $v_d$  may contribute to the IAV of  $O_3$ ...**

128: cut "physics"

Response: We have made this change as requested.

145: I find the placement/existence of this sentence strange. the authors don't investigate the same parameterizations that Wu et al. do.

Response: We agree with the reviewer, and have removed this sentence.

153: refs for strong empirical relationship

Response: In response to the reviewer comment, we have added references to this statement:

**...strong empirical relationship between photosynthesis ( $A_n$ ) and stomatal conductance ( $g_s$ ) (e.g. Ball et al., 1987; Lin et al., 2015)...**

162-173: I see that the authors have basically organized their parameterizations according to model (w/ exception of #2)

1) The GEOS Chem parameterization

2) Zhang parameterization

3) The CESM parameterization

4) The UKCA parameterization

I didn't realize this at first and the parameterizations chosen seemed quite strange. I would urge the authors to re-frame their parameterization description (but also noting that their parameterizations are not exact replicates of a given model)

Response: We agree with the reviewer that our choice of configurations is broadly implemented in some CTMs as mentioned. We intentionally separated our choice of parameterizations from their actual implementation in CTMs because we want our result to be representative of classes of approaches of modelling  $v_d$ , as we have explained this in line 150 – 158. Furthermore, the choice of doing Z03\_BB and W98\_BB comes from recent efforts to harmonize CTM  $R_s$  with Earth System Model/Land Surface Model  $R_s$  as a viable option for improving  $v_d$  simulations (line 86). However, we agree with the reviewer that we could reframe these descriptions to be more clear, and use examples in their description. In response to the reviewer’s comment we have made the following changes:

**3) W89 with  $R_s$  calculated from a widely-used coupled  $A_n$ - $g_s$  model, the Ball-Berry model (hereafter referred to as W98\_BB) (Ball et al., 1987; Collatz et al., 1992, 1991), which is similar to that proposed by Val Martin et al. (2014), and therefore the current parameterization in Community Earth System Model (CESM). This represents Type 3 in stomatal and Type 1 in non-stomatal parametrization.**

**4) Z03 with the Ball-Berry model (Z03\_BB), which is comparable to the configuration in Centoni (2017) implemented in United Kingdom Chemistry and Aerosol (UKCA) model. This represents Type 3 in stomatal and Type 2 in non-stomatal parametrization.**

175: *It doesn’t quite make sense to me that the authors say the Zhang parameterization is “open source” in one sentence and a couple sentences later say that implementing it required personal communication with Zhiyong and Leiming.*

Response: This is a good point. We deleted the word “open-source”.

180: *Given that GEOS Chem doesn’t have a land surface model, I think the authors need to clarify how exactly  $A_{net}$  is calculated.*

Response: We have added a brief description of the  $A_n$ - $g_s$  model in the new supplemental material section:

**A brief description of photosynthesis-stomatal conductance ( $A_n$ - $g_s$ ) module in TEMIR (a manuscript is in prep)**

**TEMIR largely follows Oleson et al. (2013), where net photosynthetic rate ( $A_n$ ,  $\mu\text{mol CO}_2 \text{ m}^{-2} \text{ s}^{-1}$ ), stomatal conductance for water ( $g_{sw}$ ,  $\mu\text{mol m}^{-2} \text{ s}^{-1}$ ) and  $\text{CO}_2$  concentration in leaf mesophyll ( $c_i$ ,  $\text{mol mol}^{-1}$ ) are solved simultaneously by the following coupled set of equations:**

$$A_n = \frac{g_{sw}}{1.6} (c_a - c_i) \quad (S7)$$

$$g_{sw} = \beta_t g_0 + g_1 \frac{A_n}{c_s} RH_s \quad (S8)$$

$$A_n = A - R_d \quad (S9)$$

**Here,  $c_a$  is  $\text{CO}_2$  concentration ( $\text{mol mol}^{-1}$ ),  $\beta_t$  is soil moisture stress factor (unitless),  $g_0$  is minimum stomatal conductance ( $\mu\text{mol m}^{-2} \text{ s}^{-1}$ ),  $A_n$  is net photosynthetic rate ( $\mu\text{mol CO}_2 \text{ m}^{-2} \text{ s}^{-1}$ ),  $A$**



is gross photosynthetic rate ( $\mu\text{mol CO}_2 \text{ m}^{-2} \text{ s}^{-1}$ ) and  $R_d$  is dark respiration rate ( $\mu\text{mol CO}_2 \text{ m}^{-2} \text{ s}^{-1}$ ). Furthermore,  $c_s$  and  $RH_s$  are the  $\text{CO}_2$  concentration ( $\text{mol mol}^{-1}$ ) and relative humidity (unitless) at leaf surface.  $A$  is calculated following Bonan et al. (2011), which is based on Farquhar et al. (1980) and Collatz et al. (1992):

$$\Theta_{cj}A_i^2 - (A_c + A_j)A_i + A_cA_j = 0 \quad (S10)$$

$$\Theta_{ip}A^2 - (A_i + A_p)A + A_iA_p = 0 \quad (S11)$$

For C3 plants,  $\Theta_{cj} = 0.98$  and  $\Theta_{ip} = 0.95$ . For C4 plants,  $\Theta_{cj} = 0.80$  and  $\Theta_{ip} = 0.95$ . Rubisco-limited rate ( $A_c$ ,  $\mu\text{mol CO}_2 \text{ m}^{-2} \text{ s}^{-1}$ ), light-limited rate ( $A_j$ ,  $\mu\text{mol CO}_2 \text{ m}^{-2} \text{ s}^{-1}$ ), product-limited rate ( $A_p$ ,  $\mu\text{mol CO}_2 \text{ m}^{-2} \text{ s}^{-1}$ ) and  $R_d$  are calculated as:

$$A_c = \begin{cases} \frac{V_{c \max}(c_i - \Gamma_*)}{c_i + K_c(1 + \frac{0.21P_{\text{atm}}}{K_o})} & \text{for } C_3 \text{ plants} \\ V_{c \max} & \text{for } C_4 \text{ plants} \end{cases} \quad (S12)$$

$$A_j = \begin{cases} \frac{J(c_i - \Gamma_*)}{4c_i + 8\Gamma_*} & \text{for } C_3 \text{ plants} \\ 0.23\phi & \text{for } C_4 \text{ plants} \end{cases} \quad (S13)$$

$$A_c = \begin{cases} 3T_p & \text{for } C_3 \text{ plants} \\ k_p \frac{c_i}{P_{\text{atm}}} & \text{for } C_4 \text{ plants} \end{cases} \quad (S14)$$

$$R_d = \begin{cases} 0.015V_{c \max} & \text{for } C_3 \text{ plants} \\ 0.025V_{c \max} & \text{for } C_4 \text{ plants} \end{cases} \quad (S15)$$

Here,  $V_{c \max}$ ,  $\Gamma_*$ ,  $P_{\text{atm}}$ ,  $J$ ,  $\phi$ ,  $T_p$  and  $k_p$  are the maximum rate of carboxylation ( $\mu\text{mol m}^{-2} \text{ s}^{-1}$ ),  $\text{CO}_2$  compensation point ( $\text{mol mol}^{-1}$ ), atmospheric pressure (Pa), electron transport rate ( $\mu\text{mol m}^{-2} \text{ s}^{-1}$ ), absorbed photosynthetically active radiation (PAR) ( $\text{W m}^{-2}$ ), triose phosphate utilization rate ( $\mu\text{mol m}^{-2} \text{ s}^{-1}$ ) and initial slope of C4  $\text{CO}_2$  response curve ( $\mu\text{mol Pa}^{-1} \text{ m}^{-2} \text{ s}^{-1}$ ).  $K_c$  and  $K_o$  are the Michaelis-Menten constants for  $\text{CO}_2$  and  $\text{O}_2$  (Pa). Furthermore,  $J$  is calculated as the smaller root of the following equation:

$$0.7J^2 + (1.955\phi + J_{\max})J + 1.955\phi = 0 \quad (S16)$$

Where  $J_{\max}$  is the maximum potential rate of electron transport ( $\mu\text{mol m}^{-2} \text{ s}^{-1}$ ). As  $J_{\max}$ ,  $\phi$ ,  $V_{c \max}$  and the variables related to  $V_{c \max}$  ( $\Gamma_*$ ,  $J_{\max}$ ,  $T_p$ ,  $R_d$ ) differ between sunlit and shaded leaves, the above set of equations are solved separately for sunlit and shaded leaves.

The parameters ( $V_{c \max}$ ,  $\Gamma_*$ ,  $K_c$ ,  $K_o$ ,  $J_{\max}$ ,  $T_p$ ,  $R_d$ ) are functions of vegetation temperature ( $T_v$ ), and the temperature scaling formulae are given at eq. 8.9 to eq. 8.14, while the effect of temperature acclimation (Kattge and Knorr, 2007) on  $J_{\max}$  and  $V_{c \max}$  are given at eq. 8.15 and 8.16 in Oleson et al. (2013). Other details of the model formalism (e.g. canopy scaling and effect of  $\beta_t$  on  $V_{c \max}$ ) also follow Chapter 8 in Oleson et al. (2013), therefore we will focus on describing the main differences between CLM 4.5 and TEMIR.

First, TEMIR is driven entirely by assimilated meteorology. Instead of solving the whole surface energy balance equation, TEMIR consistently calculates  $T_v$  from 2-meter air temperature ( $T_2$ , K)

and sensible heat flux ( $H$ ,  $\text{W m}^{-2}$ ) using Monin-Obukhov similarity theory (Monin and Obukhov, 1954):

$$T_v = T_2 + \frac{H}{\rho c_p} (r_{a,h} + r_{b,h}) \quad (S16)$$

Where  $\rho$ ,  $c_p$ ,  $r_{a,h}$  and  $r_{b,h}$  are air density ( $\text{kg m}^{-3}$ ), specific heat of air at constant pressure ( $\text{J kg}^{-1} \text{K}^{-1}$ ), aerodynamic and laminar boundary-layer resistance ( $\text{s m}^{-1}$ ) of heat, respectively.

Secondly, MERRA-2 only provides soil moisture output at two levels (surface and root zone), which is not compatible with the multi-layer soil module in CLM. Therefore, instead of aggregating  $\beta_i$  from multiple soil layers, TEMIR calculates  $\beta_i$  from the root-zone soil wetness of MERRA-2. Soil wetness ( $s$ ) is first converted into soil matric potential ( $\psi$ , mm) using the following equation:

$$\psi = \psi_{sat} s^{-B} \quad (S17)$$

Where  $\psi_{sat}$  and  $B$  are the soil matric potential (mm) at saturation and Clapp-Hornberger exponent (Clapp and Hornberger, 1978), which are related to soil property. Then  $\beta_i$  is calculated as:

$$\beta_t = \frac{\psi_c - \psi}{\psi_c - \psi_0} \left( \frac{\theta_{sat} - \theta_{ice}}{\theta_{sat}} \right), 0 \leq \beta_t \leq 1 \quad (S18)$$

Where  $\psi_c$  and  $\psi_0$  are the soil matric potential (mm) at which stomata are full close or fully open, and the term in the bracket account for the fact that frozen water are not available for plants.

182-183: *It's fine not to test Ra and Rb, but i suggest that the authors do not use this qualifier. This isn't well understood (Does Fares et al. even show this?)*

Response: In response to the reviewer's comment we have deleted this qualifier:

**...which is numerically stable (Sun et al., 2012). Since discrepancies in  $R_e$  parameterizations typically dominates the uncertainty of deposition velocity of O3  $v_d$  (Fares et al., 2010; e.g. Wu et al., 2018)...**

188-9: *has this model been evaluated? or used previously?*

Response: An evaluation paper of this model is in prep by collaborators who hope to have this submitted shortly in a Discussion format, and we intend to add this citation if possible before publicatio.

194-5: *what are these variables used for?*

Response: These variables are needed to drive the dry deposition parameterizations, as they require land cover classification (basically PFT) and LAI. Soil property is required for running the  $A_n-g_s$  model. In response to the reviewer's question we have added the following text to our manuscript:

...We use the CLM land surface dataset (Lawrence and Chase, 2007), which contains information for land cover, per-grid cell coverage of each plant functional type (PFT), and PFT-specific LAI, which are required to drive the dry deposition parametrizations, and soil property, which is required to drive the  $A_n-g_s$  model in addition to PFT and PFT-specific LAI.

195: presumably the authors' decisions about land type mapping (& differences for "W89" vs "Z03") impact the authors' results... one implication of this is that the authors' statement in the abstract or introduction that the only thing different across parameterizations is the model structure is not necessarily true

Response: The reviewer raises an excellent point. We agree that this is one of the key uncertainty of our approach and deserves more discussion. This is mostly limited to herbaceous and shrub land type as the CLM forest PFT correspond pretty well to W98/Z03 land types. In response to the reviewer's comment, we added the following:

... do not resolve croplands into such detail. Having land cover maps that distinguish between more crop types could potentially improve the performance of Z03. **The evaluation for herbaceous land types also suggests that as CLM PFT do not have exact correspondence with W98 and Z03 land types, our results over herbaceous land types are subject uncertainty in land type mapping (e.g. tundra vs grassland, specific vs generic crops, C3 vs C4 grass).**

197: I would suggest cutting the "(eg. leaf physiological and soil hydraulic constants)" - becoming more specific here doesn't help readers when the parameterizations are not laid out and we have no idea what these terms do/stand for

Response: This was removed as suggested.

198: what's z0?

Response: We have clarified this in the manuscript:

... while land-cover specific **roughness length** ( $z_0$ ) values follow Geddes et al. (2016).

198: how is leaf wetness calculated? how is snow calculated?

Response: We have added the following to our manuscript:

...follow Geddes et al. (2016). **Leaf is set to be wet when either latent heat flux  $< 0 \text{ W m}^{-2}$  or precipitation  $> 0.2 \text{ mm hr}^{-1}$ . Fractional coverage of snow for Z03 is parameterized as a land-type specific function of snow depth following the original manuscript of Z03, while W98 flags grid cells with albedo  $> 0.4$  or permanently glaciated as snow-covered.**

203: *how do the authors scale PFT-specific LAI? is there an established method of doing this? presumably this has implications for the findings*

Response: We choose to derive scaling factors as the direct disaggregation method of Lawrence and Chase (2007) is very difficult to replicate, and derived the grid-cell level scaling factor at  $2^{\circ} \times 2.5^{\circ}$  by comparing the monthly mean LAI at each year with that of the 30-year mean. In theory PFT-specific LAI can be simulated by land surface model, but that will be even more uncertain and less empirically-constrained than using satellite LAI. In response to the reviewer comment, we clarify our approach in the manuscript:

**We use ~~this data set to derive~~ the interannual scaling factors as the ratio between the monthly LAI at specific year and that of the 30-year mean of GIMMS LAI3g, that can be applied to **scale** the baseline CLM-derived LAI (Lawrence and Chase, 2007) **for each month over 1982 to 2011...****

217: *I think the authors need to articulate here or in the introduction the various effects that high CO<sub>2</sub> may have on ozone dry deposition velocity and the various uncertainties in our understanding of CO<sub>2</sub> fertilization (& reference previous work examining this)*

Response: We added the following:

**...enhanced cuticular O<sub>3</sub> uptake under leaf surface wetness (Altimir et al., 2006; Potier et al., 2015, 2017; Sun et al., 2016). Furthermore, terrestrial atmosphere-biosphere exchange is also directly affected by CO<sub>2</sub>, as CO<sub>2</sub> can drive increases in LAI (Zhu et al., 2016) while inhibiting  $g_s$  (Ainsworth and Rogers, 2007). These can have important implications on  $v_d$ , as shown by Sanderson et al. (2007), where doubling current CO<sub>2</sub> level reduces  $g_s$  by 0.5 – 2.0 mm s<sup>-1</sup>, and by Wu et al. (2012) where  $v_d$  increases substantially due to CO<sub>2</sub> fertilization at 2100. Observations from the Free Air CO<sub>2</sub> Enrichment (FACE) experiments also CO<sub>2</sub> fertilization and inhibition of  $g_s$  effects, but the impacts are variable and species specific such that extrapolation of these effects to global forest cover is cautioned (Norby and Zak, 2011).**

229: *is the proper/up-to-date way of referencing GEOS-Chem?*

Response: We have replaced the citation to Bey et al. (2001) with a link to the GEOS-Chem model, which is up-to-date and we believe is consistent with the GEOS-Chem community's approach (in addition to including citations to the most relevant developments in the GEOS-Chem chemistry, as we have done).

237: *binned = jargon*

Response: We changed the sentence to:

**Both of the maps are ~~binned~~ remapped from their native resolutions to  $0.25^{\circ} \times 0.25^{\circ}$ .**

243-246: discussing about dry deposition of other species and impacts on ozone requires introducing some concepts (or cutting talking about dry deposition of other species)

Response: We removed the sentence talking about dry deposition of other species.

249-251: this seems like a strange choice to me. it's not differences in transport per se, it's differences in background ozone caused by changes in ozone dry deposition. why wouldn't the authors want to capture this? because it contributes to nonlinear responses to ozone dry deposition?

Response: We agree with reviewer's comment that perturbation in  $v_d$  causes changes in background  $O_3$ , and this can be potentially important. Our main objective is to study the local uncertainty in  $O_3$  due to local uncertainty in  $v_d$ . Therefore, we choose to limit our study to regions with sufficiently high  $v_d$ , where the changes and uncertainties in surface  $O_3$  are more likely to be dominated by the direct effect of  $v_d$  rather than changes in background  $O_3$ , and avoid the potential non-linearity as suggested by the reviewer. In response to the reviewer's comment, we have clarified this in our manuscript:

~~Nevertheless, we~~ **We use this sensitivity to identify areas where local uncertainty and variability in  $v_d$  is expected to affect local surface  $O_3$  concentration, and we use the assumption of linearity to estimate those impacts to a first order (e.g. Wong et al. 2018).**

**...are expected to be attributed more to ~~chemical transport~~ changes in background  $O_3$  rather than...**

249: what is the baseline simulation?

Response: We make the following change:

**...where the monthly average  $v_d$  is greater than  $0.25 \text{ cm s}^{-1}$  in the ~~baseline~~ unperturbed GEOS-Chem simulation...**

254: Why not CLIM+LAI+CO2 as well?

Response: As we show later, over these 30 years,  $CO_2$  has very minor effect on  $v_d$  (fig. 9). In response to the reviewer's question, we have added the following:

**...largely based on the evaluation presented in Silva and Heald (2018). We do not include the evaluation of  $v_d$  from [Clim+LAI+CO<sub>2</sub>] scenario as we find that the impact of  $CO_2$  concentration on  $v_d$  is negligible over the period of concern, as we will show in subsequent sections.**

261-3: How many sites does this cut?

Response: This removes 1/3 of the original data (25 data sets). In response to the reviewer's question, we have added this:

~~While this leads to reduction of dataset size comparing to~~ **removes 1/3 of the original data sets used in Silva and Heald (2018)...**

265: *Fractional coverage of what? (please spell out in text) Why are these figures shown? they are not very useful for the reader*

Response: For fractional coverage, we refer to “each major land type” in line 267. We do agree that our description did not help readers to understand the graph. In response to the reviewer questions, we have made the following changes:

**Nearly all the observations are clustered in Europe and North America, except three sites in the tropical rainforest and one site in tropical deciduous forest in Thailand. For most major land types, there are significant mismatches between the locations of flux measurements and the dominant land cover fraction, which may hinder the spatial representativeness of our evaluation.**

270-1: *Not sure what the point of this sentence is*

Response: We agree that the statement is unnecessary. We have removed the sentence.

273: *it seems strange to me that the authors would generalize such as bias, given that it's unclear if the bias is caused by a particular attribute of a land type or process, and that the land type-specific biases differ across the parameterizations*

Response: We agree with the reviewer that it may not be a good choice to generalize such bias. We have made the following change:

~~As summarized in Table 2, each parameterization shows distinct biases over specific land types (we subsequently refer to this as the “land-type specific bias” unique to each parameterization).~~ **The performance metrics of each parameterization at each land type are summarized in table 2.**

282: *what does N=5 mean? 5 sites? 5 data points?*

Response: Thanks for pointing out this ambiguity. We have made the following changes:

**... by the four dry deposition parameterizations, with  $N$  referring to number of data points (1 data point = 1 seasonal mean).**

288: *if the authors are implying ambient chemistry is happening then they should just say it*

Response: As suggested in earlier response, this sentence contains unnecessary speculation and therefore we have deleted the sentence.

300: *meaning that the authors do not leverage it*

Response: Yes. We have clarified this in our manuscript:

**...as most global land cover data sets do not resolve croplands into such detail. Having land cover maps that distinguish between more crop types could potentially improve the performance of Z03...**

301-302: *I'm not sure that the following lines illustrate this; in other words, i think BB "generally but not universally leads to improvements" is not supported by the actual findings — it seems to be for Z03 — but not for Wesely — which may suggest that we need to be paying attention to nonstomatal deposition estimates too.*

Response: We agree that non-stomatal deposition should not be overlooked, and we agree that the improvement of Z03\_BB over Z03 is more significant than that of W98\_BB over W98. We find that W98\_BB and W98 have comparable performance over forests, but W98\_BB significantly outperform W98 over herbaceous land types. We also agree that nonstomatal parameterization probably contributes to the different responses between W98\_BB vs W98 and Z03\_BB vs Z03. We changed our wording as follows:

**...improving spatial distribution of mean  $v_d$ . The different responses to substituting native  $g_s$  with that from Ball-Berry model highlight the significant differences in parameterizing non-stomatal uptake between W98 and Z03, which further suggests that the uncertainty in non-stomatal deposition should not be overlooked.**

313-4: *what particular problem has been highlighted?*

Response: This refers to the mismatch between EC footprint and model resolution. In response to the reviewer comment, we have clarified this in our manuscript:

**~~This problem~~ The mismatch between model resolution and the footprint of site-level measurements...**

315: *sampling biases meaning that the authors are not evaluating most locations on earth, right? the authors are sampling the time/place of the measurements*

Response: This is correct and we acknowledge our ambiguity in wording. We make the following change:

**... the evaluation may be further compromised by inherent spatial sampling biases (fig. 1).**

317-320: *not sure what the point of this paragraph is. what is the hypothesis being investigated?*

Response: The main purpose of the section is to show that our model implementation gives reasonable result at seasonal scale. Comparing the W98 result from our implementation with that from GC further supports our argument. In response to the reviewer question, we have added the following wording:

**W98 run with static LAI, providing further evidence that our implementation of W98 is reliable...**

334-5: *recommend that the authors don't speculate here or elsewhere*

Response: We agree that it is unnecessary. We removed the speculative statement:

**In India, Australia, western US, and polar tundra Mediterranean region, July mean daytime  $v_d$  is low (0.2 - 0.5 cm s<sup>-1</sup>). ~~which could be due to either the high temperature or the sparsity of vegetation (or a combination of both).~~**

349-50: *on a similar note as the above comment, how do the authors know this?*

Response: We agree that we should provide more information to support our argument, and will make our explanation much clearer. We added the soil moisture stress factor map as figure S2. In July, over southern Africa, the soil stress factor is exceptionally low, indicating that drought stress does strongly limit  $g_s$  over the region. We have also changed our wording to be more cautious in our interpretation (instead of “because”, we state, “which may be due to”). We changed line 350 to:

**...which may be due to the explicit consideration of soil moisture limitation to  $A_n$  and  $g_s$  (demonstrated by the spatial overlap with soil moisture stress factors shown in Fig. S2)...**

And in the Supplemental Information:

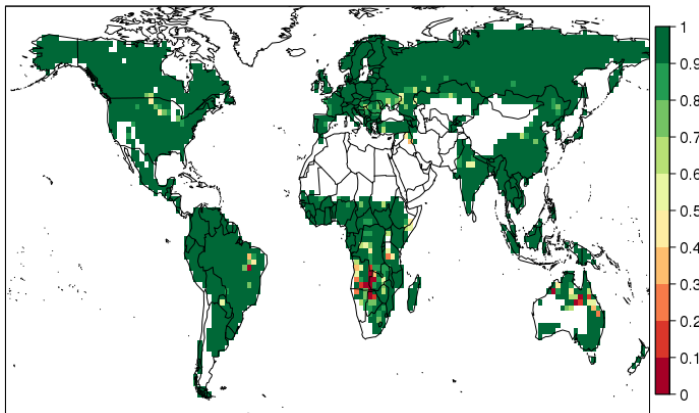


**Figure S2. July average soil moisture stress factor ( $\beta_i$ ).  $\beta_i = 1$  represents no soil moisture stress, while smaller  $\beta_i$  means stronger soil moisture stress and more stomatal closure.  $\beta_i = 0$  signifies that soil moisture stress is so strong that it completely shuts down stomatal activity.**

353: *"is not desiccated"?*

Response: We have clarified this in our manuscript as follows:

**... as long as the soil does not desiccate ~~become too dry to support stomatal opening~~...**



358: *i don't think the authors show this; they just speculate that this is the cause.*

Response: In response to the reviewer's comment, we have omitted this comment.

368: *will the authors more carefully articulate what Centoni finds so that the reader knows how to compare the findings*

Response: We agree this reference may not be ideal since Centoni (2017) did not explicitly talk about all four parameterizations. We have removed this reference:

**...We find  $\Delta O_3$  is the largest in tropical rainforests for all the parameterizations (up to 5 to 8 ppbv), ~~which agrees with the result from Centoni (2017) ...~~**

370: *i assume that the authors are identifying the hot spot regions through their large delta O3. related: perhaps the authors are missing a delta on the  $v_{d,i}$  in Equation 3.*

Response: We thank the reviewer for catching this oversight. We have amended equation (3) to:

$$\Delta O_3 \approx \beta \frac{\Delta \overline{v_{d,i}}}{v_{dW98}} \quad (3)$$

378: *are the authors really "exploring the importance of seasonality in predictions of  $v_d$  and their subsequent impact" with their current approach? (see comment below for line 404)*

404: *are the authors actually showing the impacts on seasonality? showing the impact in each season is not the same as showing the impact on seasonality (a couple of easy calculations could help here)*

Response: We agree with the reviewer that "showing the impacts in different season" is not equivalent to "showing the impact on seasonality". In response to the reviewers' comments, we have clarified our intentions:

**To explore the impact of different prediction of  $v_d$  on surface  $O_3$  in different seasons, importance of seasonality in prediction of  $v_d$  and their subsequent impact...**

**...not only affects the mean of predicted surface ozone, but also has different impacts in different seasons, ~~the seasonality, of predicted surface ozone...~~**

382-4: *i suggest a semi colon connecting these two sentences*

Response: Changed as suggested

385: *"shifts from the south to the north relative to July"*

Response: Changed as suggested

387: i'm not a fan of the authors' use of the term hydroclimate — it's vague — can the authors just say soil moisture or VPD or leaf wetness?

Response: We agree that “hydroclimate” is vague. We have clarified this in the manuscript:

**... driven primarily by the response to hydroclimate-related parameters such as soil moisture, VPD and leaf wetness, in addition to and land type-specific parameters...**

398: the suggestion that “hydroclimate [is] a key driver of process uncertainty” seems limited to the tropics/subtropics. am i correct in this interpretation? if so, this should be emphasized.

Response: We agree with this interpretation. We have clarified our interpretation as follow:

**These findings identify hydroclimate as a key driver of process uncertainty of vd over tropics and subtropics, and therefore its impact on the spatial distribution of surface ozone concentrations, independent of land type-based biases, in these regions.**

409: briefly describe this method such as the limitations/strengths of it

Response: We add this to our manuscript:

**We use Theil-Sen method (Sen, 1968), which is less susceptible to outliers than least-square methods, to estimate trends...**

413: what trends? trends in meteorology, LAI, and/or CO2?

Response: We are referring to  $v_d$ . We have clarified this:

**Figure 9 shows the potential impact of ~~these trends~~ the trends in  $v_d$  on...**

415: how is the annual change in vd estimated? is it using the Theil-Sen method? this part needs better explanation; the reader needs to at least have some concept of what the method used is

Response: We have clarified our methods as follows:

$$\Delta O_{30y,i} \approx \beta \times m_{v_d,i} \times 30 \quad (4)$$

where  $\Delta O_{30y,i}$  and  $m_{v_d,i}$  is are the absolute change in ozone inferred to a first order as a result of the trend of  $v_d$  and the normalized Theil-Sen slope (% yr<sup>-1</sup>) of  $v_d$ , for parameterization  $i$  the over the 30-years (1982-2011).

423-4: but they are small or nonsignificant per the first line of the paragraph?

Response: Our wording here was indeed confusing. We have clarified this by making the following changes:

**In [Clim] simulations (where LAI is held constant), ~~the trend of July daytime vd is either small or non-significant over the vast majority of the NH.~~ significant decreasing trends in July daytime vd are simulated by the Z03, W98\_BB and Z03\_BB parameterizations. An exception is observed in the region of ~~over~~ Mongolia, where significant increasing trend in T (warming) and decreasing trend in RH (drying) detected in the MERRA-2 surface meteorological field in July daytime results in significant decreasing trends using the Z03, W98\_BB and Z03\_BB parameterizations.**

439: *or it may decrease as plants acclimate or as nutrients become limiting*

We acknowledge that the sensitivity of terrestrial biosphere to CO<sub>2</sub> can be highly variable. In response to the reviewer's comment, we have elaborated and included citations to related literature:

**We note that the importance of the CO<sub>2</sub> effect could grow as period of study further extend to allow larger range of atmospheric CO<sub>2</sub> concentration (Hollaway et al., 2017; Sanderson et al., 2007). in the coming decades, since the 439 sensitivity of stomatal conductance to atmospheric CO<sub>2</sub> may increase (Franks et al., 2013).**

452: *assuming that ozone dry deposition should be a strong function of LAI*

Response: We have clarified this statement to include this correction:

**...since both stomatal and non-stomatal conductance in W98 are assumed to be strong functions of LAI...**

455: *"complex"*

Response: Changed as advised

466: *"suggesting"*

Response: Changed as advised

466: *suggestion to cut "natural" here and in other spots - natural IAV has ambiguous meaning*

Response: Cut as advised

475: *heterogeneity?*

Response: We changed this line:

... show more spatial ~~discontinuities~~ **heterogeneity** compared to W98 and Z03.

478: soil moisture data?

The advent of microwave remote sensing data provides excited opportunities for assimilating soil moisture. However, converting soil moisture into soil matric potential, which is measures of attraction between soil matrix and water, and therefore ecophysiologicaly relevant, requires data of soil property, which is less constrained globally. In response to this comment, we have made the following clarification:

**Given the uncertainty in soil data (Folberth et al., 2016)... global soil property maps (Dai et al., 2019)...**

480: refs for good performance at site level?

Response: We have added a reference as follows:

**... despite their relatively good performance in site-level evaluation (e.g. Wu et al., 2011).**

495-6: whether IAV in  $v_d$  at Blodgett is caused by chemistry is unknown

Response: We agree that our wording is ambiguous. Rather than claiming chemistry causing IAV, we have reworded this sentence as follows:

**In Blodgett Forest, where  $O_3$  uptake is more controlled by gas-phase reactions (fares et al., 2010; Wolfe et al., 2011), we...**

491-497: steps on how authors calculated averages and CVs for long term data needed

Response: We agree with the reviewer that this subsection would benefit from some clarification. As most of the IAV section presents result for July, we now recalculate and present the July  $CV_{v_d}$  for all the 3 sites based on the raw data, and the details of calculation is given in supplemental material. We calculated July mean daytime  $v_d$  for each year by averaging the individual hourly averages to avoid hourly sampling bias, and derive  $CV_{v_d}$  by dividing the standard deviation by the mean of July mean  $v_d$  over all years. The recalculated numbers do not change our conclusion significantly. In response to the reviewer's suggestion, we have made the following changes to our manuscript:

**We compare the simulated IAV of  $v_d$  July  $CV_{v_d}$  from all four deposition parameterizations with those recorded by publicly available long-term observations. Hourly  $v_d$  is calculated using eq. (1) from raw data. We filter out the data points with extreme ( $> 2 \text{ cm s}^{-1}$ ) or negative  $v_d$ , and without enough turbulence ( $u^* < 0.25 \text{ m s}^{-1}$ ). As  $v_d$  in each daytime hours are not uniformly sampled in the observational datasets, we calculate the mean diurnal cycle, and then calculate the daytime average July of  $v_d$  for each year from the mean diurnal cycle, from which  $CV_{v_d}$  can be calculated.**

The IAV predicted by all four parameterizations at Harvard Forest is between 3% to 7.9%, which is 2 to 6 times lower than that presented in the observations (~~19~~ **18%**). ~~by Clifton et al. (2017)~~. We find similar underestimates by all four parameterizations compared to the long-term observation from Hyytiala (Junninen et al., 2009; Keronen et al., 2003; <https://avaa.tdata.fi/web/smart/smear/download>), where observed  $CV_{vd}$  (~~11~~**16%**) is significantly higher than that predicted by the deposition parameterizations (3.5% - 7.1%). In Blodgett Forest, where  $O_3$  uptake is more controlled by **attributable to** gas-phase reactions (Fares et al., 2010; Wolfe et al., 2011), we find that the models underestimate the observed annual  $CV_{vd}$  more seriously (~1%– 3% compared to ~~12~~ **18%** in the observations)

499: *Olivia has a new paper on this*

Response: We agree that Olivia's new paper is an excellent reference of furthering our discussion. We have added this reference:

**Clifton et al. (2017**~~2019~~**) attribute this to the IAV in deposition to wet soil and dew-wet leaves, and in-canopy chemistry under stressed condition for forests over northeastern U.S. in non-stomatal deposition, while acknowledging the obscurity of the mechanisms driving such variability, Some of these processes (e.g. in-canopy chemistry, wetness slowing soil ozone uptake) are not represented by existing parameterizations, contributing to their** ~~implying the difficulty in reproducing the observed IAV by existing parameterizations.~~

526: *a vague reference to an effort in asia doesn't do much to help the reader*

Response: We add the reference to the measurement in Asia as follow:

**We know of only one multi-season direct observational record in Asia (Matsuda et al., 2005) and none in Africa...**

527: *"constrain"; why all of a sudden call it gaseous dry deposition?*

Response: We agree that our paper does not discuss about other gaseous species. We clarified this:

**To better constraint regional  $O_3$  dry deposition, effort must be made in making new observations of gaseous dry deposition...**

528: *what do the authors mean by reported? do they mean in the peer reviewed literature? there are many reasons why people report fluxes rather than deposition velocities in peer-reviewed publications, and previous work doesn't simply exist to provide deposition velocities for future model evaluation! many datasets are available by contacting the research groups that made them.*

Response: We agree that our wording could be misinterpreted and requires clarification. We have simplified the text in our manuscript:

~~We also find that many existing ozone flux measurements are not usable for our evaluation purposes, since only FO3 is reported in detail instead of vd. Evaluation and development of ozone dry deposition parameterizations would be greatly benefited if result of ozone flux measurements is reported in both FO3 and vd, or even have publically available ozone flux and other related micrometeorological variables, which allows both direct evaluation of vd and solves the mismatch between coarse model grids and the site (e.g. Wu et al., 2011, 2018).~~  
**Evaluation and development of ozone dry deposition parameterizations will continue to benefit from publicly available ozone flux measurements and related micrometeorological variables that allow for partitioning measured flux into individual deposition pathways (e.g. Clifton et al., 2017; 2019, Fares et al., 2010, Wu et al., 2018).**

536: *do the authors actually show that the four parameterizations differ most in leafy parts of the world? if not, i suggest rephrasing*

Response: We have rephrased this statement.

**We find that these discrepancies are in general a function of both location and season. In NH summer,  $v_d$  simulated by the 4 parameterizations are considerably different in many ~~vegetation-dominated~~ regions over the world.**

542-544: *is this something that is assumed widely?*

Response: We have reworded this statement:

**This demonstrates the potential impact of parameterization choice (or, process uncertainty) on  $v_d$  is neither spatiotemporally uniform nor negligible in ~~most vegetated~~ **many** regions over the world.**

543: *demonstrates that*

Response: Changed as advised

549: *why “at least increase the spatiotemporal representativeness if not the absolute accuracy” - is there some limitation of the Ducker dataset that I am missing?*

Response: This is because FLUXNET-based data can provide a constraint stomatal deposition, but with limited opportunity to constrain other individual pathways. Potentially, if the biases in stomatal and non-stomatal deposition offsets each other, constraining stomatal deposition may lead to substantial biases in  $v_d$ . Whether better constrained  $g_s$  leads to significantly better constrained  $v_d$  we believe is still an open research question and is something we are investigating in a follow up study. In response to the reviewer’s question, we have added the following text to the manuscript:

**...increase the spatiotemporal representativeness, if not the absolute accuracy, of dry deposition parameterization, since it would be difficult to constrain non-stomatal sinks with**

**this method. Further research is required to more directly verify whether better constrained  $g_s$  leads to improved  $v_d$  simulation.**

554-6: *the authors could do a better job at illustrating why they are linking these two ideas*

Response: We clarified our statement as follow:

**The predicted IAV from all four models is smaller than what long-term observations suggest, but **its potential contribution to IAV in  $O_3$**  is still comparable to the long-term variability of background ozone over similar timescales in U.S. summer (Brown-Steiner et al., 2018; Fiore et al., 2014).**

561-3: *yet the authors barely make use of long-term datasets that are available!*

Response: Our intention was to draw attention to the fact that our experiment shows many interesting and notable impacts occurring in parts of the world where there are no available long-term observations to our knowledge, and therefore are these effects are difficult to evaluate. We have clarified by replacing this sentence in question with the following:

~~**The scarcity of long-term ozone deposition measurement poses significant difficulty in evaluating the model predictions over interannual (and in particular multidecadal) timescales.**~~ **While our results show notable impacts across the globe, in many regions there are no available long-term observation to evaluate the model predictions over interannual timescales.**

583: *what does low baseline  $v_d$  actually mean?*

Response: Here we were referring to the mean  $v_d$  in the unperturbed GEOS-Chem simulation. We deleted the word “baseline” to avoid confusion.

586:  $v_d$

Response: We have made this correction.

587: *do the authors mean the simulation year for the 30% testing?*

Response: We refer to the whole sensitivity simulation. This has been clarified:

**...and possibly the **choice of simulation year for the sensitivity simulation...****

588: *is this somewhat inherently in the LAI product?*

Response: This is an interesting question and can be answered in two dimensions. First, LAI retrieval is land cover-dependent (Fang et al., 2013). LAI products spanning before MODIS era

(2000) mostly use static land cover (e.g. Liu et al., 2012; Zhu et al., 2013) that may not even correctly capture the impact land use and land cover change (LULCC) on LAI. Also, at least in those parameterizations, changes in land type causes changes in LAI-independent parameters (e.g. in-canopy aerodynamic resistance, cuticular resistance), which also cannot be captured by LAI changes. In response to the reviewer comment, we have made the following modification to the text:

**...source of variability for  $v_d$ , and even long-term LAI retrieval (Fang et al., 2013).**

593-600: *as is, this seems like a stretch to me*

Response: We agree that this is a speculative element of our discussion. We meant to emphasize that uncertainty in gaseous dry deposition is not exclusive to O<sub>3</sub>. We want to encourage similar research attention on the uncertainty in dry deposition of other gases (e.g. NO<sub>2</sub>, SO<sub>2</sub>). We have reworded this statement to avoid speculation:

**The impact of dry deposition parameterization choice ~~may be generalizable to other trace gases~~ may also have impacts which we have not explored in this study on other trace gases....**

608: what is the difference between a model-observation integration and an empirical study?

Response: We have reworded this sentence to avoid confusion:

**~~This makes a strong case for additional measurements (e.g. Kammer et al., 2019; Li et al., 2018; Stella et al., 2011a), empirical studies (e.g. Ducker et al., 609 2018) and model-observation integrations (e.g. Silva et al., 2019) of ozone dry deposition at different timescales, which would 610 be greatly facilitated by an open data sharing infrastructure (e.g. Baldocchi et al., 2001; Junninen et al., 2009).~~ This makes a strong case for additional measurement and model studies of ozone dry deposition across different timescales, which would be greatly facilitated by an open data sharing infrastructure (e.g. Baldocchi et al., 2001; Junninen et al., 2009).**



We thank the referee for their positive and constructive comments on our manuscript. We provide our response to each individual reviewer comment (shown in italics) below, including detailed changes to the manuscript (additions in red).

*My only general criticism is that the figures need to be presented in a larger form that will be easier for readers to see.*

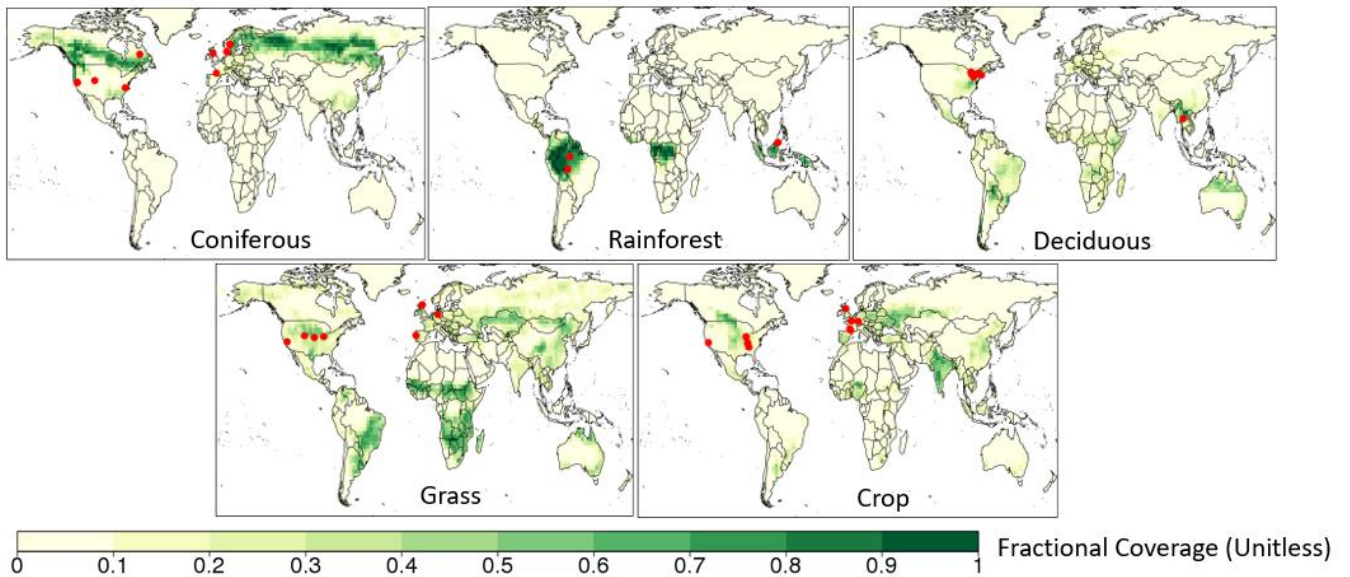
Response: We acknowledge that some of the figures are difficult to see, and our manuscript would benefit from addressing this. We have made improvements to Figure 1, 8, and 9 (see below) that we hope will help with readability.

*Line 660 – 661: The blue dots are very difficult to see on these figures. The figures should be made larger!*

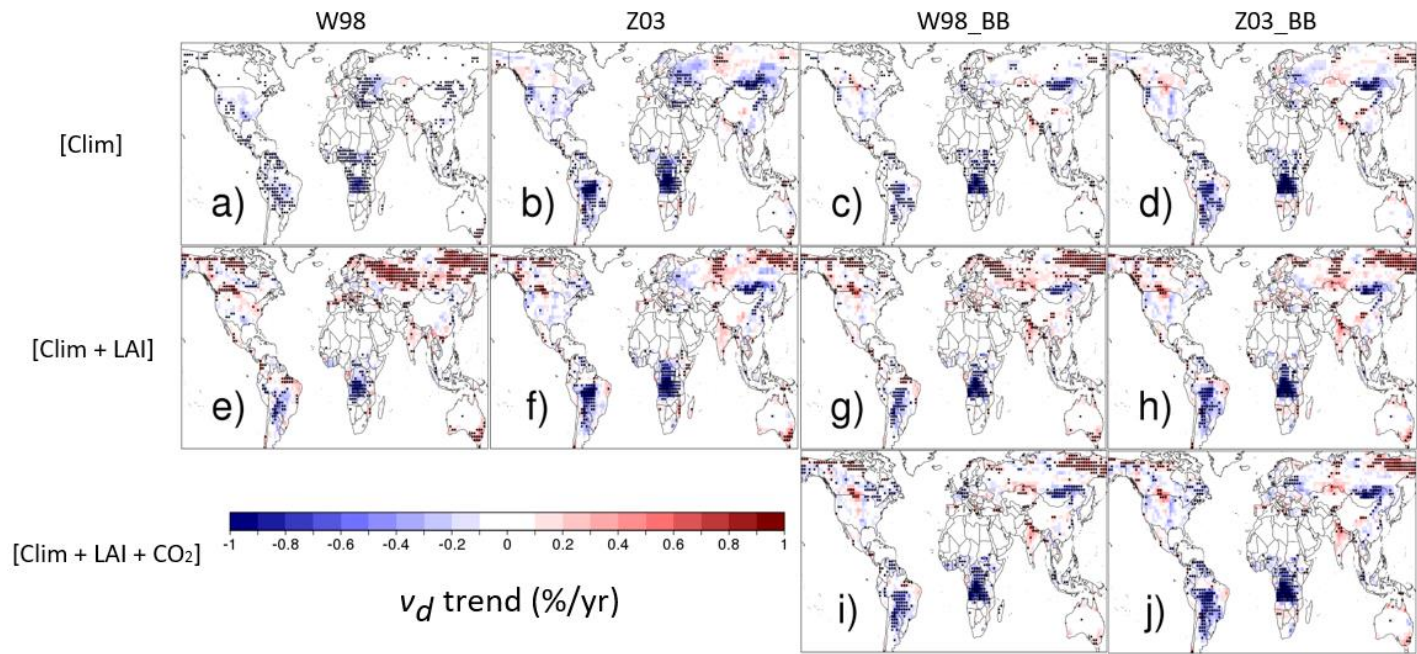
Figure 1 has been changed to show larger red dots that make them easier to see.

Furthermore, Figure 8 and Figure 9 have been adjusted to remove white space to allow for larger panels, and zooms into the Earth's land surface by removing areas around the edges where results were minor.

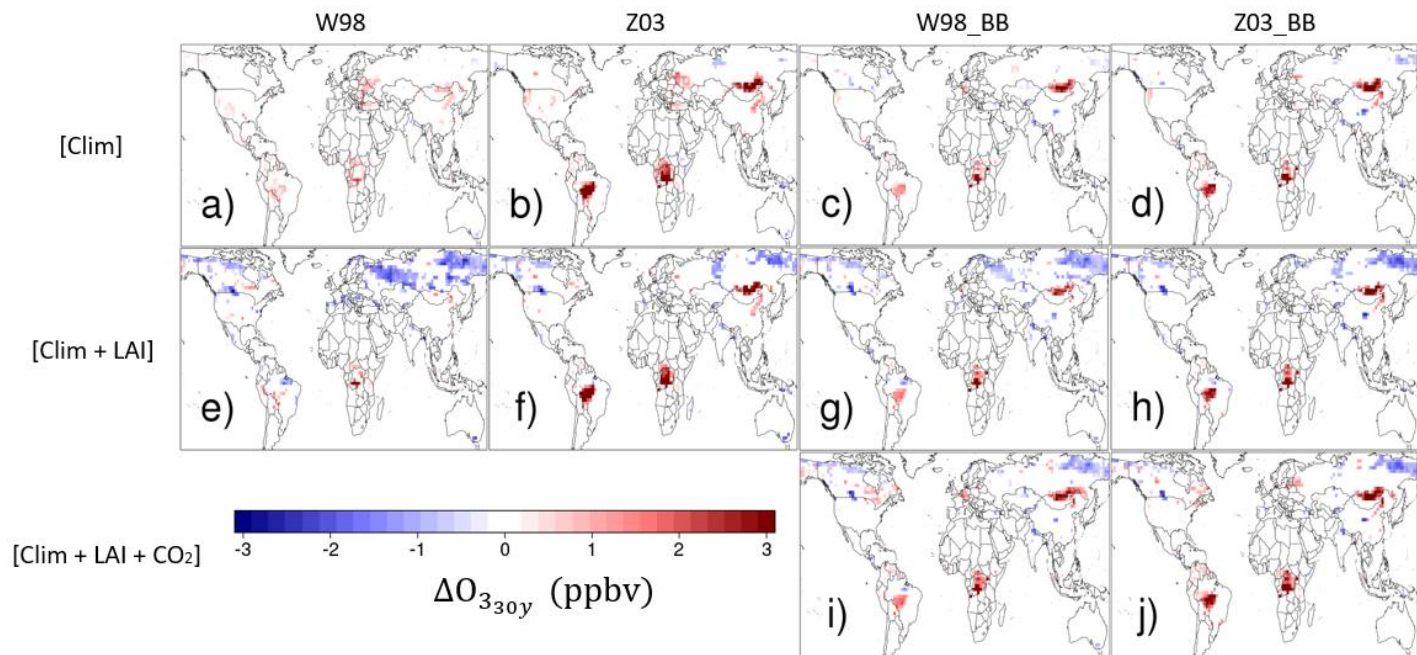
New figure 1:



New figure 8:



New figure 9:



Specific comments:

*p. 1, line 27: Should be “The trend in July ...”, not “trends”.*

Response: We have made this correction.

*p. 2, line 62: Should be “... compiled ...”.*

Response: We have made this correction.

*p. 2, line 63: Should be “measurements from the EC and GM ...”.*

Response: We have made this correction.

*p. 7, line 205: Should be “... simulation described in the next sub-section.”*

Response: We have made this correction.

*p. 7, line 211: Should be “... to investigate how ...”.*

Response: We have made this correction.

*p. 7, line 216: Should be “... the increase in atmospheric ...”.*

Response: We have made this correction.

*p. 8, line 233: Should be “... developed by NOAA’s National Centers for Environmental Prediction (NCEP) and the NASA Global ...”.*

Response: We changed the sentence to:

**...developed by National Centers for Environmental Prediction (NCEP) of National Oceanic and Atmospheric Administration (NOAA) and...**

*p. 13, line 409: Should be “... We use the Theil-Sen method ...”.*

Response: We have made this correction.

*p. 14, lines 430-431: I believe it should be “... a concomitant decrease in July mean surface ozone ...”.*

Response: We changed the sentence to:

**...a concomitant ~~increase~~ decrease in July mean surface ozone...**

*p. 15, line 461: Should be “... as they allow for ...”.*

Response: We have made this correction.

*p. 16, line 497: Should be “... This suggests that the IAV ...”.*

Response: We have made this correction.

*p. 17, line 527: Should be “... To better constrain regional dry ...”.*

Response: We have made this correction.

*p. 17, line 530: Should be “... would be greatly benefited if results of ozone flux measurements were reported as both ...”.*

Response: In response to comment from another referee, we have already the sentence to:

**~~We also find that many existing ozone flux measurements are not usable for our evaluation purposes, since only FO3 is reported in detail instead of vd.~~ Evaluation and development of ozone dry deposition parameterizations will continue to benefit from publicly available ozone flux measurements and related micrometeorological variables that allow for partitioning measured flux into individual deposition pathways (e.g. Clifton et al., 2017; 2019, Fares et al., 2010, Wu et al., 2018).**

*p. 17, line 538: Should be “... a vast majority of land in ...”.*

Response: We have made this correction.

*p. 18, line 558: Should be “... mainly concentrates in the drier part of ...”.*

Response: We have made this correction.

*p. 18, line 562: Should be “... deposition measurements poses ...”.*

Response: In response to comment from another referee, we have already changed line 562 to:

**~~The scarcity of long-term ozone deposition measurement poses significant difficulty in evaluating the model predictions over interannual (and in particular multidecadal) timescales.~~ While our results show notable impacts across the globe, in many regions there are no available long-term observation to evaluate the model predictions over interannual timescales.**

*p. 18, line 566: Should be "... The magnitudes of trends are ...".*

Response: We have made this correction.

*p. 19, line 597: I believe it should be something like ... "... contribute to understanding the role of gaseous dry deposition on air quality, but also to biogeochemical cycling."*

Response: We changed the sentence to:

**...contribute to understanding the role of gaseous dry deposition role on air quality, but also to biogeochemical eyele cycling...**

*p. 19, line 600: Should be "... global nitrogen cycles."*

Response: We have made this correction.

*p. 19, line 607: Should be "... scarcity of measurements."*

Response: In response to comment from another referee, we have already changed the sentence to:

**~~The scarcity of long-term ozone deposition measurement poses significant difficulty in evaluating the model predictions over interannual (and in particular multidecadal) timescales.~~ While our results show notable impacts across the globe, in many regions there are no available long-term observation to evaluate the model predictions over interannual timescales.**

# 1 Importance of Dry Deposition Parameterization Choice in Global 2 Simulations of Surface Ozone

3 Anthony Y.H. Wong<sup>1</sup>, Jeffrey A. Geddes<sup>1</sup>, Amos P.K. Tai<sup>2,3</sup>, Sam J. Silva<sup>4</sup>

4 <sup>1</sup>Department of Earth and Environment, Boston University, Boston, MA, USA

5 <sup>2</sup>Earth System Science Programme, Faculty of Science, The Chinese University of Hong Kong, Hong Kong

6 <sup>3</sup>Institute of Energy, Environment and Sustainability, and State Key Laboratory of Agrobiotechnology, The Chinese University  
7 of Hong Kong, Hong Kong

8 <sup>4</sup>Department of Civil and Environmental Engineering, Massachusetts Institute of Technology, Cambridge, MA, USA

9 *Correspondence to:* Jeffrey A. Geddes (jgeddes@bu.edu)

10 **Abstract.** Dry deposition is ~~the second largest~~ major sink of tropospheric ozone. Increasing evidence has shown that ozone  
11 dry deposition actively links meteorology and hydrology with ozone air quality. However, there is little systematic  
12 investigation on the performance of different ozone dry deposition parameterizations at the global scale, and how  
13 parameterization choice can impact surface ozone simulations. Here we present the results of the first global, multi-decade  
14 modelling and evaluation of ozone dry deposition velocity ( $v_d$ ) using multiple ozone dry deposition parameterizations. We use  
15 consistent assimilated meteorology and satellite-derived leaf area index (LAI) to drive four ozone dry deposition  
16 parameterizations simulate  $v_d$  over 1982-2011 driven by four sets of ozone dry deposition parameterization that are  
17 representative of the current approaches of global ozone dry deposition modelling over 1982-2011, such that the differences  
18 in simulated  $v_d$  are entirely due to differences in deposition model structures. In addition, we use the surface ozone sensitivity  
19 to  $v_d$  predicted by a chemical transport model to estimate the impact of mean and variability of ozone dry deposition velocity  
20 on surface ozone. Our estimated  $v_d$  from four different parameterizations are evaluated against field observations, and while  
21 performance varies considerably by land cover types, our results suggest that none of the parameterizations are universally  
22 better than the others. Discrepancy in simulated mean  $v_d$  among the parameterizations is estimated to cause 2 to 5 ppbv of  
23 discrepancy in surface ozone in the Northern Hemisphere (NH) and up to 8 ppbv in tropical rainforest in July, and up to 8 ppbv  
24 in tropical rainforests and seasonally dry tropical forests in Indochina in December. Parameterization-specific biases based on  
25 individual land cover type and hydroclimate are found to be the two main drivers of such discrepancies. We find statistically  
26 significant trends in the multiannual time series of simulated July daytime  $v_d$  in all parameterizations, driven by warming and  
27 drying (southern Amazonia, southern African savannah and Mongolia) or greening (high latitudes). The ~~trends-trend~~ in July  
28 daytime  $v_d$  is estimated to be 1 % yr<sup>-1</sup> and leads to up to 3 ppbv of surface ozone changes over 1982-2011. The interannual  
29 coefficient of variation (CV) of July daytime mean  $v_d$  in NH is found to be 5%-15%, with spatial distribution that varies with  
30 the dry deposition parameterization. Our sensitivity simulations suggest this can contribute between 0.5 to 2 ppbv to  
31 interannual variability (IAV) in surface ozone, but all models tend to underestimate interannual CV when compared to long-  
32 term ozone flux observations. We also find that IAV in some dry deposition parameterizations are more sensitive to LAI while

33 others are more sensitive to climate. Comparisons with other published estimates of the IAV of background ozone confirm  
34 that ozone dry deposition can be an important part of natural surface ozone variability. Our results demonstrate the importance  
35 of ozone dry deposition parameterization choice on surface ozone modelling, and the impact of IAV of  $v_d$  on surface ozone,  
36 thus making a strong case for further measurement, evaluation and model-data integration of ozone dry deposition on different  
37 spatiotemporal scales.

## 38 **1 Introduction**

39 Surface ozone ( $O_3$ ) is one of the major air pollutants that poses serious threats to human health (Jerrett et al., 2009) and plant  
40 productivity (Ainsworth et al., 2012; Reich, 1987; Wittig et al., 2007). Ozone exerts additional pressure on global food security  
41 and public health by damaging agricultural ecosystems and reducing crop yields (Avnery et al., 2011; McGrath et al., 2015;  
42 Tai et al., 2014). Dry deposition, by which atmospheric constituents are removed from the atmosphere and transferred to the  
43 Earth's surface through turbulent transport or gravitational settling, is the second-largest and terminal sink of tropospheric  $O_3$   
44 (Wild, 2007). Terrestrial ecosystems are particularly efficient at removing  $O_3$  via dry deposition through stomatal uptake and  
45 other non-stomatal pathways (Wesely and Hicks, 2000) (e.g., cuticle, soil, reaction with biogenic volatile organic compounds  
46 (BVOCs) (Fares et al., 2010; Wolfe et al., 2011). Meanwhile, stomatal uptake of  $O_3$  inflicts damage on plants by initiating  
47 reactions that impair their photosynthetic and stomatal regulatory capacity (Hoshika et al., 2014; Lombardozzi et al., 2012;  
48 Reich, 1987). Widespread plant damage has the potential to alter the global water cycle (Lombardozzi et al., 2015) and suppress  
49 the land carbon sink (Sitch et al., 2007), as well as to generate a cascade of feedbacks that affect atmospheric composition  
50 including ozone itself (Sadiq et al., 2017; Zhou et al., 2018). Ozone dry deposition is therefore key in understanding how  
51 meteorology (Kavassalis and Murphy, 2017), climate, and land cover change (Fu and Tai, 2015; Ganzeveld et al., 2010; Geddes  
52 et al., 2016; Heald and Geddes, 2016; Sadiq et al., 2017; Sanderson et al., 2007; Young et al., 2013) can affect air quality and  
53 atmospheric chemistry at large.

54

55 Analogous to other surface-atmosphere exchange processes (e.g., sensible and latent heat flux),  $O_3$  dry deposition flux ( $F_{O_3}$ )  
56 is often expressed as the product of ambient  $O_3$  concentrations at the surface ( $[O_3]$ ) and a transfer coefficient (dry deposition  
57 velocity,  $v_d$ ) that describes the efficiency of transport (and removal) to the surface from the measurement height:

58

$$F_{O_3} = [O_3]v_d \quad (1)$$

59 Also analogous to other surface fluxes,  $F_{O_3}$ ,  $[O_3]$ , and hence  $v_d$  can be directly measured by the eddy covariance (EC) method  
60 (e.g. Fares et al., 2014; Gerosa et al., 2005; Lamaud et al., 2002; Munger et al., 1996; Rannik et al., 2012) with random  
61 uncertainty of about 20% (Keronen et al., 2003; Muller et al., 2010). Apart from EC,  $F_{O_3}$  and  $v_d$  can also be estimated from  
62 the vertical profile of  $O_3$  by exploiting flux-gradient relationship (Foken, 2006) (termed the gradient method, GM) (e.g. Gerosa  
63 et al., 2017; Wu et al., 2016, 2015). A recent [review-study](#) (Silva and Heald, 2018) ~~has~~ compiled 75 sets of ozone deposition  
64 measurement from the EC and GM ~~methods~~ across different seasons and land cover types over the past 30 years.

65

66 At the site level, ozone dry deposition over various terrestrial ecosystems can be simulated comprehensively by 1-D chemical  
67 transport models (Ashworth et al., 2015; Wolfe et al., 2011; Zhou et al., 2017), which are able to ~~account for~~ simulate the  
68 effects of vertical gradients inside the canopy environment, and gas-phase reaction with BVOCs in addition to surface sinks.  
69 Regional and global models, which lack the fine-scale information (e.g. vertical structure of canopy, in-canopy BVOCs  
70 emissions) and horizontal resolution for resolving the plant canopy in such detail, instead represent plant canopy foliage as 1  
71 to 2 big leaves, and rely on parameterizing  $v_d$  is parameterized as a network of resistances, which account for the effects of  
72 turbulent mixing via aerodynamic ( $R_a$ ), molecular diffusion via quasi-laminar sublayer resistances ( $R_b$ ), and surface sinks via  
73 surface resistance ( $R_c$ ):

74

$$v_d = \frac{1}{R_a + R_b + R_c} \quad (2)$$

75

76 A diverse set of parameterizations of ozone dry deposition are available and used in different models and monitoring networks.  
77 Examples include the Wesely parameterization (1989) and modified versions of it (e.g. Wang et al., 1998), the Zhang et al.  
78 parameterization (Zhang et al., 2003), the Deposition of O<sub>3</sub> for Stomatal Exchange model (Emberson et al., 2000; Simpson et  
79 al., 2012), and the Clean Air Status and Trends Network (CASTNET) deposition estimates (Meyers et al., 1998). The  
80 calculation of  $R_a$  (mostly based on Monin-Obukhov similarity theory) and  $R_b$  across these parameterizations often follow a  
81 standard formulation from micrometeorology (Foken, 2006; Wesely and Hicks, 1977, 2000; Wu et al., 2011) and thus does  
82 not vary significantly. The main difference between the ozone dry deposition parameterizations lies on the surface resistance  
83  $R_c$ . This resistance includes stomatal resistance ( $R_s$ ), which can be computed by a Jarvis-type multiplicative algorithm (Jarvis,  
84 1976) where  $R_s$  is the product of its minimum value and a series of response functions to individual environmental conditions.  
85 Such conditions typically include air temperature ( $T$ ), photosynthetically available radiation ( $PAR$ ), vapour pressure deficit  
86 ( $VPD$ ) and soil moisture ( $\theta$ ), with varying complexity and functional forms.

87

88 Such formalism is empirical in nature and does not adequately represent the underlying ecophysiological processes affect  $R_s$   
89 (e.g. temperature acclimation). An advance of these efforts includes harmonizing  $R_s$  with that computed by land surface models  
90 (Ran et al., 2017a; Val Martin et al., 2014), which calculate  $R_s$  by coupled photosynthesis-stomatal conductance ( $A_n-g_s$ ) models  
91 (Ball et al., 1987; Collatz et al., 1992, 1991). Such coupling should theoretically give a more realistic account of  
92 ecophysiological controls on  $R_s$ . Indeed, it has been shown that the above approach may better simulate  $v_d$  than the  
93 multiplicative algorithms that only considers the effects  $T$  and  $PAR$  (Val Martin et al., 2014; Wu et al., 2011). The non-stomatal  
94 part of  $R_c$  often consists of cuticular ( $R_{cut}$ ), ground ( $R_g$ ) and other miscellaneous types of resistances (e.g., lower canopy  
95 resistance ( $R_{lc}$ ) in Wesely (1989)). Due to very limited measurements and mechanistic understanding towards non-stomatal  
96 deposition, non-stomatal resistances are often constants (e.g.,  $R_g$ ) or simply scaled with leaf area index (LAI) (e.g.,  $R_{cut}$ )  
97 (Simpson et al., 2012; Wang et al., 1998; Wesely, 1989), while some of the parameterizations (Zhang et al., 2003; Zhou et al.,



98 2017) incorporate the observation of enhanced cuticular O<sub>3</sub> uptake under leaf surface wetness (Altimir et al., 2006; Potier et  
99 al., 2015, 2017; Sun et al., 2016). Furthermore, terrestrial atmosphere-biosphere exchange is also directly affected by CO<sub>2</sub>, as  
100 CO<sub>2</sub> can drive increases in LAI (Zhu et al., 2016) while inhibiting g<sub>s</sub> (Ainsworth and Rogers, 2007). These can have important  
101 implications on v<sub>d</sub>, as shown by Sanderson et al. (2007), where doubling current CO<sub>2</sub> level reduces g<sub>s</sub> by 0.5 – 2.0 mm s<sup>-1</sup>, and  
102 by Wu et al. (2012) where v<sub>d</sub> increases substantially due to CO<sub>2</sub> fertilization at 2100. Observations from the Free Air CO<sub>2</sub>  
103 Enrichment (FACE) experiments also CO<sub>2</sub> fertilization and inhibition of g<sub>s</sub> effects, but the impacts are variable and species  
104 specific such that extrapolation of these effects to global forest cover is cautioned (Norby and Zak, 2011).  
105  
106

107 Various efforts have been made to evaluate and assess the uncertainty in modelling ozone dry deposition using field  
108 measurements. Hardacre et al. (2015) evaluate the performance of simulated monthly mean v<sub>d</sub> and F<sub>O<sub>3</sub></sub> by 15 chemical transport  
109 models (CTM) from the Task Force on Hemispheric Transport of Air Pollutant (TF HTAP) against seven long-term site  
110 measurements, 15 short-term site measurements, and modelled v<sub>d</sub> from 96 CASTNET sites. This work ~~found that the seasonal~~  
111 ~~cycle is well-simulated across models, while suggests demonstrating~~ that the difference in land cover classification is the main  
112 source of discrepancy between models. In this case, most of the models in TF HTAP use the same class of dry deposition  
113 parameterization (Wang et al., 1998; Wesely, 1989), so a global evaluation of *different* deposition parameterizations was not  
114 possible. Also, the focus in this intercomparison study was on seasonal, but not other (e.g. diurnal, daily, interannual)  
115 timescales. Using an extended set of measurements, Silva and Heald (2018) evaluate the v<sub>d</sub> output from the Wang et al. (1998)  
116 parameterization used by the GEOS-Chem chemical transport model. They show that diurnal and seasonal cycles are generally  
117 well-captured, while the daily variability is not well-simulated. They find that differences in land type and LAI, rather than  
118 meteorology, are the main reason behind model-observation discrepancy at the seasonal scale, and eliminating this model bias  
119 results in up to 15% change in surface O<sub>3</sub>. This study is also limited to a single parameterization. Using parameterizations that  
120 are explicitly sensitive to other environmental variables (e.g. Simpson et al., 2012; Zhang et al., 2003) could conceivably lead  
121 to different conclusions.  
122

123 Other efforts have been made to compare the performance of different parameterizations. Centoni (2017) find that two different  
124 dry deposition parameterizations, Wesely (1989) versus Zhang et al. (2003), implemented in the same chemistry-aerosol model  
125 (United Kingdom Chemistry Aerosol model, UKMA), result in up to a 20% difference in simulated surface O<sub>3</sub> concentration.  
126 This study demonstrates that uncertainty in v<sub>d</sub> can have large potential effect on surface O<sub>3</sub> simulation. Wu et al. (2018)  
127 compare v<sub>d</sub> simulated by five North-American dry deposition parameterizations to a long-term observational record at a single  
128 mixed forest in southern Canada, and find a large spread between the simulated v<sub>d</sub>, with no single parameterization uniformly  
129 outperforming others. They further acknowledge that as each parameterization is developed with its own set of limited  
130 observations, it is natural that their performance can vary considerably under different environments, and advocate for an  
131 “ensemble” approach to dry deposition modelling. This highlights the importance of parameterization choice as a key source

132 of uncertainty in modelling ozone dry deposition. Meanwhile, in another evaluation at a single site, Clifton et al. (2017) show  
133 that the GEOS-Chem parameterization largely underestimates the interannual variability (IAV) of  $v_d$  in Harvard Forest based  
134 on the measurement from 1990 to 2000, although they ~~were unable to conclude~~ do not show how the IAV of  $v_d$  may contribute  
135 to the IAV of  $O_3$ .

136

137 These developments have made a substantial contribution to our understanding of the importance of  $O_3$  dry deposition in  
138 atmospheric chemistry models. Still, pertinent questions remain about the impact of dry deposition model ~~physics~~—on  
139 simulations of the global distribution of ozone and its long-term variability. Here, we build on previous works by posing and  
140 answering the following questions:

- 141 1) How does the global distribution of mean  $v_d$  vary with different dry deposition parameterizations, and what drives the  
142 discrepancies among them? How much might the choice of deposition parameterization affect spatial distribution of  
143 surface ozone concentration simulated by a chemical transport model?
- 144 2) How are the IAV and long-term trends of  $v_d$  different across deposition parameterizations, and what drives the  
145 discrepancies among them? Do they potentially contribute different predictions of the long-term temporal variability  
146 in surface ozone?

147 The answers to such question could have important consequences on our ability to predict long-term changes in atmospheric  
148  $O_3$  concentrations as a function of changing climate and land cover characteristics. In general, there is a high computational  
149 cost to thorough and large-scale evaluations of different dry deposition parameterizations embedded in CTMs. In this study,  
150 we explore these questions using a strategy that combines an offline dry deposition modelling framework incorporating long-  
151 term assimilated meteorological and land surface remote sensing data, in combination with a set of CTM sensitivity  
152 simulations.

## 153 **2 Method**

### 154 **2.1 Dry deposition parameterization**

155 ~~A detailed description of the common dry deposition parameterizations we explore can be found in Wu et al. (2018).~~ Here we  
156 consider several “big-leaf” models commonly used by global chemical transport models. More complex multilayer models  
157 require the vertical profiles of leaf area density for different biomes which are generally not available for regional and global  
158 models. From the wide range of literature on dry deposition studies, we observe that  $R_s$  is commonly modelled through one of  
159 the following approaches:

- 160 1) Multiplicative algorithm that considers the effects of LAI, temperature and radiation (Wang et al., 1998).
- 161 2) Multiplicative algorithm that considers the effects of LAI, temperature, radiation and water stress (e.g. Meyers et al.,  
162 1998; Pleim and Ran, 2011; Simpson et al., 2012; Zhang et al., 2003).

163 3) Coupled  $A_n$ - $g_s$  model, which exploit the strong empirical relationship between photosynthesis ( $A_n$ ) and stomatal  
164 conductance ( $g_s$ ) (e.g. Ball et al., 1987; Lin et al., 2015) and to simulate  $A_n$  and  $g_s = 1/R_s$  simultaneously (e.g. Ran et  
165 al., 2017b; Val Martin et al., 2014).

166 Similarly, their functional dependence of non-stomatal surface resistances can be classified into two classes:

- 167 1) Mainly scaling with LAI, with in-canopy aerodynamics parameterized as function of friction velocity ( $u_*$ ) or radiation  
168 (Meyers et al., 1998; Simpson et al., 2012; Wang et al., 1998)
- 169 2) Additional dependence of cuticular resistance on relative humidity (Pleim and Ran, 2011; Zhang et al., 2003)

170

171 With these considerations, we identify four common parameterizations that are representative of the types of approaches  
172 described above:

173 1) The version of Wesely (1989) with the modification from Wang et al. (1998) (hereafter referred to as W98), which is  
174 used extensively in global CTMs (Hardacre et al., 2015) and comprehensively discussed by Silva and Heald (2018).  
175 This represents Type 1 in both stomatal and non-stomatal parametrizations.

176 2) The Zhang et al. (2003) parameterization (hereafter referred to as Z03), which is used in many North American air  
177 quality modelling studies (e.g. Huang et al., 2016; Kharol et al., 2018) and Canadian Air and Precipitation Monitoring  
178 Network (CAPMoN) (e.g. Zhang et al., 2009). This represents Type 2 in both stomatal and non-stomatal  
179 parameterizations

180 3) W89 with  $R_s$  calculated from a widely-used coupled  $A_n$ - $g_s$  model, the Ball-Berry model (hereafter referred to as  
181 W98\_BB) (Ball et al., 1987; Collatz et al., 1992, 1991), which is similar to that proposed by Val Martin et al. (2014),  
182 and therefore the current parameterization in Community Earth System Model (CESM). This represents Type 3 in  
183 stomatal and Type 1 in non-stomatal parametrization.

184 4) Z03 with the Ball-Berry model (Z03\_BB), which is comparable to the configuration in Centoni (2017) implemented  
185 in United Kingdom Chemistry and Aerosol (UKCA) model. This represents Type 3 in stomatal and Type 2 in non-  
186 stomatal parametrization.

187

188 Another important consideration in choosing Z03 and W98 is that they both have ~~open-source~~ parameters for all major land  
189 types over the globe, making them widely applicable in global modelling. We extract the source code (Wang et al., 1998) and  
190 parameters (Baldocchi et al., 1987; Jacob et al., 1992; Jacob and Wofsy, 1990; Wesely, 1989) of W98 from GEOS-Chem CTM  
191 ([http://wiki.seas.harvard.edu/geos-chem/index.php/Dry\\_deposition](http://wiki.seas.harvard.edu/geos-chem/index.php/Dry_deposition)). The source code of Z03 are obtained through personal  
192 communication with Zhiyong Wu and Leiming Zhang, which follows the series of papers that described the development and  
193 formalism of the parameterization (Brook et al., 1999; Zhang et al., 2001, 2002, 2003). The Ball-Berry  $A_n$ - $g_s$  model (Ball et  
194 al., 1987; Collatz et al., 1992, 1991; Farquhar et al., 1980) and its solver are largely based on the algorithm of CLM  
195 (Community Land Model) version 4.5 (Oleson et al., 2013), which is numerically stable (Sun et al., 2012). ~~Since  $R_c$  typically~~  
196 ~~dominates the deposition velocity of  $O_3$  (Fares et al., 2010; Wu et al., 2018), we We~~ use identical formulae of  $R_a$  and  $R_b$

197 (Paulson, 1970; Wesely and Hicks, 1977) for each individual parameterizations, allowing us to focus our analysis on  
198 differences in parameterizations of  $R_c$  alone. Table [A1-S1](#) gives a brief description on the formalism of each of the dry  
199 deposition parameterizations.

## 200 **2.2 Dry deposition model configuration, inputs, and simulation**

201 The above parameterizations are re-implemented in R language (R core team, 2017) in the modeling framework of the  
202 Terrestrial Ecosystem Model in R (<http://www.cuhk.edu.hk/sci/essc/tgabi/tools.html>), and driven by gridded surface  
203 meteorology and land surface data sets. The meteorological forcing chosen for this study is the Modern-Era Retrospective  
204 Analysis for Research and Application-2 (MERRA-2) (Gelaro et al., 2017), an assimilated meteorological product at hourly  
205 time resolution spanning from 1980 to present day. MERRA-2 contains all the required surface meteorological fields except  
206  $VPD$  and  $RH$ , which can be readily computed from  $T$ , specific humidity ( $q$ ) and surface air pressure ( $P$ ). We use the CLM land  
207 surface dataset (Lawrence and Chase, 2007), which contains information for land cover, per-grid cell coverage of each plant  
208 functional type (PFT), and PFT-specific LAI, which are required to drive the dry deposition parameterizations, and soil  
209 property, which is required to drive the  $A_n-g_s$  model in addition to PFT and PFT-specific LAI. CLM land types are mapped to  
210 the land type of W98 following Geddes et al. (2016). The mapping between CLM and Z03 land types are given in Table [A2S2](#).  
211 Other relevant vegetation and soil parameters (~~e.g. leaf physiological and soil hydraulic constants~~) are also imported from  
212 CLM 4.5 (Oleson et al., 2013), while land cover specific roughness length ( $z_{0r}$ ) values follow Geddes et al. (2016). Leaf is set  
213 to be wet when either latent heat flux  $< 0 \text{ W m}^{-2}$  or precipitation  $> 0.2 \text{ mm hr}^{-1}$ . Fractional coverage of snow for Z03 is  
214 parameterized as a land-type specific function of snow depth following the original manuscript of Z03, while W98 flags grid  
215 cells with albedo  $> 0.4$  or permanently glaciated as snow-covered.

216

217

218 As the IAV of LAI could be an important factor in simulating  $v_d$ , the widely-used third generation Global Inventory Modelling  
219 and Mapping Studies Leaf Area Index product (GIMMS LAI3g, abbreviated as LAI3g in this paper) (Zhu et al., 2013), which  
220 is a global time series of LAI with 15-day temporal frequency and 1/12 degree spatial resolution spanning from late 1981 to  
221 2011, is incorporated in this study. We ~~use this data set to~~ derive the interannual scaling factors that can be applied to scale the  
222 baseline CLM-derived LAI (Lawrence and Chase, 2007) for each month over 1982 to 2011. All the input data are aggregated  
223 into horizontal resolution of  $2^\circ \times 2.5^\circ$  to align with the CTM sensitivity simulation described in the next sub-section. To  
224 represent sub-grid land cover heterogeneity, grid cell-level  $v_d$  is calculated as the sum of  $v_d$  over all sub-grid land types weighted  
225 by their percentage coverage in the grid cell (a.k.a tiling or mosaic approach, e.g. Li et al., 2013). This reduces the information  
226 loss when land surface data is aggregated to coarser spatial resolution, and allows us to retain PFT-specific results for each  
227 grid box in the offline dry deposition simulations.

228

229 We run three sets of 30-years (1982-2011) simulations with the deposition parameterizations to investigate ~~the~~ how  $v_d$   
230 simulated by different parameterizations responds to different environmental factors over multiple decades. The settings of the  
231 simulations are summarized in Table 1. The first set, [Clim], focuses on meteorological variability alone, driven by MERRA-  
232 2 meteorology and a multiyear (constant) mean annual cycle of LAI derived from LAI3g. The second set, [Clim+LAI],  
233 combines the effects of meteorology and IAV in LAI, driven by the same MERRA-2 meteorology plus the LAI time series  
234 from LAI3g. As the increase in atmospheric CO<sub>2</sub> level over multidecadal timescales may lead to significant reduction in  $g_s$  as  
235 plants tend to conserve water (e.g. Franks et al., 2013; Rigden and Salvucci, 2017), we introduce the third set of simulation,  
236 [Clim+LAI+CO<sub>2</sub>], which is driven by varying meteorology and LAI, plus the annual mean atmospheric CO<sub>2</sub> level measured  
237 in Mauna Loa (Keeling et al., 2001) (for the first two sets of simulations, atmospheric CO<sub>2</sub> concentration held constant at 390  
238 ppm). Since W98 and Z03 do not respond to changes in CO<sub>2</sub> level, only W98\_BB and Z03\_BB are run with [Clim+LAI+CO<sub>2</sub>]  
239 to evaluate this impact. We focus on the daytime (solar elevation angle > 20°)  $v_d$ , as both  $v_d$  and surface O<sub>3</sub> concentration  
240 typically peak around this time. We calculate monthly means, filtering out the grid cells with monthly total daytime < 100  
241 hours, which would be an indication of dormant biosphere.

242

243 In summary, we present for the first time a unique set of global dry deposition velocity predictions over the last 30 years driven  
244 by identical meteorology and land cover, so that discrepancies (in space and time) among the predicted  $v_d$  are a result  
245 specifically of dry deposition parameterizations alone.

### 246 2.3 Chemical transport model sensitivity experiments

247 We quantify the sensitivity of surface O<sub>3</sub> to variations in  $v_d$  using a global 3D CTM, GEOS-Chem version 11.01 ([www.geos-](http://www.geos-chem.org)  
248 [chem.org](http://www.geos-chem.org)) (Bey et al., 2001), which includes comprehensive HO<sub>x</sub>-NO<sub>x</sub>-VOC-O<sub>3</sub>-BrO<sub>x</sub> chemical mechanisms (Mao et al., 2013)  
249 and is widely used to study tropospheric ozone (e.g. Hu et al., 2017; Travis et al., 2016; Zhang et al., 2010). The model is  
250 driven by the assimilated meteorological data from the GEOS-FP (Forward Processing) Atmospheric Data Assimilation  
251 System (GEOS-5 ADAS) (Rienecker et al., 2008), which is jointly developed by National Centers for Environmental  
252 Prediction (NCEP) of National Oceanic and Atmospheric Administration (NOAA) and the Global Modelling and Assimilation  
253 Office (GMAO). The model is run with a horizontal resolution of 2°×2.5°, and 47 vertical layers. The dry deposition module,  
254 which has been discussed above (W98), is driven by the monthly mean LAI retrieved from Moderate Resolution Imaging  
255 Spectroradiometer (MODIS) (Myneni et al., 2002) and the 2001 version of Olson land cover map (Olson et al., 2001). Both of  
256 the maps are binned-remapped from their native resolutions to 0.25°×0.25°.

257

258 We propose to estimate the sensitivity of surface O<sub>3</sub> concentrations to uncertainty/changes in  $v_d$  by the following equation:

259

$$\Delta O_3 = \beta \frac{\Delta v_d}{v_d}$$

260 where  $\Delta O_3$  is the response of monthly mean daytime surface  $O_3$  to fractional change in  $v_d$  ( $\Delta v_d/v_d$ ), and  $\beta$  accounts for the  
261 sensitivity of surface  $O_3$  concentration in a grid box to the perturbation in  $v_d$  within that grid box. To estimate  $\beta$ , we run two  
262 simulations for the year 2013, one with default setting and another where we perturb  $v_d$  by +30%. ~~Since not every gaseous~~  
263 ~~species deposit with the same functional relationships as  $O_3$ , we only adjust the  $v_d$  of  $O_3$  to avoid perturbing the chemistry~~  
264 ~~resulting from the deposition of other chemically relevant species (e.g. PAN,  $HNO_3$ ).~~ Thus, this approach could represent a  
265 conservative estimate of  $O_3$  sensitivity to  $v_d$  if the impacts on other species result in additional effects on  $O_3$ . ~~Nevertheless, we~~  
266 ~~use this sensitivity to estimate the potential impact of  $v_d$  simulation on surface  $O_3$  concentration to a first order in subsequent~~  
267 ~~sections. This approach is based on the reasonably linear response of surface  $O_3$  to  $v_d$  over comparable range of  $v_d$  change~~  
268 ~~(Wong et al., 2018). We use this sensitivity to identify areas where local uncertainty and variability in  $v_d$  is expected to affect~~  
269 ~~local surface  $O_3$  concentration, and we use the assumption of linearity to estimate those impacts to a first order (e.g. Wong et~~  
270 ~~al. 2018). In the Supplemental Methods, we justify this first order assumption mathematically, as well as demonstrate the~~  
271 ~~impact of using a second order approximation, and estimate the uncertainty using an assumption of linearity to be within 30%.~~  
272 ~~However, we note this first-order assumption may not be able to capture the effects of chemical transport, changes in~~  
273 ~~background ozone and non-linearity in chemistry, which can contribute to response of  $O_3$  concentration to  $v_d$ . Our experiment~~  
274 ~~could help identify regions where more rigorous modelling efforts could be targeted in future work.~~ We limit our analysis to  
275 grid cells where the monthly average  $v_d$  is greater than  $0.25 \text{ cm s}^{-1}$  in the baseline-unperturbed GEOS-Chem simulation, since  
276 changes in surface  $O_3$  elsewhere are expected to be attributed more to chemical transport change in background  $O_3$  rather than  
277 the local perturbation of  $v_d$  (Wong et al., 2018).

### 278 3. Evaluation of Dry Deposition Parameterizations

279 We first compare our offline simulations of seasonal mean daytime average  $v_d$  that result from the four parameterizations in  
280 the [Clim] and [Clim+LAI] scenarios with an observational database largely based on the evaluation presented in Silva and  
281 Heald (2018). ~~We do not include the evaluation of  $v_d$  from [Clim+LAI+ $CO_2$ ] scenario as we find that the impact of  $CO_2$~~   
282 ~~concentration on  $v_d$  is negligible over the period of concern, as we will show in subsequent sections.~~ We use two unbiased and  
283 symmetrical statistical metrics, normalized mean bias factor (*NMBF*) and normalized mean absolute error factor (*NMAEF*), to  
284 evaluate our parameterizations. Positive *NMBF* indicates that the parameterization overestimates the observations by a factor  
285 of  $1 + NMBF$  and the absolute gross error is *NMAEF* times the mean observation, while negative *NMBF* implies that the  
286 parameterization underestimates the observations by a factor of  $1 - NMBF$  and the absolute gross error is *NMAEF* times the  
287 mean model prediction (Yu et al., 2006). We use the simulated subgrid land type-specific predictions of  $v_d$  that correctly match  
288 the land type and the averaging window indicated by the observations. We exclude instances where the observed land type  
289 does not have a match within the model grid box. While this ~~removes 1/3 of the original data sets used in leads to a reduction~~  
290 ~~of dataset size comparing to~~ Silva and Heald (2018), this means that mismatched land-cover types can be ignored as a factor  
291 in model bias.

292

293 Figure 1 shows the fractional coverage within each grid cell and the geographic locations of O<sub>3</sub> flux observation sites for each  
294 major land type. Nearly all the observations are clustered in Europe and North America, except three sites in the tropical  
295 rainforest and one site in tropical deciduous forest in Thailand. ~~For most major land types, there are significant mismatches~~  
296 ~~between the locations of flux measurements and the dominant land cover fraction, which may hinder the spatial~~  
297 ~~representativeness of our evaluation.~~ The resulting *NMBF* and *NMAEF* for five major land type categories are shown in Table  
298 2, and the list of sites and their descriptions are given in Table [A3S3](#). In general, the numerical ranges of both *NMBF* and  
299 *NMAEF* are similar to that of Silva and Heald (2018), and no single parameterization of the four parameterizations outperforms  
300 the others across all five major land types. ~~Here, we focus on describing how our implementation of the dry deposition~~  
301 ~~parameterizations produce consistent comparisons with earlier results.~~

302

303 ~~As summarized in Table 2, each parameterization shows distinct biases over specific land types (we subsequently refer to~~  
304 ~~this as the “land-type specific bias” unique to each parameterization).~~ ~~The performance metrics of each parameterization at~~  
305 ~~each land type are summarized in table 2.~~ Comparing the two multiplicative parameterizations (W98 and Z03), we find that  
306 W98 performs satisfactorily over deciduous forests and tropical rainforests, while strongly underestimating daytime  $v_d$  over  
307 coniferous forests. In contrast, Z03 performs better in coniferous forests but worse in tropical rainforests and deciduous  
308 forests. The severe underestimation of daytime  $v_d$  by Z03 over tropical rainforests has previously been attributed to persistent  
309 canopy wetness, and hence stomatal blocking imposed by the parameterization (Centoni, 2017). ~~The simple linear VPD~~  
310 ~~response function in Z03 may overestimate the sensitivity of  $g_s$  to VPD under the high temperature in tropical rainforest.~~ We  
311 also note that even for the same location,  $v_d$  can vary significantly between seasons (Rummel et al., 2007) and management  
312 practices (Fowler et al., 2011), which models may fail to capture due to limited representations of land cover. Given the  
313 small sample size ( $N = 5$ ), diverse environments, and large anthropogenic intervention in the tropics, the disparity in  
314 performance metrics may not fully reflect the relative model performance. Baseline cuticular resistances in Z03 under dry  
315 and wet canopy are 1.5 and 2 times that of coniferous forests, respectively (Zhang et al., 2003), such that the enhancement of  
316 cuticular uptake by wetness may not compensate the reduced  $g_s$  over tropical rainforests, and, to a lesser extent, deciduous  
317 forests. ~~The higher cuticular uptake may explain the better performance of Z03 over W98 over coniferous forests, where~~  
318 ~~strong non-stomatal (though not necessarily cuticular) ozone sinks are often observed (e.g. Gerosa et al., 2005; Wolfe et al.,~~  
319 ~~2011).~~

320

321 Over grasslands, W98 has higher positive biases, while Z03 has higher absolute errors. This is because for datasets at high  
322 latitudes, the dominant grass PFT is arctic grass, which is mapped to “tundra” land type (Geddes et al., 2016). While tundra  
323 is parameterized similarly to grasslands in W98, this is not the case in Z03. Combined with the general high biases at other  
324 sites for these parameterizations, the large low biases for “tundra” sites in Z03 lower the overall high biases but leads to  
325 higher absolute errors.

326

327 Over croplands, the positive biases and absolute errors are relatively large for both W98 and Z03 (with Z03 performing worse  
328 in general than W98). ~~This may be attributed to the lack of response to VPD over all crop and grass land types in Z03.~~ The  
329 functional and physiological diversity with the “crop” land type also contributes to the general difficulty in simulating  $v_d$  over  
330 cropland. Even though Z03 has individual parameterizations for 4 specific crop types (rice, sugar, maize and cotton), this  
331 advantage is difficult to fully leverage as most global land cover data sets do not resolve croplands into such detail. Having  
332 land cover maps that distinguish between more crop types could potentially improve the performance of Z03. The evaluation  
333 for herbaceous land types also suggests that as CLM PFT do not have exact correspondence with W98 and Z03 land types, our  
334 results over herbaceous land types are subject to the uncertainty in land type mapping (e.g. tundra vs grassland, specific vs  
335 generic crops, C3 vs C4 grass).

336

337

338 Substituting the native  $g_s$  in W98 and Z03 by that simulated by Ball-Berry model (the W98\_BB and Z03\_BB runs) generally,  
339 though not universally, leads to improvement in model performance against the observations. W98\_BB has considerably  
340 smaller biases and absolute errors than W98 over grassland. While having little effect on the absolute error, W98\_BB improves  
341 the biases over coniferous forest and cropland compared to W98, but worsens the biases over rainforests and deciduous forests.  
342 In contrast, Z03\_BB is able to improve the model-observation agreement over all 5 land types when compared to Z03. This  
343 finding echoes that from Wu et al. (2011), who explicitly show the advantage of replacing the  $g_s$  of Wesely (1989) with the  
344 Ball-Berry model in simulating  $v_d$  over a forest site, and in addition shows the potential of Ball-Berry model in improving  
345 spatial distribution of mean  $v_d$ . The different responses to substituting native  $g_s$  with that from Ball-Berry model highlight the  
346 significant differences in parameterizing non-stomatal uptake between W98 and Z03, which further suggests that the  
347 uncertainty in non-stomatal deposition should not be overlooked.

348

349 The minimal impact that results from using LAI that matches the time of observation is not unexpected, since the  
350 meteorological and land cover information from a  $2^\circ \times 2.5^\circ$  grid cell may not be representative of the typical footprint of a site  
351 measurement (on the order of  $10^{-3}$  to  $10^1$  km<sup>2</sup>, e.g. Chen et al., 2009, 2012). ~~This problem~~ The mismatch between model  
352 resolution and the footprint of site-level measurements has also been highlighted in previous evaluation efforts in global-  
353 scale CTMs (Hardacre et al., 2015; Silva and Heald, 2018). Furthermore, the sample sizes for all land types are small ( $N \leq$   
354 16) and the evaluation may be further compromised by inherent sampling biases.

355

356 In addition to the evaluation against field observation, we find good correlation ( $R^2 = 0.94$ ) between the annual mean  $v_d$  from  
357 GEOS-Chem at 2013 and the 30-year mean  $v_d$  of W98 run with static LAI, providing further evidence that our  
358 implementation of W98 is reliable. Overall, our evaluation shows that the quality of our offline simulation of dry deposition  
359 across the four parameterizations in this work is largely consistent with previous global modelling evaluation efforts.



#### 360 4. Impact of Dry Deposition Parameterization Choice on Long-Term Averages

361 Here we summarize the impact that the different dry deposition parameterizations may have on simulations of the spatial  
362 distribution of  $v_d$  and on the inferred surface  $O_3$  concentrations. We begin by comparing the simulated long-term mean  $v_d$   
363 across parameterizations, then use a chemical transport model sensitivity experiment to estimate the  $O_3$  impacts.

364

365 Figure 2 shows the 30-year July daytime average  $v_d$  simulated by W98 over vegetated surfaces (defined as the grid cells with  
366 >50% plant cover), and Figure 3 shows the difference between the W98 and the W98\_BB, Z03, Z03\_BB predictions  
367 respectively. We first focus on results from July because of the coincidence of high surface  $O_3$  level, biospheric activity and  
368  $v_d$  in the Northern Hemisphere (NH), and will subsequently discuss the result for December, when such condition holds for  
369 the Southern Hemisphere (SH). W89 simulates the highest July mean daytime  $v_d$  in Amazonia (1.2 to 1.4  $cm\ s^{-1}$ ), followed by  
370 other major tropical rainforests, and temperate forests in northeastern US. July mean daytime  $v_d$  in other temperate regions in  
371 North America and Eurasia typically range from 0.5 to 0.8  $cm\ s^{-1}$ , while in South American and African savannah, and most  
372 parts of China, daytime  $v_d$  is around 0.4 to 0.6  $cm\ s^{-1}$ . In India, Australia, western US, and polar tundra Mediterranean region,  
373 July mean daytime  $v_d$  is low (0.2-0.5  $cm\ s^{-1}$ ). ~~which could be due to either the high temperature or the sparsity of vegetation~~  
374 ~~(or a combination of both).~~

375

376 The other three parameterizations (W98\_BB, Z03, Z03\_BB) simulate substantially different spatial distributions of daytime  
377  $v_d$ . In North America, we find W98\_BB, Z03 and Z03\_BB produce lower  $v_d$  (by -0.1 to -0.4  $cm\ s^{-1}$ ) compared to W98 in  
378 deciduous forest-dominated northeastern US and slightly higher  $v_d$  in boreal forest-dominated regions of Canada. Z03 and  
379 Z03\_BB produce noticeably lower  $v_d$  (by up to -0.2  $cm\ s^{-1}$ ) in arctic tundra and grasslands in western US. In southeastern US,  
380 W98\_BB and Z03\_BB simulate a slightly higher  $v_d$  (by up to +0.1  $cm\ s^{-1}$ ), while Z03 suggests a slightly lower  $v_d$  (by up to -  
381 0.1  $cm\ s^{-1}$ ). W98\_BB simulates a lower (-0.1 to -0.4  $cm\ s^{-1}$ )  $v_d$  in tropical rainforests, with larger reductions concentrated in  
382 southern Amazonia, where July is within the dry season, while the northern Amazonia is not (Malhi et al., 2008). Z03 and  
383 Z03\_BB simulate much smaller (-0.4 to -0.6  $cm\ s^{-1}$ )  $v_d$  in all tropical rainforests.

384

385 Over the midlatitudes in Eurasia, Australia and South America except Amazonia, W98\_BB, Z03 and Z03\_BB generally  
386 simulate a lower daytime  $v_d$  by up to 0.25  $cm\ s^{-1}$ , possibly due to the dominance of grasslands and deciduous forests, where  
387 W98 tends to be more high-biased than other parameterizations when compared to the observations of  $v_d$ . In southern African  
388 savannah, W98\_BB and Z03\_BB suggest a much lower daytime  $v_d$  (by -0.1 to -0.4  $cm\ s^{-1}$ ) because of explicit consideration of  
389 soil moisture limitation to  $A_n$  and  $g_s$ . ~~(demonstrated by the spatial overlap with soil moisture stress factors shown in Fig. S2).~~  
390 Z03\_BB simulates a particularly high daytime  $v_d$  over the high-latitude coniferous forests (+0.1 to +0.3  $cm\ s^{-1}$ ). W98\_BB and  
391 Z03\_BB produce higher daytime daytime  $v_d$  (up to +0.15  $cm\ s^{-1}$ ) in India and South China due to temperature acclimation  
392 (Kattge and Knorr, 2007), which allows more stomatal opening under the high temperature that would largely shut down the

393 stomatal deposition in W98 and Z03, as long as the soil does not ~~desiccate~~become too dry to support stomatal opening. This  
394 is guaranteed by the rainfall from summer monsoon in both regions. Low  $v_d$  is simulated by Z03 and Z03\_BB in the grasslands  
395 near Tibetan plateau because the grasslands are mainly mapped to tundra land type, which typically has low  $v_d$  as discussed in  
396 section 3.

397  
398 Our results suggest that the global distribution of simulated mean  $v_d$  depends substantially on the choice of dry deposition  
399 parameterization, driven primarily by the response to hydroclimate-related parameters such as soil moisture, VPD and leaf  
400 wetness, in addition to ~~and~~ land type-specific parameters, which could impact the spatial distribution of surface ozone predicted  
401 by chemical transport models. To estimate the impact on surface ozone of an individual parameterization “ $i$ ” compared to the  
402 W98 predictions (which we use as a baseline), we apply the following equation:

$$403 \quad \Delta O_{3,i} \approx \beta \frac{\Delta \overline{v_{d,i}}}{\overline{v_{d,W98}}} \quad (3)$$

404 where  $\Delta O_{3,i}$  is the estimated impact on simulated  $O_3$  concentrations in a grid box,  $\Delta \overline{v_{d,i}}$  is the difference between  
405 parameterization  $i$  and W98 simulated mean daytime  $v_d$  in that grid box,  $\overline{v_{d,W98}}$  is W98 output mean daytime  $v_d$  for that grid  
406 box, and  $\beta$  is the sensitivity of surface ozone to  $v_d$  calculated by the method outlined in Section 2.3

407  
408 Figure 4 shows the resulting estimates of  $\Delta O_3$  globally. We find  $\Delta O_3$  is the largest in tropical rainforests for all the  
409 parameterizations (up to 5 to 8 ppbv), ~~which agrees with the result from Centoni (2017)~~. Other hotspots of substantial  
410 differences are boreal coniferous forests, eastern US, continental Europe, Eurasian steppe and the grassland in southwestern  
411 China, where  $\Delta O_3$  is either relatively large or the signs disagree among parameterizations. In India, Indochina and South China,  
412  $\Delta O_3$  is relatively small but still reaches up to up to -2 ppbv. We find that  $\Delta O_3$  is not negligible (1-4 ppbv) in many regions with  
413 relatively high population density, which suggests that the choice of dry deposition parameterization can be relevant to the  
414 uncertainty in the study of air quality and its implication on public health. We note that we have not estimated  $\Delta O_3$  for some  
415 regions with low GEOS-Chem-predicted  $v_d$  ( $< 0.25 \text{ cm s}^{-1}$ , as described in section 2.3), but where the disagreement in  $v_d$   
416 between parameterizations can be large (e.g., southern African savannah, see Figure 3). Given this limitation, the impacts on  
417  $O_3$  we have summarized may therefore be spatially conservative.

418  
419 To explore the impact of different prediction of  $v_d$  on surface  $O_3$  in different seasons, importance of seasonality in predictions  
420 of  $v_d$  and their subsequent impact, we repeat the above analyses for December. Figure 5 shows the 1982-2011 mean December  
421 daytime  $v_d$  predicted by W98, while Figure 6 shows the difference between W98 and the Z03, W98\_BB, Z03\_BB respectively.  
422 High latitudes in the NH are excluded due to the small number of daytime hours. Z03 and Z03\_BB simulate substantially  
423 lower in daytime  $v_d$  at NH midlatitudes because Z03 and Z03\_BB allow partial snow cover but W98 and W98\_BB only allow  
424 total or no snow cover. At midlatitudes, the snow cover is not high enough to trigger the threshold of converting vegetated to  
425 snow covered ground in W98 and W98\_BB, resulting in lower surface resistance, and hence higher daytime  $v_d$  comparing to

426 Z03 and Z03\_BB. ~~In~~ in Amazonia, the hotspot of difference in daytime  $v_d$  shifts from the south to the north relative to July,  
427 which is in the dry season (Malhi et al., 2008). These results for December, together with our findings from July, suggest that  
428 the discrepancy in simulated daytime  $v_d$  between W98 and other parameterizations is due to the explicit response to  
429 hydroclimate in the former compared to the latter. Given that field observations indicate a large reduction of  $v_d$  in dry season  
430 in Amazonia (Rummel et al., 2007), the lack of dependence of hydroclimate can be a drawback of W98 in simulating  $v_d$  in  
431 Amazonia.

432

433 Figure 7 shows the resulting estimates of  $\Delta O_3$  globally for December using Equation 3. In all major rainforests,  $\Delta O_3$  is smaller  
434 in December due to generally lower sensitivity compared to July. A surprising hotspot of both daytime  $\Delta v_d$  and  $\Delta O_3$  is the  
435 rainforest/tropical deciduous forest in Myanmar and its eastern bordering region, which also has distinct wet and dry season.  
436 The proximity of December to the dry season, which starts at January (e.g. Matsuda et al., 2005), indicates that the consistent  
437  $\Delta v_d$  between W98 and other parameterizations is driven by hydroclimate as in Amazonia. Comparison with field measurements  
438 (Matsuda et al., 2005) suggests that the W98\_BB and Z03\_BB capture daytime  $v_d$  better than W98, while Z03 may  
439 overemphasize the effect of such dryness. The above reasoning also explains some of the  $\Delta v_d$  in India and south China across  
440 the three parameterizations. These findings identify hydroclimate as a key driver of process uncertainty of  $v_d$  over tropics and  
441 subtropics, and therefore its impact on the spatial distribution of surface ozone concentrations, independent of land type-based  
442 biases, in these regions.

443

444 Overall, these results demonstrate that the discrepancy in the spatial distribution of simulated mean daytime  $v_d$  resulting from  
445 choice of dry deposition parameterization can have an important impact on the global distribution of surface  $O_3$  predicted by  
446 chemical transport models. We find that the response to hydroclimate by individual parametrization not only affects the mean  
447 of predicted surface ozone, but also ~~the seasonality, of~~ has different impacts in different seasons ~~predicted surface~~  $O_3$ , which is  
448 complementary to the findings of Kavassalis and Murphy (2017) that mainly focus on how shorter-term hydrometeorological  
449 variability may modulate surface  $O_3$  through dry deposition.

450

## 451 **5. Impact of Dry Deposition Parameterization Choice on Trends and Interannual Variability**

452 Here we explore the impact that different dry deposition parameterizations may have on predictions of IAV and trends in  $v_d$   
453 and on the inferred surface  $O_3$  concentrations. We use the Theil-Sen method (Sen, 1968), which is less susceptible to outliers  
454 than least-square methods, to estimate trends in July daytime  $v_d$  (and any underlying meteorological variables), and use p-value  
455  $< 0.05$  to estimate significance.

456

457 Figure 8 shows the trend in July mean daytime  $v_d$  from 1982-2011 predicted by each of the parameterizations and scenarios  
458 ([Clim], [Clim + LAI], and [Clim + LAI + CO<sub>2</sub>]). Figure 9 shows the potential impact of these trends in  $v_d$  on July daytime  
459 surface ozone, which we estimate to a first order using the following equation:

460 
$$\Delta O_{3\ 30y,i} \approx \beta \times (\text{Annual \% change in } v_{d,i}) m_{v_{d,i}} \times 30 \text{ years} \quad (4)$$

461 where  $\Delta O_{3\ 30y,i}$  ~~is and~~  $m_{v_{d,i}}$  ~~are~~ the absolute change in ozone inferred to a first order as a result of the trend of  $v_d$  and the  
462 normalized Theil-Sen slope (% yr<sup>-1</sup>) of  $v_{d,i}$  for parameterization  $i$  over the 30-years (1982-2011).

463

464 In [Clim] simulations (where LAI is held constant), ~~the trend of July daytime  $v_d$  is either small or non significant over the vast~~  
465 ~~majority of the NH significant decreasing trends in July daytime  $v_d$  are simulated by the Z03, W98\_BB and Z03\_BB. An~~  
466 ~~exception is observed in the region of Mongolia, where significant increasing trend in  $T$  (warming) and decreasing trend in  $RH$~~   
467 ~~(drying) detected in the MERRA-2 surface meteorological field in July daytime results in significant decreasing trends using~~  
468 ~~the Z03, W98\_BB and Z03\_BB parameterizations.~~ This trend is not present in the W98 parameterization as this formulation  
469 does not respond to the long-term drying. We find some decreasing trends in  $v_d$  across parts of central Europe and the  
470 Mediterranean to varying degrees across the parameterizations. In the SH, we find consistent decreasing trends across all four  
471 parameterizations in southern Amazonia and southern African savannah due to warming and drying, which we estimate could  
472 produce a concomitant increase in July mean surface ozone of between 1 to 3 ppbv (Figure 9).

473

474 In [Clim+LAI] scenario, all four parameterizations simulate a significant increasing trend of  $v_d$  over high latitudes, which is  
475 consistent with the observed greening trend over the region (Zhu et al., 2016). We estimate this could produce a concomitant  
476 ~~increase decrease~~ in July mean surface ozone of between 1 to 3 ppbv. The parameterizations generally agree in terms of the  
477 spatial distribution of these trends in O<sub>3</sub>. Exceptions include a steeper decreasing trend in most of Siberia predicted by W98,  
478 while the trend is more confined in the eastern and western Siberia in the other three parameterizations. Including the effect of  
479 CO<sub>2</sub>-induced stomatal closure ([Clim+LAI+CO<sub>2</sub>] runs) partially offset the increase of  $v_d$  in high latitudes, but does not lead to  
480 large changes in both the magnitudes and spatial patterns of  $v_d$  trend. We find negligible trends in daytime  $v_d$  for December in  
481 all cases. These results show that across all dry deposition model parameterizations, LAI and climate, more than increasing  
482 CO<sub>2</sub>, can potentially drive significant long-term changes in  $v_d$  and should not be neglected when analyzing the long-term  
483 change in air quality over 1982-2011. We note that the importance of the CO<sub>2</sub> effect could grow as period of study further  
484 extend to allow larger range of atmospheric CO<sub>2</sub> concentration (Hollaway et al., 2017; Sanderson et al., 2007). ~~in the coming~~  
485 ~~decades, since the sensitivity of stomatal conductance to atmospheric CO<sub>2</sub> may increase (Franks et al., 2013).~~

486

487 We go on to explore the impact of parameterization choice in calculations of IAV in  $v_d$ . Figure 10 shows the coefficient of  
488 variation of linearly detrended July daytime  $v_d$  ( $CV_{v_d}$ ). Figure 11 shows the potential impact this has on IAV in surface ozone,  
489 which we estimate to a first order by the following equation:

490 
$$\sigma_{O_3,i} \approx \beta \times CV_{v_d,i} \quad (5)$$

491 where  $\sigma_{O_3,i}$  is the estimated interannual standard deviation in surface ozone resulting from IAV in  $v_d$  given predicted by dry  
492 deposition parameterization  $i$ . In both cases, we show only the [Clim] and [Clim+LAI] runs, since IAV in  $CO_2$  has negligible  
493 impact on interannual variability in  $v_d$ .

494

495 Using the W98 parameterization, IAV in predicted  $v_d$  and  $O_3$  is considerably smaller in the [Clim] run than that for the [Clim  
496 + LAI] run, since both the stomatal and non-stomatal conductance in W98 are assumed to be strong functions of LAI rather  
497 than meteorological conditions. This implies that long-term simulations with W98 and constant LAI can potentially  
498 underestimate the IAV of  $v_d$  and surface ozone. In contrast, IAV in  $v_d$  calculated by the Z03 parameterization is nearly the  
499 same for the [Clim] and [Clim+LAI] runs. In Z03,  $g_s$  is also directly influenced by  $VPD$  in addition to temperature and radiation,  
500 and non-stomatal conductance in Z03 is much more dependent on meteorology than W98, leading to high sensitivity to climate.  
501 Though the Ball-Berry model also responds to meteorological conditions, it considers relatively complicated-complex  $A_n-g_s$   
502 regulation and includes temperature acclimation, which could dampen its sensitivity to meteorological variability compared to  
503 the direct functional dependence on meteorology in the Z03 multiplicative algorithm. Thus, the climate sensitivity of W98\_BB  
504 and Z03\_BB is in between Z03 and W98, as is indicated by more moderate difference between  $\sigma_{O_3,i}$  from [Clim] and [Clim+LAI]  
505 runs in Figure 11.

506

507 For regional patterns of  $CV_{v_d}$  and  $\sigma_{O_3}$ , we focus on the [Clim+LAI] runs (Fig. 10e to 10h and Fig. 11e to 11h) as it-they allows  
508 allow for a comparison of all 4 parameterizations and contain all the important factors of controlling  $v_d$ . In North America, we  
509 estimate modest IAV in  $v_d$  across all 4 parameterizations ( $CV_{v_d} < 15\%$ ) in most places. We find this results in relatively low  
510  $\sigma_{O_3}$  in northeastern US, and larger  $\sigma_{O_3}$  in central and southeast US (in the range of 0.3 to 2 ppbv). These results are of a similar  
511 magnitude to the standard deviation of summer mean background ozone suggested by Fiore et al. (2014) over similar time  
512 period, confirming-suggesting that IAV of dry deposition can be a potentially important component of the natural-IAV of  
513 surface ozone in summer over North America.

514

515 All parameterizations produce larger  $CV_{v_d}$  (and therefore larger  $\sigma_{O_3}$ ) in southern Amazonia compared to northern and central  
516 Amazonia, but we find substantial discrepancies across parameterizations. The estimated impact on IAV in  $O_3$  ( $\sigma_{O_3}$ ) in southern  
517 Amazonia ranges from less than 1 ppbv predicted by the W98 and W98\_BB parameterizations, to exceeding 1.5 - 2.5 ppbv  
518 predicted by the Z03 parameterization. IAV is also relatively large in central Africa. We find that the parameterizations which  
519 include a Ball-Berry formulation (W98\_BB and Z03\_BB) estimate higher IAV in this region (with  $\sigma_{O_3}$  varying between 1 to  
520 4 ppbv), compared to the W98 and Z03 parameterizations ( $\sigma_{O_3}$  up to 2ppbv). We also note that the Ball-Berry formulations  
521 show more spatial discontinuities-heterogeneity compared to W98 and Z03. In our implementation of the Ball-Berry model,  
522 impact of soil moisture on  $g_s$  is parameterized as a function of root-zone soil matric potential, which makes  $g_s$  very sensitive  
523 to variation in soil wetness when the its climatology is near the point that triggers limitation on  $A_n$  and  $g_s$ . Given the large

524 uncertainty in ~~soil data (Folberth et al., 2016)~~global soil property map (Dai et al., 2019), such sensitivity could be potentially  
525 artificial, which should be taken into consideration when implementing Ball-Berry parameterizations in large-scale models  
526 despite their relatively good performance in site-level evaluation (Wu et al., 2011).

527

528 Across Europe, the magnitude of IAV predicted by all four parameterizations show relatively good spatial consistency.  
529 Simulated  $CV_{vd}$  is relatively low in western and northern Europe (<10%), which we estimate translates to less than 1 ppbv of  
530  $\sigma_{O_3}$ . We find larger  $CV_{vd}$  (and therefore large  $\sigma_{O_3}$ ) over parts of southern Russia and Siberia ( $\sigma_{O_3}$  up to 2.5 ppbv) from all  
531 parameterizations except W98. The local geographic distribution of  $CV_{vd}$  and  $\sigma_{O_3}$  also significantly differs among the  
532 parameterizations. Z03 and Z03\_BB simulate larger  $CV_{vd}$  in eastern Siberia than W98\_BB, while W98\_BB and Z03\_BB predict  
533 larger  $CV_{vd}$  over the southern Russian steppe than Z03. Finally, all four parameterizations estimate relatively low  $CV_{vd}$  and  $\sigma_{O_3}$   
534 in India, China and Southeast Asia.

535

536 We compare the simulated IAV ~~of July~~  $CV_{vd}$  from all four deposition parameterizations with those recorded by publicly  
537 available long-term observations. Hourly  $v_d$  is calculated using eq. (1) from raw data. We filter out the data points with extreme  
538 (> 2 cm s<sup>-1</sup>) or negative  $v_d$ , and without enough turbulence ( $u_* < 0.25$  m s<sup>-1</sup>). As  $v_d$  in each daytime hours are not uniformly  
539 sampled in the observational datasets, we calculate the mean diurnal cycle, and then calculate the daytime average July of  $v_d$   
540 for each year from the mean diurnal cycle, from which  $CV_{vd}$  can be calculated.

541 The IAV predicted by all four parameterizations at Harvard Forest is between 3% to 7.9%, which is 2 to 6 times lower than  
542 that presented in the observations (~~1918%~~), ~~by Clifton et al. (2017)~~. We find similar underestimates by all four  
543 parameterizations compared to the long-term observation from Hyytiala (Junninen et al., 2009; Keronen et al., 2003;  
544 <https://avaa.tdata.fi/web/smart/smear/download>), where observed  $CV_{vd}$  (~~4416%~~) is significantly higher than that predicted by  
545 the deposition parameterizations (3.5% - 7.1%). In Blodgett Forest, ~~where O<sub>3</sub> uptake is more controlled by gas-phase reactions~~  
546 ~~(Fares et al., 2010; Wolfe et al., 2011)~~, we find that the models underestimate the observed annual  $CV_{vd}$  more seriously (~1%  
547 - 3% compared to ~~4218%~~ in the observations). This ~~suggest~~ suggests that the IAV of  $v_d$  may be underestimated across all  
548 deposition parameterizations we investigated (and routinely used in simulations of chemical transport). ~~(Clifton et al. (~~  
549 ~~2019)~~ ~~Clifton et al. (2017)~~ attribute this to the IAV in deposition to wet soil and dew-wet leaves, and in-canopy chemistry  
550 under stressed condition for forests over northeastern U.S. Some of these processes (e.g. in-canopy chemistry, wetness slowing  
551 soil ozone uptake) are not represented by existing parameterizations, contributing to their in-non-stomatal deposition, while  
552 acknowledging the obscurity of the mechanisms driving such variability, implying the difficulty in reproducing the observed  
553 IAV ~~by existing parameterizations~~. The scarcity of long-term ozone flux measurements (Fares et al., 2010, 2017; Munger et  
554 al., 1996; Rannik et al., 2012) limits our ability to benchmark the IAV in our model simulations with observational datasets.

555

556 In summary, when both the variability in LAI and climate are considered, the IAV in simulated  $v_d$  translates to IAV in surface  
557 O<sub>3</sub> of 0.5 – 2ppbv in July for most region. Such variability is predicted to be particularly strong in southern Amazonian and

558 central African rainforest, where the predicted IAV in July surface  $O_3$  due to dry deposition can be as high as 4 ppbv. This  
559 suggests that IAV of  $v_d$  can be an important part of the natural variability of surface  $O_3$ . The estimated magnitude of IAV is  
560 also dependent of the choice of  $v_d$  parameterization, which highlights the importance of  $v_d$  parameterization choice on  
561 modelling IAV of surface  $O_3$ .

## 562 **6 Discussion and Conclusion**

563 We present the results of multidecadal global modelling of ozone dry deposition using four different ozone deposition  
564 parameterizations that are representative of the major types of approaches of gaseous dry deposition modelling used in global  
565 chemical transport models. The parameterizations are driven by the same assimilated meteorology and satellite-derived LAI,  
566 which minimizes the uncertainty of model input across parameterization and simplifies interpretation of inter-model  
567 differences. The output is evaluated against field observations and shows satisfactory performance. One of our main goals was  
568 to investigate the impact of dry deposition parameterization choice on long-term averages, trends, and IAV in  $v_d$  over a  
569 multidecadal timescale, and estimate the potential concomitant impact on surface ozone concentrations to a first order using a  
570 sensitivity simulation approach driven by the GEOS-Chem chemical transport model.

571

572 We find that the performance of the four dry deposition parameterizations against field observations varies considerably over  
573 land types, and these results are consistent with other evaluations, reflecting the potential issue that dry deposition  
574 parameterizations can often be overfit to a particular set of available observations, requiring caution in their application at  
575 global scales. We also find that using more ecophysiological realistic output  $g_s$  predicted by the Ball-Berry model can  
576 generally improve model performance, but at the cost of high sensitivity to relatively unreliable soil data. However, the number  
577 of available datasets of ozone dry deposition observation are still small and concentrated in North America and Europe. We  
578 know of only one multi-season direct observational record in Asia (Matsuda et al., 2005) and none in Africa, where air quality  
579 can be an important issue. To better constraint regional  $O_3$  dry deposition, effort must be made in making new observations of  
580 gaseous dry deposition (Fares et al., 2017) especially in the under-sampled regions. ~~We also find that many existing ozone~~  
581 ~~flux measurements are not usable for our evaluation purposes, since only  $F_{O_3}$  is reported in detail instead of  $v_d$ .~~ Evaluation and  
582 development of ozone dry deposition parameterizations will continue to benefit from publicly available ozone flux  
583 measurements and related micrometeorological variables that allow for partitioning measured flux into individual deposition  
584 pathways (e.g. Clifton et al., 2017, 2019; Fares et al., 2010; Wu et al., 2011, 2018). ~~Evaluation and development of ozone dry~~  
585 ~~deposition parameterizations would be greatly benefited if result of ozone flux measurements is reported in both  $F_{O_3}$  and  $v_d$ ,~~  
586 ~~or even have publically available ozone flux and other related micrometeorological variables, which allows both direct~~  
587 ~~evaluation of  $v_d$  and solves the mismatch between coarse model grids and the site (e.g. Wu et al., 2011, 2018).~~

588

589 We find substantial disagreement in the spatial distribution between the mean daytime  $v_d$  predicted by the different  
590 parameterizations we tested. We find that these discrepancies are in general a function of both location and season. In NH  
591 summer,  $v_d$  simulated by the 4 parameterizations are considerably different in many ~~vegetation-dominated~~ regions over the  
592 world. We estimate that this could lead to around 2 to 5 ppbv in uncertainty of surface ozone concentration simulations over a  
593 vast majority of land in the NH. In tropical rainforests, where leaf wetness is prevalent and the dry-wet season dynamics can  
594 have large impact on  $v_d$  (Rummel et al., 2007), we estimate the uncertainty due to dry deposition model choice could even  
595 lead to an uncertainty in surface ozone of up to 8 ppbv. We also find noticeable impacts in parameterization choice during SH  
596 summer, but we note that due to the unreliability of  $\beta$  at low  $v_d$ , we have not assessed its impact on surface ozone in many  
597 high-latitude regions of the NH. In general, we find hydroclimate to be an important driver of the uncertainty. This  
598 demonstrates that the potential impact of parameterization choice (or, process uncertainty) of  $v_d$  is neither spatiotemporally  
599 uniform nor negligible in ~~most-vegetated~~many regions over the world. More multi-seasonal observations are especially needed  
600 over seasonally dry ecosystems where the role of hydroclimate in deposition parameterizations need to be evaluated. Recently,  
601 standard micrometeorological measurements have been used to derive  $g_s$  and stomatal deposition of  $O_3$  over North America  
602 and Europe (Ducker et al., 2018), highlighting the potential of using global networks of micrometeorological observation (e.g.  
603 FLUXNET (Baldocchi et al., 2001)) to benchmark and calibrate  $g_s$  of dry-deposition parameterizations, which could at least  
604 increase the spatiotemporal representativeness, if not the absolute accuracy, of dry deposition parameterizations, since it would  
605 be difficult to constrain non-stomatal sinks with this method. Further research is required to more directly verify whether better  
606 constrained  $g_s$  leads to improved  $v_d$  simulation.-

607  
608 Over the majority of vegetated regions in the NH, we estimate the IAV of mean daytime  $v_d$  is generally on the order of 5 to  
609 15% and may contribute between 0.5 to 2 ppbv of IAV in July surface  $O_3$  over the thirty-year period considered here, with  
610 each parameterization simulating different geographic distribution of where IAV is highest. The predicted IAV from all four  
611 models is smaller than what long-term observations suggest, but its potential contribution to IAV in  $O_3$  is still comparable to  
612 the long-term variability of background ozone over similar timescales in U.S. summer (Brown-Steiner et al., 2018; Fiore et al.,  
613 2014). This would seem to confirm that  $v_d$  may be a substantial contributor to natural IAV of  $O_3$  in summer, at least in U.S. In  
614 the southern Hemisphere, the IAV mainly concentrates in the drier part of tropical rainforests. The Ball-Berry  
615 parameterizations simulate large and spatially discontinuous  $CV_{v_d}$  and  $\sigma_{O_3}$  due to their sensitivity to soil wetness. Globally, we  
616 find that IAV of  $v_d$  in W98 is mostly driven by LAI, while in other parameterizations climate generally plays a more important  
617 role. We therefore emphasize that temporal matching of LAI is important for consistency when W98 is used in long-term  
618 simulations. While our results show notable impacts across the globe, in many regions there are no available long-term  
619 observation to evaluate the model predictions over interannual timescales. The scarcity of long term ozone deposition  
620 measurement poses significant difficulty in evaluating the model predictions over interannual (and in particular multidecadal)  
621 timescales.- This information is helpful in designing and identifying sources of error in model experiments that involve  
622 variability of  $v_d$ .



624 We are also able to detect statistically significant trends in July daytime  $v_d$  over several regions. The magnitudes of ~~trend-trends~~  
625 are up to 1% per year and both climate and LAI contribute to the trend. All four deposition parameterizations identify three  
626 main hotspots of decreasing July daytime  $v_d$  (southern Amazonia, southern African savannah, Mongolia), which we link mainly  
627 to increasing surface air temperature and decreasing relative humidity. Meanwhile, extensive areas at high latitudes experience  
628 LAI-driven increasing July daytime  $v_d$ , consistent with the greening trend in the region (Zhu et al., 2016). We don't find a  
629 strong influence of CO<sub>2</sub>-induced stomatal closure in the trend over this time period. Over the 30-years we estimate the trend  
630 in July daytime  $v_d$  could translate approximately to 1 to 3 ppbv of ozone changes in the areas of impact, indicating the potential  
631 effect of long-term changes in  $v_d$  on surface ozone. This estimate should be considered conservative, since we are unable to  
632 reliably test the sensitivity of ozone to regions with low  $v_d$  with our approach.

633

634 While the approach we have presented here allows us to explore the role of dry deposition parameterization choice on  
635 simulations of long-term means, trends, and IAV in ozone dry deposition velocity, there remain some limitations and  
636 opportunities for development. First, we only used one LAI and assimilated meteorological product. The geographic  
637 distribution of trend and IAV of  $v_d$  may vary considerably as the LAI and meteorological products used due to their inherent  
638 uncertainty (e.g. Jiang et al., 2017). While we expect the qualitative conclusions about how LAI and climate controls the  
639 modelled trend and IAV of  $v_d$  to be robust to the choice of data set, the magnitude and spatial variability could be affected.  
640 Second, the estimated effects on surface O<sub>3</sub> are a first-order inference based on a linear approximation of the impact that  $v_d$   
641 has directly on O<sub>3</sub>. We have not applied our analysis to regions with low ~~baseline~~-GEOS-Chem  $v_d$ , where other components of  
642 parameterization (e.g. definition and treatment of snow cover, difference in ground resistance) may have major impact on  $v_d$   
643 prediction (Silva and Heald, 2018), nor accounted for the role that  $v_d$  variability can have on other chemical species which  
644 would have feedbacks on O<sub>3</sub>. Moreover, the sensitivity of surface ozone to ~~dry deposition velocity~~ $v_d$  may be dependent on the  
645 choice of chemical transport model (here, the GEOS-Chem model has been used), and possibly the choice of simulation year  
646 for the sensitivity simulation. Finally, we have neglected the effect of land use and land cover change on global PFT  
647 composition at this stage, which can be another source of variability for  $v_d$ , and even long-term LAI retrieval (Fang et al.,  
648 2013). Nevertheless, the relatively high *NMAEF* of simulated  $v_d$  and the inherent uncertainty in input data (land cover, soil  
649 property, assimilated meteorology and LAI) are considered as the major source of uncertainty in our predictions of  $v_d$ .

650

651 The impact of dry deposition parameterization choice may also have impacts which we have not explored in this study on  
652 other trace gases may be generalizable to other trace gases with deposition velocity controlled by surface resistance, and for  
653 which stomatal resistance is an important control of surface resistance (e.g. NO<sub>2</sub>). As  $v_d$  has already been recognized as a major  
654 source of uncertainty in deriving global dry deposition flux of NO<sub>2</sub> and SO<sub>2</sub> (Nowlan et al., 2014), systematic investigation on  
655 the variability and uncertainty of  $v_d$  for other relevant chemical species does not only contribute to understanding the role of  
656 gaseous dry deposition ~~role~~ on air quality, but also to biogeochemical eyelecycling. Particularly, gaseous dry deposition has

657 been shown to be a major component in nitrogen deposition (Geddes and Martin, 2017; Zhang et al., 2012), highlighting the  
658 potential importance of understanding the role of  $v_d$  parameterization in modelling regional and global nitrogen cycles.  
659  
660 Here we have built on the recent investigations of modelled global mean (Hardacre et al., 2015; Silva and Heald, 2018) and  
661 observed long-term variability (Clifton et al., 2017) of  $O_3$   $v_d$ . We are able to demonstrate the substantial impact of  $v_d$   
662 parameterization on modelling the global mean and IAV of  $v_d$ , and their non-trivial potential impact on simulated seasonal  
663 mean and IAV of surface ozone. We demonstrate that the parameterizations with explicit dependence on hydroclimatic  
664 variables have higher sensitivity to climate variability than those without. Difficulties in evaluating predictions of  $v_d$  for many  
665 regions of the world (e.g. most of Asia and Africa) persist due to the scarcity of measurements. This makes a  
666 strong case for additional measurements (e.g. Kammer et al., 2019; Li et al., 2018; Stella et al., 2011a), empirical studies (e.g.  
667 Dueker et al., 2018) and model observation integrations (e.g. Silva et al., 2019) of ozone dry deposition at different timescales,  
668 which would be greatly facilitated by an open data sharing infrastructure This makes a strong case for additional measurement  
669 and model studies of ozone dry deposition across different timescales, which would be greatly facilitated by an open data  
670 sharing infrastructure (e.g. Baldocchi et al., 2001; Junninen et al., 2009).

## 671 Code Availability

672 The source code and output of the dry deposition parameterizations can be obtained by contacting the corresponding author  
673 ([jgeddes@bu.edu](mailto:jgeddes@bu.edu)).

## 674 Appendix

|       | W98  | Z03   | W98_BB  | Z03_BB   |
|-------|--|---|---|--|
| $R_a$ | $R_a = \frac{1}{\kappa u_*} \left[ \ln\left(\frac{z}{z_0}\right) - \Psi\left(\frac{z}{L}\right) + \Psi\left(\frac{z_0}{L}\right) \right]$ <p>When <math>\zeta \geq 0</math>, <math>\Psi(\zeta) = -5\zeta</math></p> <p>When <math>\zeta &lt; 0</math>, <math>\Psi(\zeta) = 2 \ln\left(\frac{1 + \sqrt{1 - 16\zeta}}{2}\right)</math></p> |   |   |  |
| $R_b$ | $R_b = \frac{2}{\kappa u_*} \left(\frac{S\zeta}{Pr}\right)^{2/3}$  |   |   |  |
| $R_s$ | $R_s = r_s(PAR, LAI) f_r \frac{D_{H_2O}}{D_{O_3}}$   | $R_s = \frac{r_s(PAR, LAI)}{(1 - w_{st}) f_r f_{vp} a f_{\psi}} \frac{D_{H_2O}}{D_{O_3}}$ | $g_s = g_0 + m \frac{A_{\overline{n}}}{C_s} h_s$ $R_s = \frac{1}{g_s} \frac{D_{H_2O}}{D_{O_3}}$ | $g_s = g_0 + m \frac{A_{\overline{n}}}{C_s} h_s$ $R_s = \frac{1}{(1 - w_{st}) g_s} \frac{D_{H_2O}}{D_{O_3}}$ |

|   |  |  |             |             |
|---|--|--|-------------|-------------|
| Cuticular Resistance ( $R_{cut}$ )                | $R_{cut} = \frac{R_{cut0}}{LAI}$                       | For dry surface,<br>$R_{cut} = \frac{R_{cutd0}}{e^{0.02RH} LAI^{0.25} u_x}$<br>For wet surface,<br>$R_{cut} = \frac{R_{cutw0}}{LAI^{0.5} u_x}$ | Same as W98 | Same as Z03 |
| In-canopy aerodynamic resistance ( $R_{ac}$ )     | Prescribed   | $R_{ac} = \frac{LAI^{0.25}}{R_{ac0} u_x}$  |             |             |
| Ground Resistance ( $R_g$ )                       | Prescribed   |  |             |             |
| Lower canopy aerodynamic resistance ( $R_{alc}$ ) | $R_{alc} = 100 \left( 1 + \frac{1000}{R + 10} \right)$ | -  |             |             |
| Lower canopy surface resistance ( $R_{cle}$ )     | Prescribed   | -  |             |             |

675 **Table A1:** Brief description of the four dry deposition parameterizations.  $\kappa$  = von Karman constant,  $u_x$  = friction velocity,  $z$  =  
676 reference height,  $z_0$  = roughness length,  $L$  = Obukhov length,  $Sc$  = Schmidt's number,  $Pr$  = Prandtl number for air,  $LAI$  = leaf  
677 area index,  $PAR$  = photosynthetically active radiation,  $D_x$  = Diffusivity of species  $x$  in air,  $f_T$  = temperature ( $T$ ) stress function,  
678  $f_{vpd}$  = vapour pressure deficit ( $VPD$ ) stress function,  $f_\psi$  = leaf water potential ( $\psi$ ) stress function,  $w_{st}$  = stomatal blocking fraction,  
679  $A_n$  = Net photosynthetic rate,  $g_0$  = minimum stomatal conductance,  $m$  = Ball-Berry slope,  $C_s$  =  $CO_2$  concentration on leaf  
680 surface,  $h_s$  = relative humidity on leaf surface,  $RH$  = relative humidity,  $h$  = canopy height,  $R$  = downward shortwave radiation  
681

| CLM PFT                             | Z03 surface type           |
|-------------------------------------|----------------------------|
| Needleleaf evergreen tree—temperate | Evergreen needleleaf trees |
| Needleleaf evergreen tree—boreal    |                            |
| Needleleaf deciduous tree—boreal    | Deciduous needleleaf trees |
| Broadleaf evergreen tree—tropical   | Tropical broadleaf trees   |
| Broadleaf deciduous tree—tropical   | Deciduous broadleaf trees  |
| Broadleaf deciduous tree—temperate  |                            |
| Broadleaf deciduous tree—boreal     |                            |
| Broadleaf evergreen shrub—temperate | Thorn shrubs               |

|                                     |                  |
|-------------------------------------|------------------|
| Broadleaf deciduous shrub—temperate | Deciduous shrubs |
| Broadleaf deciduous shrub—boreal    |                  |
| C <sub>3</sub> -arctic grass        | Tundra           |
| C <sub>3</sub> -grass               | Short-grass      |
| C <sub>4</sub> -grass               | Corn*            |
| C <sub>3</sub> -crop                | Crops            |

682 **Table A2:** Mapping between CLM PFT and Z03 surface-type.

683 \*C<sub>4</sub>-grasses are mapped to corn due to the similarity in photosynthetic pathway, and hence stomatal control

684

| Land-Type         | Longitude | Latitude | Season | Mean daytime $v_a$ (cm s <sup>-1</sup> ) | Citation                 |
|-------------------|-----------|----------|--------|--|--------------------------|
| Deciduous Forest  | -80.9°    | 44.3°    | Summer | 0.92                                     | Padro et al., 1991       |
|                   |           |          | Winter | 0.28                                     |                          |
|                   | 99.7°     | 18.3°    | Spring | 0.38                                     | Matsuda et al., 2005     |
|                   |           |          | Summer | 0.65                                     |                          |
|                   | -72.2°    | 42.7°    | Summer | 0.61                                     | Munger et al., 1996      |
|                   |           |          | Winter | 0.28                                     |                          |
| -78.8°            | 41.6°     | Summer   | 0.83   | Finkelstein et al., 2000                 |                          |
| -75.2°            | 43.6°     | Summer   | 0.82   |  |                          |
| Coniferous Forest | -3.4°     | 55.3°    | Spring | 0.58                                     | Coe et al., 1995         |
|                   | -79.1°    | 36.0°    | Spring | 0.79                                     | Finkelstein et al., 2000 |
|                   | -120.6°   | 38.9°    | Spring | 0.58                                     | Kurpius et al., 2002     |
|                   |           |          | Summer | 0.59                                     |                          |
|                   |           |          | Autumn | 0.43                                     |                          |
|                   |           |          | Winter | 0.45                                     |                          |
|                   | -0.7°     | 44.2°    | Summer | 0.48                                     | Lamaud et al., 1994      |
|                   | 105.5°    | 40.0°    | Summer | 0.39                                     | Turnipseed et al., 2009  |
|                   | -66.7°    | 54.8°    | Summer | 0.26                                     | Munger et al., 1996      |
|                   | 11.1°     | 60.4°    | Spring | 0.31                                     | Hole et al., 2004        |
|                   |           |          | Summer | 0.48                                     |                          |
| Autumn            |           |          | 0.20   |  |                          |
| Winter            |           |          | 0.074  |  |                          |
| 8.4°              | 56.3°     | Spring   | 0.68   | Mikkelsen et al., 2004                   |                          |
|                   |           | Summer   | 0.80   |  |                          |

|                     |         |        |                             |                        |                                  |
|---------------------|---------|--------|-----------------------------|------------------------|----------------------------------|
|                     |         |        | Autumn                      | 0.83                   |                                  |
| Tropical Rainforest | 117.9°  | 4.9°   | Wet                         | 0.5                    | Fowler et al., 2011 <sup>#</sup> |
|                     |         |        | Wet                         | 1.0                    |                                  |
|                     | -61.8°  | -10.1° | Wet                         | 1.1                    | Rummel et al., 2007              |
|                     |         |        | Dry                         | 0.5                    |                                  |
| -60.0°              | 3.0°    | Wet    | 1.8                         | Song Miao et al., 1990 |                                  |
| Grass               | -88.2°  | 40.0°  | Summer                      | 0.56                   | Droppo, 1985                     |
|                     | -3.2°   | 57.8°  | Spring                      | 0.59                   | Fowler et al., 2001              |
|                     |         |        | Summer                      | 0.56                   |                                  |
|                     |         |        | Autumn                      | 0.42                   |                                  |
|                     | -119.8° | 37.0°  | Summer                      | 0.15                   | Padro et al., 1994               |
|                     | -8.6°   | 40.7°  | Summer                      | 0.22                   | Pio et al., 2000                 |
|                     |         |        | Winter                      | 0.38                   |                                  |
|                     | -104.8° | 40.5°  | Spring                      | 0.22                   | Stocker et al., 1993             |
| 10.5°               | 52.4°   | Spring | 0.44                        | Mészáros et al., 2009  |                                  |
| -96.4°              | 39.5°   | Summer | 0.62                        | Gao and Wesely, 1995   |                                  |
| Crops               | -2.8°   | 55.9°  | Not applicable <sup>*</sup> | 0.69                   | Coyle et al., 2009               |
|                     | -88.4°  | 40.1°  |                             | 0.53                   | Meyers et al., 1998              |
|                     |         |        |                             | 0.12                   |                                  |
|                     | -87.0°  | 36.7°  |                             | 0.85                   | 0.39                             |
|                     |         |        |                             | 0.40                   |                                  |
|                     | -86.0°  | 34.3°  |                             | 0.76                   | Padro et al., 1994               |
|                     | -120.7° | 36.8°  |                             | 0.41                   | Pilegaard et al., 1998           |
|                     | 8.0°    | 48.7°  |                             | 0.60                   | Stella et al., 2011              |
|                     | 2.0°    | 48.9°  |                             | 0.47                   |                                  |
|                     | 0.6°    | 44.4°  |                             | 0.37                   |                                  |
| 1.4°                | 43.8°   |        |                             |                        |                                  |

685 **Table A3:** Information of all the measurement sites included in model evaluation

686 <sup>\*</sup>Crops are heavily influenced by management practices rather than natural seasonality. Thus, two data sets in the same location  
687 generally represent before and after certain a crop phenology or human management event.

688 <sup>#</sup>The two measurements are taken at a rainforest and an oil palm plantation nearby.

689

690 **Author Contributions**

691 AYHW and JAG developed the ideas behind this study, formulated the methods, and designed the model experiments. AYHW  
692 wrote the dry deposition code and ran the chemical transport model simulations. Data analysis was performed by AYHW, with  
693 input and feedback from JAG. APKT provided the photosynthesis model code, and co-supervised the dry deposition code  
694 development. SJS compiled the dry deposition observations used for evaluation. Manuscript preparation was performed by  
695 AYHW, reviewed by JAG, and commented, edited, and approved by all authors.

696 **Acknowledgement**

697 This work was funded by an NSF CAREER grant (ATM-1750328) to project PI J.A. Geddes; and the Vice-Chancellor  
698 Discretionary Fund (Project ID: 4930744) from The Chinese University of Hong Kong (CUHK) given to the Institute of  
699 Environment, Energy and Sustainability. Funding support to SJS was provide by a National Science Foundation grant to C.L.  
700 Heald (ATM-1564495). We also thank the Global Modelling and Assimilation Office (GMAO) at NASA Goddard Flight  
701 Center for providing the MERRA-2 data, Ranga Myneni for GIMMS LAI3g product, Petri Keronen and Ivan Mammarella for  
702 the flux measurements in Hyytiala, Silvano Fares and Allen Goldstein for the flux measurement in Blodgett Forest, and  
703 Leiming Zhang and Zhiyong Wu for the source code of Z03.

704

705

706

707

708

709

710

711

712

713

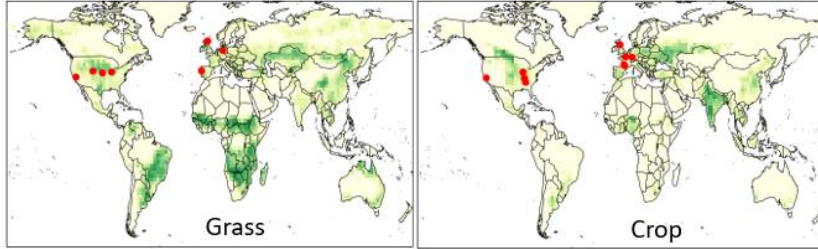
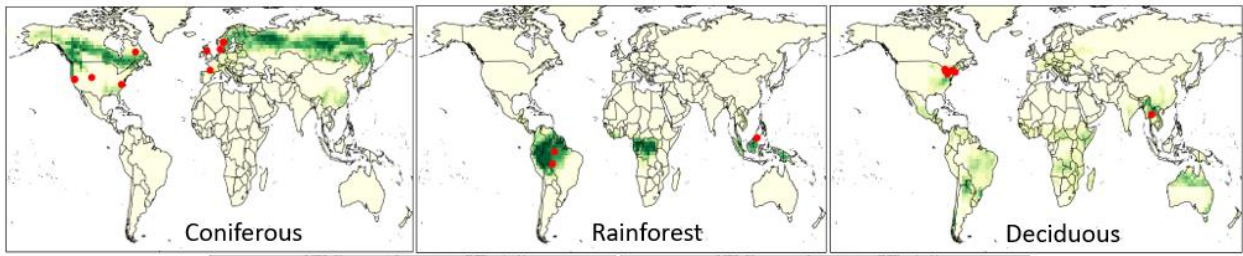
714

715

716

717

718

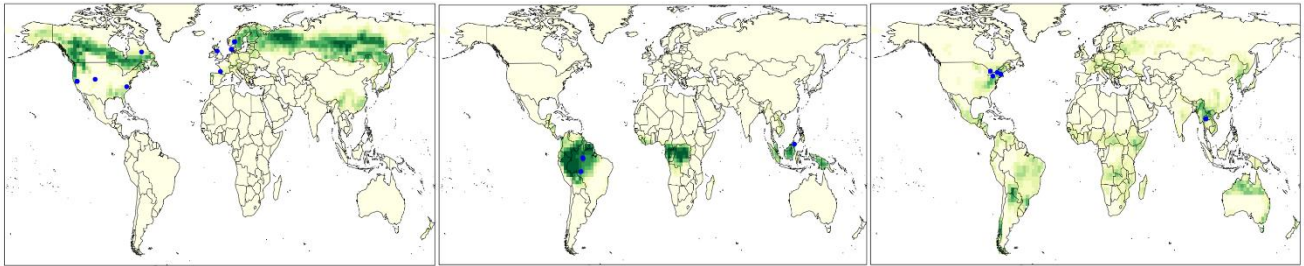


719

Coniferous

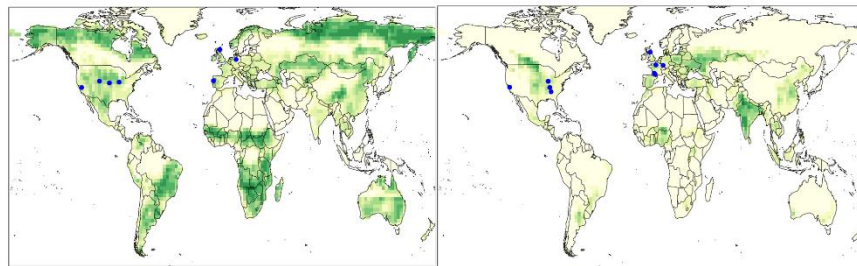
Rainforest

Deciduous



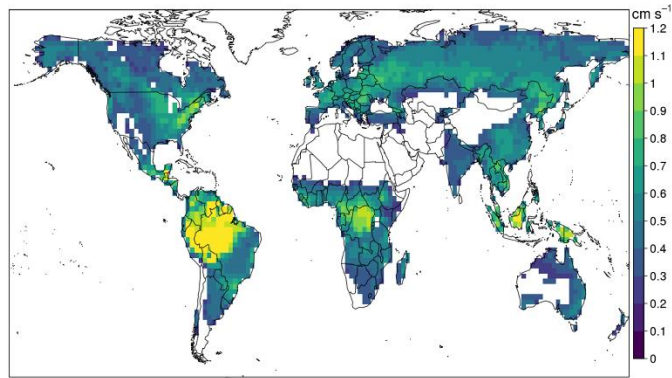
Grass

Crop



720

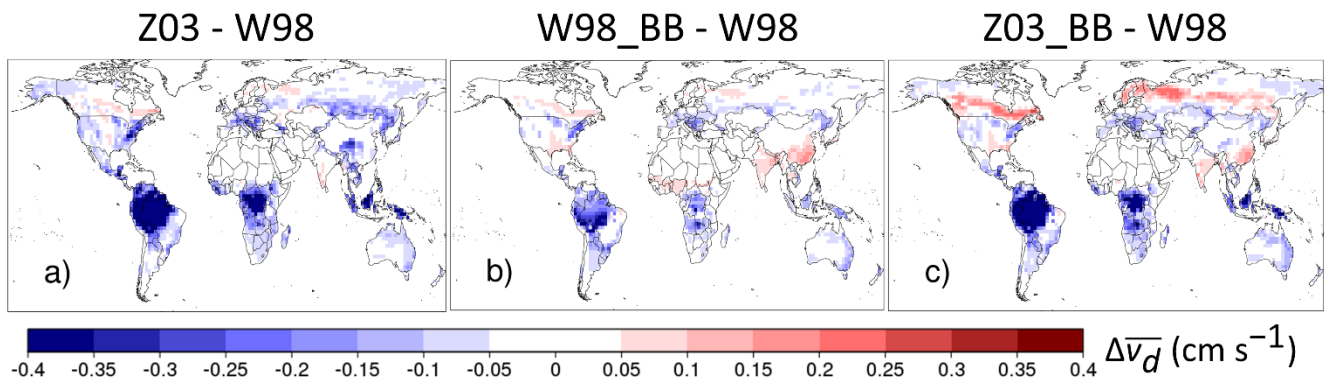
721 **Figure 1:** Fractional coverage of each major land type at each grid cell. Blue dots indicate the locations of the observational  
 722 sites.



723

724 **Figure 2:** 1982-2011 July mean daytime  $v_d$  (solar elevation angle  $> 20^\circ$ ) over vegetated land surface simulated by W98.

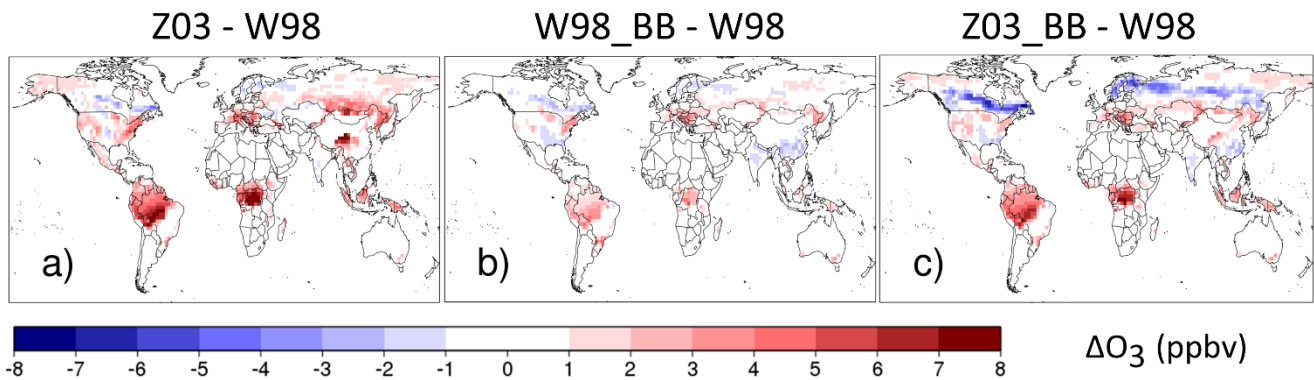
725



726

727 **Figure 3:** Differences of 1982-2011 July mean daytime  $v_d$  ( $\Delta\bar{v}_d$ ) between three other parameterizations (Z03, W98\_BB and  
728 Z03\_BB) and W98 over vegetated land surface.

729

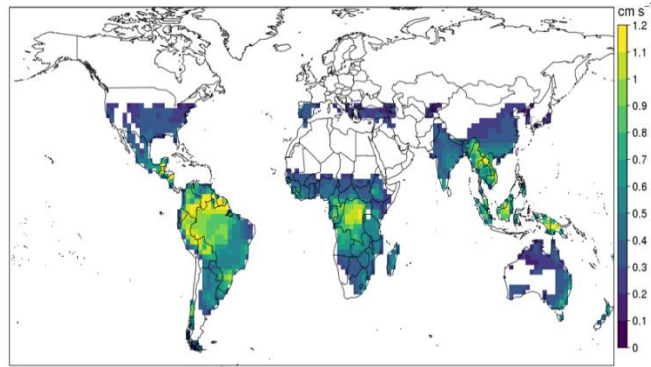


730

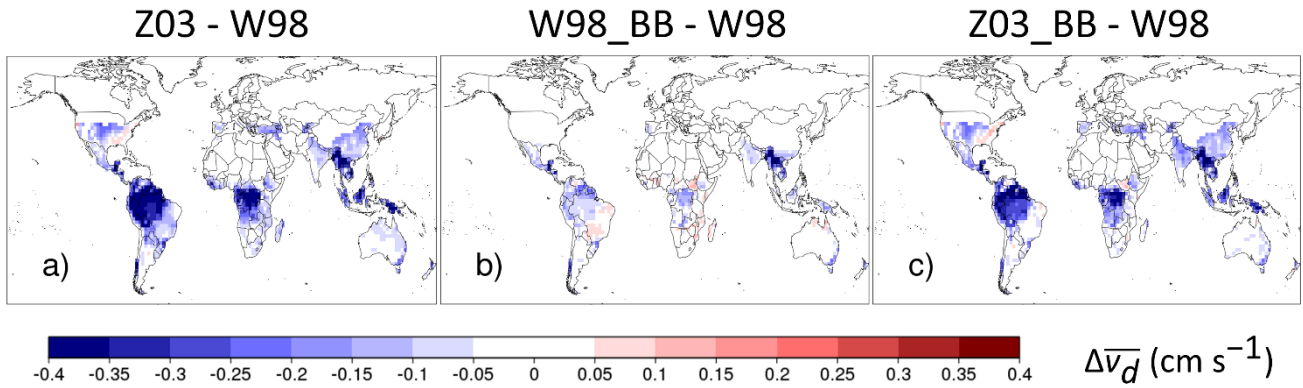
731 **Figure 4:** Estimated difference in July mean surface ozone ( $\Delta O_3$ ) due to the discrepancy of simulated July mean daytime  $v_d$   
732 among the parameterizations.



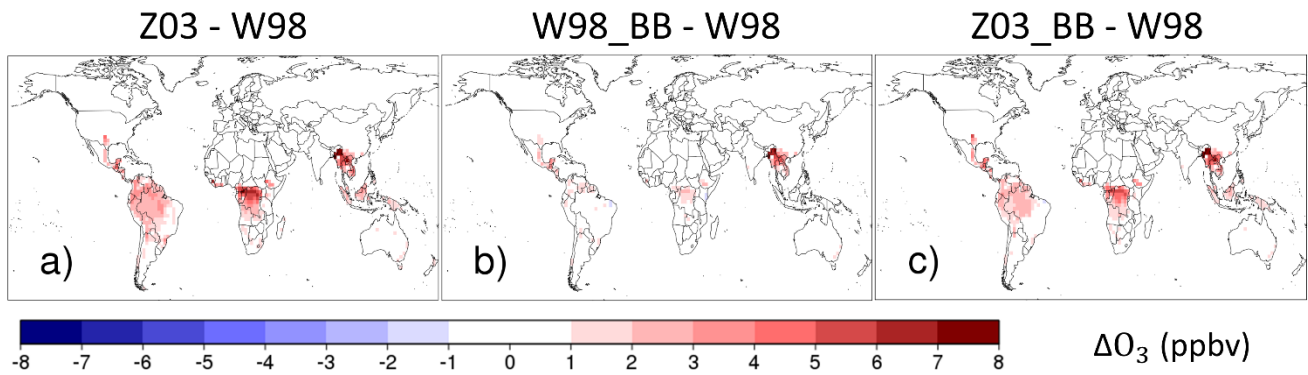
733  
734  
735  
736



737  
738 **Figure 5:** 1982-2011 December mean daytime  $v_d$  (solar elevation angle  $> 20^\circ$ ) over vegetated land surface simulated by  
739 W98. The data over high latitudes over Northern Hemisphere is invalid due to insufficient daytime hours over the month ( $<$   
740 100 hours month $^{-1}$ )  
741



742  
743 **Figure 6:** Differences of 1982-2011 December mean daytime  $v_d$  ( $\Delta \bar{v}_d$ ) between three other parameterizations (Z03, W98\_BB  
744 and Z03\_BB) and W98 over vegetated land surface.  
745  
746

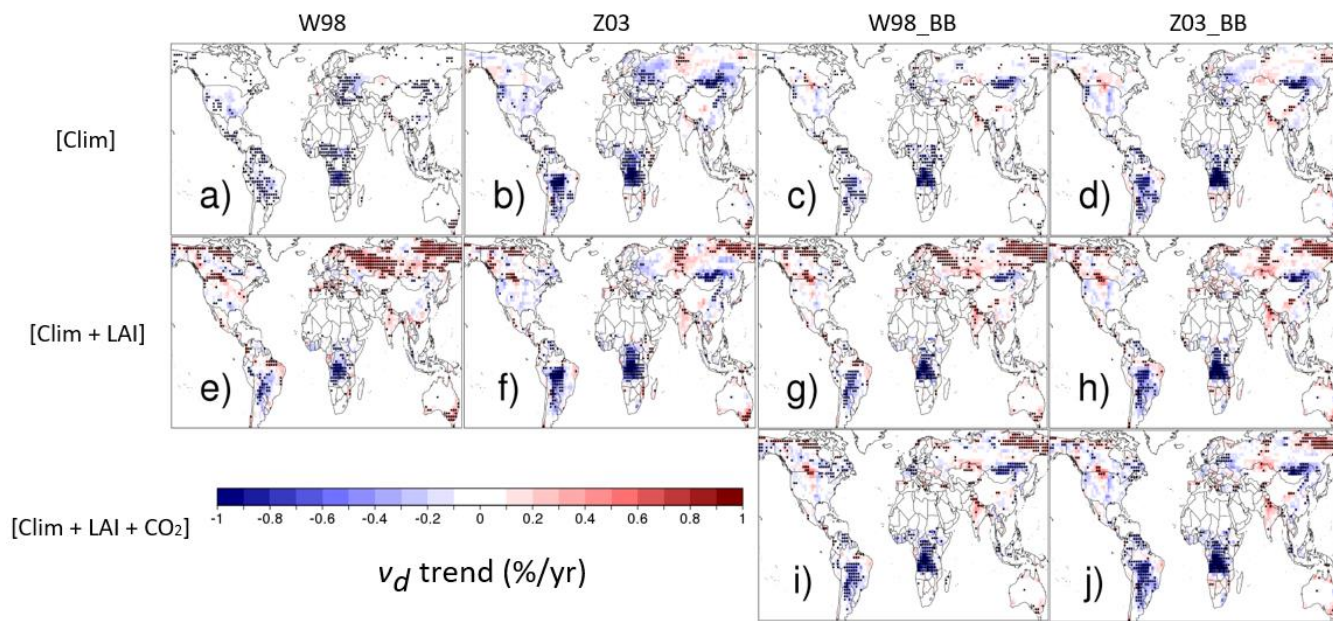


747

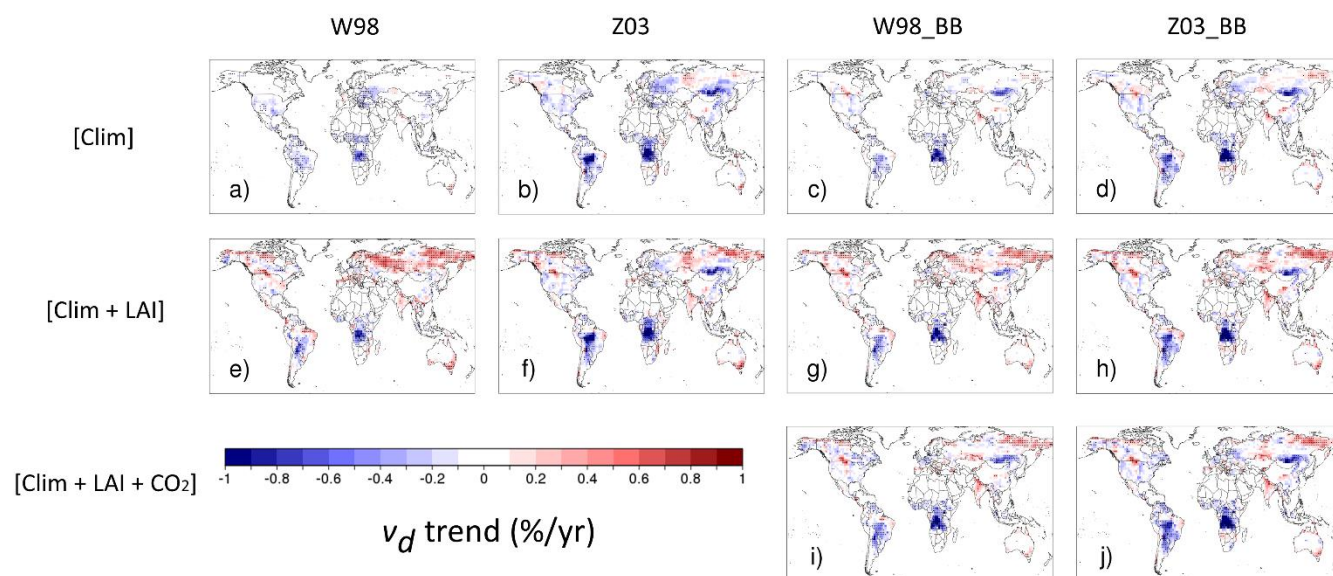
748 **Figure 7:** Estimated difference in December mean surface ozone ( $\Delta O_3$ ) due to the discrepancy of simulated December mean  
 749 daytime  $v_d$  among the parameterizations.

750

751

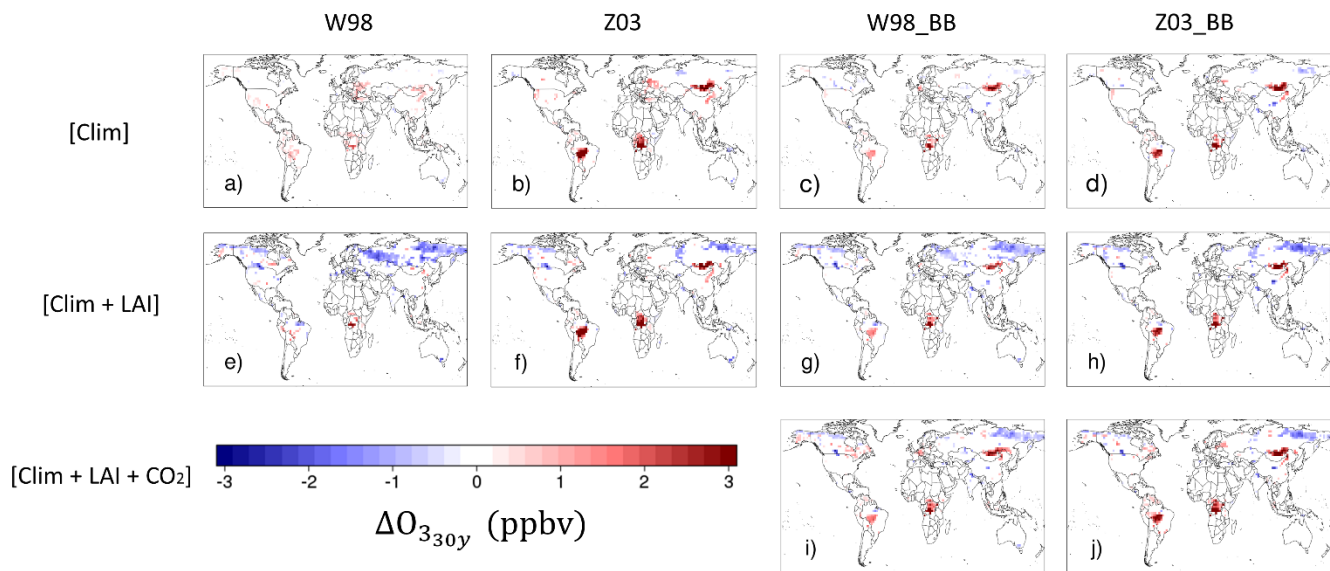
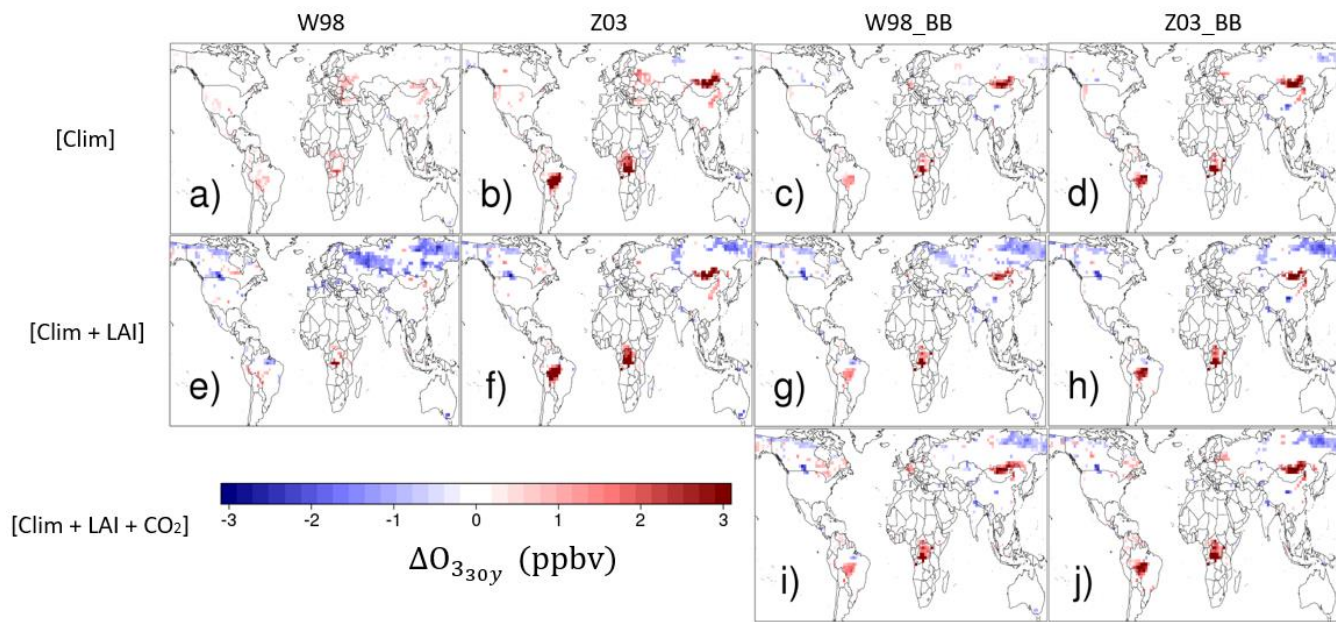


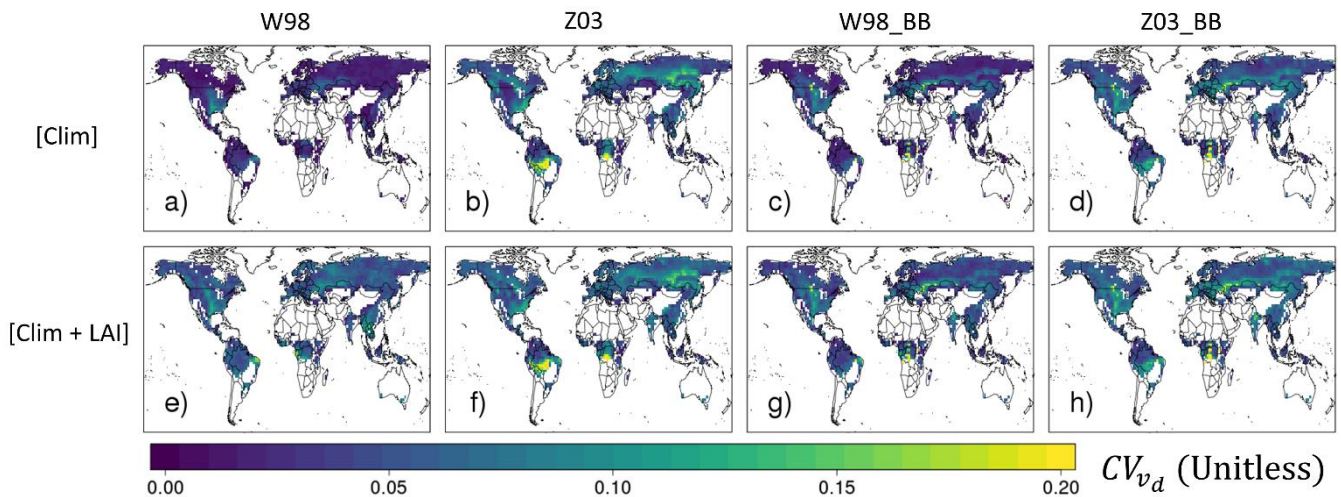
752



753

754 **Figure 8:** Trends of July mean daytime  $v_d$  during 1982-2011 over vegetated land surface. Black dots indicate statistically755 significant trends ( $p < 0.05$ )

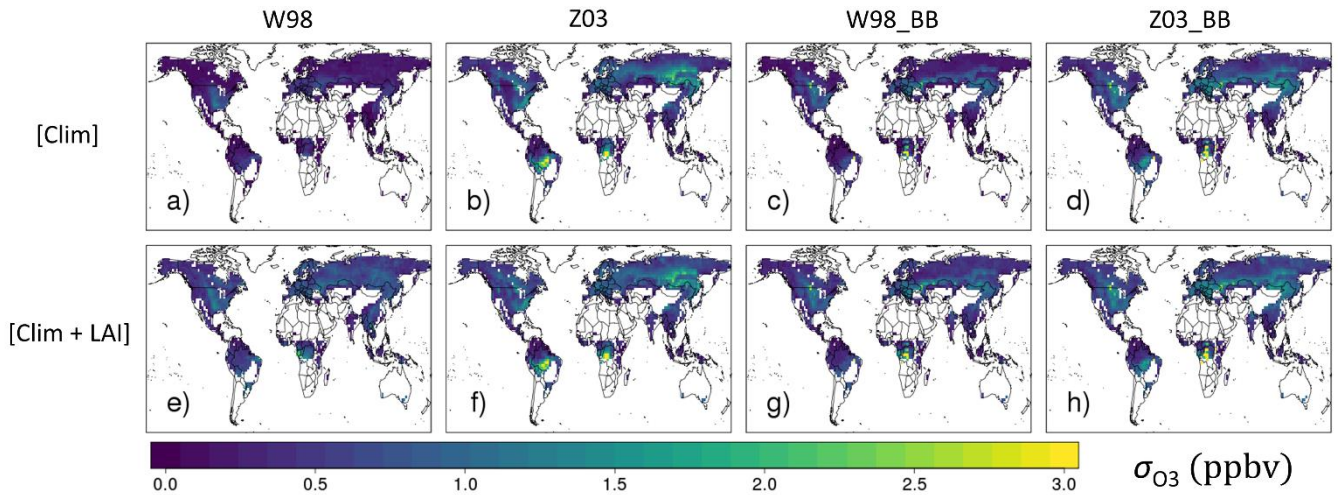




762

763 **Figure 10:** Interannual coefficient of variation of linearly detrended July mean daytime  $v_d$  ( $CV_{v_d}$ ) during 1982-2011 over

764 vegetated land surface.



765

766 **Figure 11:** Estimated contribution of IAV in July mean daytime  $v_d$  to IAV of July mean surface ozone ( $\sigma_{O_3}$ ) during 1982-

767 2011 over vegetated land surface.

768

769

770

771

772

773

774

| $v_d$ simulation            | Meteorology            | LAI                       | Atmospheric CO <sub>2</sub> concentration |
|-----------------------------|------------------------|---------------------------|---|
| [Clim]                      | MERRA-2<br>meteorology | LAI3g monthly climatology | 390 ppm                                   |
| [Clim+LAI]                  |                        | LAI3g monthly time series |   |
| [Clim+LAI+CO <sub>2</sub> ] |                        |                           | Manoa Loa time series                     |

776 **Table 1:** List of  $v_d$  simulations with input data

777

| Land types    | Metrics      | Static LAI   |              |              |               | Dynamic LAI  |              |              |               |
|---------------|--------------|--------------|--------------|--------------|---------------|--------------|--------------|--------------|---------------|
|               |              | W98          | Z03          | W89-BB       | Z03_BB        | W98          | Z03          | W89-BB       | Z03_BB        |
| Dec<br>(N=8)  | <i>NMBF</i>  | <b>0.134</b> | -0.367       | -0.287       | -0.142        | <b>0.119</b> | -0.376       | -0.299       | -0.153        |
|               | <i>NMAEF</i> | 0.322        | 0.369        | 0.305        | <b>0.215</b>  | 0.319        | 0.376        | 0.321        | <b>0.226</b>  |
| Con<br>(N=16) | <i>NMBF</i>  | -0.362       | -0.217       | -0.252       | <b>-0.025</b> | -0.355       | -0.209       | -0.248       | <b>-0.023</b> |
|               | <i>NMAEF</i> | 0.448        | 0.455        | 0.483        | <b>0.399</b>  | 0.427        | 0.458        | 0.470        | <b>0.394</b>  |
| Tro<br>(N=5)  | <i>NMBF</i>  | <b>0.080</b> | -0.808       | -0.086       | -0.438        | <b>0.075</b> | -0.813       | -0.090       | -0.441        |
|               | <i>NMAEF</i> | 0.423        | 0.831        | <b>0.404</b> | 0.569         | 0.422        | 0.832        | <b>0.399</b> | 0.567         |
| Gra<br>(N=10) | <i>NMBF</i>  | 0.276        | <b>0.015</b> | 0.175        | 0.097         | 0.294        | <b>0.011</b> | 0.186        | 0.110         |
|               | <i>NMAEF</i> | 0.392        | 0.479        | <b>0.307</b> | 0.318         | 0.396        | 0.467        | <b>0.302</b> | 0.311         |
| Cro<br>(N=11) | <i>NMBF</i>  | 0.297        | 0.360        | <b>0.241</b> | 0.282         | 0.318        | 0.371        | <b>0.255</b> | 0.292         |
|               | <i>NMAEF</i> | <b>0.473</b> | 0.541        | 0.474        | 0.570         | 0.485        | 0.550        | <b>0.480</b> | 0.576         |

778 **Table 2:** Performance metrics (*NMBF* and *NMAEF*) for daytime average  $v_d$  simulated by the four dry deposition

779 parameterizations-, with  $N$  referring to number of data points (1 data points = 1 seasonal mean). “Static LAI” is the result  
780 from [Clim] run, which uses 1982-2011 AVHRR monthly climatological LAI, while “Dynamic LAI” is the result from  
781 [Clim+LAI], which uses 1982-2011 AVHRR LAI time series. Dec = deciduous forest, Con = coniferous forest, Tro =  
782 tropical rainforest, Gra = grassland, Cro = cropland.  $N$  indicates the number of observational datasets involved in that  
783 particular land type. The best performing parameterization for each land type has its performance metrics bolded.

784

785

786

787

788

789

790 **References**

- 791 Ainsworth, E. A. and Rogers, A.: The response of photosynthesis and stomatal conductance to rising [CO<sub>2</sub>]: Mechanisms and  
792 environmental interactions, *Plant, Cell Environ.*, 30(3), 258–270, doi:10.1111/j.1365-3040.2007.01641.x, 2007.
- 793 Ainsworth, E. A., Yendrek, C. R., Sitch, S., Collins, W. J. and Emberson, L. D.: The Effects of Tropospheric Ozone on Net  
794 Primary Productivity and Implications for Climate Change, *Annu. Rev. Plant Biol.*, 63(1), 637–661, doi:10.1146/annurev-  
795 arplant-042110-103829, 2012.
- 796 Altimir, N., Kolari, P., Tuovinen, J.-P., Vesala, T., Bäck, J., Suni, T., Kulmala, M. and Hari, P.: Foliage surface ozone  
797 deposition: a role for surface moisture?, *Biogeosciences Discuss.*, 2, 1739–1793, doi:10.5194/bg-d-2-1739-2005, 2006.
- 798 Ashworth, K., Chung, S. H., Griffin, R. J., Chen, J., Forkel, R., Bryan, A. M. and Steiner, A. L.: FORest Canopy Atmosphere  
799 Transfer (FORCAsT) 1.0: A 1-D model of biosphere-atmosphere chemical exchange, *Geosci. Model Dev.*, doi:10.5194/gmd-  
800 8-3765-2015, 2015.
- 801 Avnery, S., Mauzerall, D. L., Liu, J. and Horowitz, L. W.: Global crop yield reductions due to surface ozone exposure: 1. Year  
802 2000 crop production losses and economic damage, *Atmos. Environ.*, 45(13), 2284–2296,  
803 doi:10.1016/j.atmosenv.2010.11.045, 2011.
- 804 Baldocchi, D., Falge, E., Gu, L., Olson, R., Hollinger, D., Running, S., Anthoni, P., Bernhofer, C., Davis, K., Evans, R.,  
805 Fuentes, J., Goldstein, A., Katul, G., Law, B., Lee, X., Malhi, Y., Meyers, T., Munger, W., Oechel, W., Paw, U. K. T.,  
806 Pilegaard, K., Schmid, H. P., Valentini, R., Verma, S., Vesala, T., Wilson, K. and Wofsy, S.: FLUXNET: A New Tool to  
807 Study the Temporal and Spatial Variability of Ecosystem-Scale Carbon Dioxide, Water Vapor, and Energy Flux Densities,  
808 *Bull. Am. Meteorol. Soc.*, doi:10.1175/1520-0477(2001)082<2415:FANTTS>2.3.CO;2, 2001.
- 809 Baldocchi, D. D., Hicks, B. B. and Camara, P.: A canopy stomatal resistance model for gaseous deposition to vegetated  
810 surfaces, *Atmos. Environ.*, 21(1), 91–101, doi:10.1016/0004-6981(87)90274-5, 1987.
- 811 Ball, J. T., Woodrow, I. E. and Berry, J. A.: A Model Predicting Stomatal Conductance and its Contribution to the Control of  
812 Photosynthesis under Different Environmental Conditions, in *Progress in Photosynthesis Research*, pp. 221–224., 1987.
- 813 Brook, J. R., Zhang, L., Di-Giovanni, F. and Padro, J.: Description and evaluation of a model of deposition velocities for  
814 routine estimates of air pollutant dry deposition over North America. Part I: Model development, *Atmos. Environ.*,  
815 doi:10.1016/S1352-2310(99)00250-2, 1999.
- 816 Brown-Steiner, B., Selin, N. E., Prinn, R. G., Monier, E., Tilmes, S., Emmons, L. and Garcia-Menendez, F.: Maximizing ozone  
817 signals among chemical, meteorological, and climatological variability, *Atmos. Chem. Phys.*, doi:10.5194/acp-18-8373-2018,  
818 2018.
- 819 Centoni, F.: Global scale modelling of ozone deposition processes and interaction between surface ozone and climate change  
820 A thesis presented for the degree The University of Edinburgh, University of Edinburgh., 2017.
- 821 Chen, B., Black, T. A., Coops, N. C., Hilker, T., Trofymow, J. A. and Morgenstern, K.: Assessing tower flux footprint  
822 climatology and scaling between remotely sensed and eddy covariance measurements, *Boundary-Layer Meteorol.*,

823 doi:10.1007/s10546-008-9339-1, 2009.

824 Chen, B., Coops, N. C., Fu, D., Margolis, H. A., Amiro, B. D., Black, T. A., Arain, M. A., Barr, A. G., Bourque, C. P. A.,  
825 Flanagan, L. B., Lafleur, P. M., McCaughey, J. H. and Wofsy, S. C.: Characterizing spatial representativeness of flux tower  
826 eddy-covariance measurements across the Canadian Carbon Program Network using remote sensing and footprint analysis,  
827 *Remote Sens. Environ.*, doi:10.1016/j.rse.2012.06.007, 2012.

828 Clifton, O. E., Fiore, A. M., Munger, J. W., Malyshev, S., Horowitz, L. W., Shevliakova, E., Paulot, F., Murray, L. T. and  
829 Griffin, K. L.: Interannual variability in ozone removal by a temperate deciduous forest, *Geophys. Res. Lett.*, 44(1), 542–552,  
830 doi:10.1002/2016GL070923, 2017.

831 Clifton, O. E., Fiore, A. M., Munger, J. W. and Wehr, R.: Spatiotemporal controls on observed daytime ozone deposition  
832 velocity over Northeastern U.S. forests during summer., 2019.

833 Coe, H., Gallagher, M. W., Choulaton, T. W. and Dore, C.: Canopy scale measurements of stomatal and cuticular O<sub>3</sub> uptake  
834 by sitka spruce, *Atmos. Environ.*, doi:10.1016/1352-2310(95)00034-V, 1995.

835 Collatz, G., Ribas-Carbo, M. and Berry, J.: Coupled Photosynthesis-Stomatal Conductance Model for Leaves of C<sub>4</sub> Plants,  
836 *Aust. J. Plant Physiol.*, 19(5), 519, doi:10.1071/PP9920519, 1992.

837 Collatz, G. J., Ball, J. T., Grivet, C. and Berry, J. A.: Physiological and environmental regulation of stomatal conductance,  
838 photosynthesis and transpiration: a model that includes a laminar boundary layer, *Agric. For. Meteorol.*, 54(2–4), 107–136,  
839 doi:10.1016/0168-1923(91)90002-8, 1991.

840 Coyle, M., Nemitz, E., Storeton-West, R., Fowler, D. and Cape, J. N.: Measurements of ozone deposition to a potato canopy,  
841 *Agric. For. Meteorol.*, doi:10.1016/j.agrformet.2008.10.020, 2009.

842 Dai, Y., Shangguan, W., Wei, N., Xin, Q., Yuan, H., Zhang, S. and Liu, S.: SOIL A review of the global soil property maps  
843 for Earth system models, , (2016), 137–158, 2019.

844 Droppo, J. G.: Concurrent measurements of ozone dry deposition using eddy correlation and profile flux methods., *J. Geophys.*  
845 *Res.*, doi:10.1029/JD090iD01p02111, 1985.

846 Ducker, J. A., Holmes, C. D., Keenan, T. F., Fares, S., Goldstein, A. H., Mammarella, I., William Munger, J. and Schnell, J.:  
847 Synthetic ozone deposition and stomatal uptake at flux tower sites, *Biogeosciences*, doi:10.5194/bg-15-5395-2018, 2018.

848 Emberson, L. D., Wieser, G. and Ashmore, M. R.: Modelling of stomatal conductance and ozone flux of Norway spruce:  
849 Comparison with field data, in *Environmental Pollution.*, 2000.

850 Fang, H., Li, W. and Myneni, R. B.: The impact of potential land cover misclassification on modis leaf area index (LAI)  
851 estimation: A statistical perspective, *Remote Sens.*, doi:10.3390/rs5020830, 2013.

852 Fares, S., McKay, M., Holzinger, R. and Goldstein, A. H.: Ozone fluxes in a *Pinus ponderosa* ecosystem are dominated by  
853 non-stomatal processes: Evidence from long-term continuous measurements, *Agric. For. Meteorol.*, 150(3), 420–431,  
854 doi:10.1016/j.agrformet.2010.01.007, 2010.

855 Fares, S., Savi, F., Muller, J., Matteucci, G. and Paoletti, E.: Simultaneous measurements of above and below canopy ozone  
856 fluxes help partitioning ozone deposition between its various sinks in a Mediterranean Oak Forest, *Agric. For. Meteorol.*, 198,



857 181–191, doi:10.1016/j.agrformet.2014.08.014, 2014.

858 Fares, S., Conte, A. and Chabbi, A.: Ozone flux in plant ecosystems: new opportunities for long-term monitoring networks to  
859 deliver ozone-risk assessments, *Environ. Sci. Pollut. Res.*, 1–9, doi:10.1007/s11356-017-0352-0, 2017.

860 Farquhar, G. D., Von Caemmerer, S. and Berry, J. A.: A Biochemical Model of Photosynthetic CO<sub>2</sub> Assimilation in Leaves  
861 of C<sub>3</sub> Species, *Planta*, 149, 78–90, doi:10.1007/BF00386231, 1980.

862 Finkelstein, P. L., Ellestad, T. G., Clarke, J. F., Meyers, T. P., Schwede, D. B., Hebert, E. O. and Neal, J. A.: Ozone and sulfur  
863 dioxide dry deposition to forests: Observations and model evaluation, *J. Geophys. Res. Atmos.*, doi:10.1029/2000JD900185,  
864 2000.

865 Fiore, A. M., Oberman, J. T., Lin, M. Y., Zhang, L., Clifton, O. E., Jacob, D. J., Naik, V., Horowitz, L. W., Pinto, J. P. and  
866 Milly, G. P.: Estimating North American background ozone in U.S. surface air with two independent global models:  
867 Variability, uncertainties, and recommendations, *Atmos. Environ.*, doi:10.1016/j.atmosenv.2014.07.045, 2014.

868 Foken, T.: 50 years of the Monin-Obukhov similarity theory, *Boundary-Layer Meteorol.*, doi:10.1007/s10546-006-9048-6,  
869 2006.

870 Fowler, D., Flechard, C., Cape, J. N., Storeton-West, R. L. and Coyle, M.: Measurements of ozone deposition to vegetation  
871 quantifying the flux, the stomatal and non-stomatal components, *Water, Air, Soil Pollut.*, doi:10.1023/A:1012243317471,  
872 2001.

873 Fowler, D., Nemitz, E., Misztal, P., di Marco, C., Skiba, U., Ryder, J., Helfter, C., Neil Cape, J., Owen, S., Dorsey, J.,  
874 Gallagher, M. W., Coyle, M., Phillips, G., Davison, B., Langford, B., MacKenzie, R., Muller, J., Siong, J., Dari-Salisburgo,  
875 C., di Carlo, P., Aruffo, E., Giammaria, F., Pyle, J. A. and Nicholas Hewitt, C.: Effects of land use on surface-atmosphere  
876 exchanges of trace gases and energy in Borneo: Comparing fluxes over oil palm plantations and a rainforest, *Philos. Trans. R.  
877 Soc. B Biol. Sci.*, doi:10.1098/rstb.2011.0055, 2011.

878 Franks, P. J., Adams, M. A., Amthor, J. S., Barbour, M. M., Berry, J. A., Ellsworth, D. S., Farquhar, G. D., Ghannoum, O.,  
879 Lloyd, J., McDowell, N., Norby, R. J., Tissue, D. T. and von Caemmerer, S.: Sensitivity of plants to changing atmospheric  
880 CO<sub>2</sub> concentration: From the geological past to the next century, *New Phytol.*, 197(4), 1077–1094, doi:10.1111/nph.12104,  
881 2013.

882 Fu, Y. and Tai, A. P. K.: Impact of climate and land cover changes on tropospheric ozone air quality and public health in East  
883 Asia between 1980 and 2010, *Atmos. Chem. Phys.*, 15(17), 10093–10106, doi:10.5194/acp-15-10093-2015, 2015.

884 Ganzeveld, L., Bouwman, L., Stehfest, E., van Vuuren, D. P., Eickhout, B. and Lelieveld, J.: Impact of future land use and  
885 land cover changes on atmospheric chemistry-climate interactions, *J. Geophys. Res.*, 115(D23), D23301,  
886 doi:10.1029/2010JD014041, 2010.

887 Gao, W. and Wesely, M. L.: Modeling gaseous dry deposition over regional scales with satellite observations-I. Model  
888 development, *Atmos. Environ.*, 29(6), 727–737, doi:10.1016/1352-2310(94)00284-R, 1995.

889 Geddes, J. A. and Martin, R. V.: Global deposition of total reactive nitrogen oxides from 1996 to 2014 constrained with satellite  
890 observations of NO<sub>2</sub> columns, *Atmos. Chem. Phys.*, doi:10.5194/acp-17-10071-2017, 2017.

891 Geddes, J. A., Heald, C. L., Silva, S. J. and Martin, R. V.: Land cover change impacts on atmospheric chemistry: Simulating  
892 projected large-scale tree mortality in the United States, *Atmos. Chem. Phys.*, 16(4), 2323–2340, doi:10.5194/acp-16-2323-  
893 2016, 2016.

894 Gelaro, R., McCarty, W., Suárez, M. J., Todling, R., Molod, A., Takacs, L., Randles, C. A., Darmenov, A., Bosilovich, M. G.,  
895 Reichle, R., Wargan, K., Coy, L., Cullather, R., Draper, C., Akella, S., Buchard, V., Conaty, A., da Silva, A. M., Gu, W., Kim,  
896 G. K., Koster, R., Lucchesi, R., Merkova, D., Nielsen, J. E., Partyka, G., Pawson, S., Putman, W., Rienecker, M., Schubert, S.  
897 D., Sienkiewicz, M. and Zhao, B.: The modern-era retrospective analysis for research and applications, version 2 (MERRA-  
898 2), *J. Clim.*, 30(14), 5419–5454, doi:10.1175/JCLI-D-16-0758.1, 2017.

899 Gerosa, G., Vitale, M., Finco, A., Manes, F., Denti, A. B. and Cieslik, S.: Ozone uptake by an evergreen Mediterranean Forest  
900 (*Quercus ilex*) in Italy. Part I: Micrometeorological flux measurements and flux partitioning, *Atmos. Environ.*, 39(18), 3255–  
901 3266, doi:10.1016/j.atmosenv.2005.01.056, 2005.

902 Gerosa, G., Marzuoli, R., Monteleone, B., Chiesa, M. and Finco, A.: Vertical ozone gradients above forests. Comparison of  
903 different calculation options with direct ozone measurements above a mature forest and consequences for ozone risk  
904 assessment, *Forests*, 8(9), doi:10.3390/f8090337, 2017.

905 Hardacre, C., Wild, O. and Emberson, L.: An evaluation of ozone dry deposition in global scale chemistry climate models,  
906 *Atmos. Chem. Phys.*, 15(11), 6419–6436, doi:10.5194/acp-15-6419-2015, 2015.

907 Heald, C. L. and Geddes, J. A.: The impact of historical land use change from 1850 to 2000 on secondary particulate matter  
908 and ozone, *Atmos. Chem. Phys.*, doi:10.5194/acp-16-14997-2016, 2016.

909 Hole, L. R., Semb, A. and Tørseth, K.: Ozone deposition to a temperate coniferous forest in Norway; gradient method  
910 measurements and comparison with the EMEP deposition module, in *Atmospheric Environment.*, 2004.

911 Hollaway, M. J., Arnold, S. R., Collins, W. J., Folberth, G. and Rap, A.: Sensitivity of midnineteenth century tropospheric  
912 ozone to atmospheric chemistry-vegetation interactions, *J. Geophys. Res. Atmos.*, 122(4), 2452–2473,  
913 doi:10.1002/2016JD025462, 2017.

914 Hoshika, Y., Carriero, G., Feng, Z., Zhang, Y. and Paoletti, E.: Determinants of stomatal sluggishness in ozone-exposed  
915 deciduous tree species, *Sci. Total Environ.*, 481(1), 453–458, doi:10.1016/j.scitotenv.2014.02.080, 2014.

916 Hu, L., Jacob, D. J., Liu, X., Zhang, Y., Zhang, L., Kim, P. S., Sulprizio, M. P. and Yantosca, R. M.: Global budget of  
917 tropospheric ozone: Evaluating recent model advances with satellite (OMI), aircraft (IAGOS), and ozonesonde observations,  
918 *Atmos. Environ.*, 167, 323–334, doi:10.1016/j.atmosenv.2017.08.036, 2017.

919 Huang, L., McDonald-Buller, E. C., McGaughy, G., Kimura, Y. and Allen, D. T.: The impact of drought on ozone dry  
920 deposition over eastern Texas, *Atmos. Environ.*, 127, 176–186, doi:10.1016/j.atmosenv.2015.12.022, 2016.

921 Jacob, D. J. and Wofsy, S. C.: Budgets of Reactive Nitrogen, Hydrocarbons, and Ozone Over the Amazon Forest during the  
922 Wet Season, *J. Geophys. Res.*, 95, 16737–16754, doi:10.1029/JD095iD10p16737, 1990.

923 Jacob, D. J., Fan, S.-M., Wofsy, S. C., Spiro, P. A., Bakwin, P. S., Ritter, J. A., Browell, E. V., Gregory, G. L., Fitzjarrald, D.  
924 R. and Moore, K. E.: Deposition of ozone to tundra, *J. Geophys. Res.*, doi:10.1029/91JD02696, 1992.

925 Jarvis, P. G.: The Interpretation of the Variations in Leaf Water Potential and Stomatal Conductance Found in Canopies in the  
926 Field, *Philos. Trans. R. Soc. B Biol. Sci.*, 273(927), 593–610, doi:10.1098/rstb.1976.0035, 1976.

927 Jerrett, M., Burnett, R. T., Pope, C. A., Ito, K., Thurston, G., Krewski, D., Shi, Y., Calle, E. and Thun, M.: Long-Term Ozone  
928 Exposure and Mortality, *N. Engl. J. Med.*, 360(11), 1085–1095, doi:10.1056/NEJMoa0803894, 2009.

929 Jiang, C., Ryu, Y., Fang, H., Myneni, R., Claverie, M. and Zhu, Z.: Inconsistencies of interannual variability and trends in  
930 long-term satellite leaf area index products, *Glob. Chang. Biol.*, doi:10.1111/gcb.13787, 2017.

931 Junninen, H., Lauri, A., Keronen, P., Aalto, P., Hiltunen, V., Hari, P. and Kulmala, M.: Smart-SMEAR: On-line data  
932 exploration and visualization tool for SMEAR stations, *Boreal Environ. Res.*, 14(4), 447–457, 2009.

933 Kattge, J. and Knorr, W.: Temperature acclimation in a biochemical model of photosynthesis: A reanalysis of data from 36  
934 species, *Plant, Cell Environ.*, 30(9), 1176–1190, doi:10.1111/j.1365-3040.2007.01690.x, 2007.

935 Kavassalis, S. C. and Murphy, J. G.: Understanding ozone-meteorology correlations: A role for dry deposition, *Geophys. Res.  
936 Lett.*, 44(6), 2922–2931, doi:10.1002/2016GL071791, 2017.

937 Keeling, C. D., Stephen, C., Piper, S. C., Bacastow, R. B., Wahlen, M., Whorf, T. P., Heimann, M. and Meijer, H. a.: Exchanges  
938 of atmospheric CO<sub>2</sub> and <sup>13</sup>CO<sub>2</sub> with the terrestrial biosphere and oceans from 1978 to 2000, *Glob. Asp. SIO Ref. Ser. Scripps  
939 Inst. Ocean. San Diego*, doi:10.1007/b138533, 2001.

940 Keronen, P., Reissell, a, Rannik, Ü., Pohja, T., Siivola, E., Hiltunen, V., Hari, P., Kulmala, M. and Vesala, T.: Ozone flux  
941 measurements over a Scots pine forest using eddy covariance method: Performance evaluation and comparison with flux-  
942 profile method, *Boreal Environ. Res.*, 8(4), 425–443 [online] Available from:  
943 [http://www.scopus.com/inward/record.url?eid=2-s2.0-  
944 0347884158&partnerID=40&md5=4ad114fb52c557d36cc8a0ec1ab8bb7e](http://www.scopus.com/inward/record.url?eid=2-s2.0-0347884158&partnerID=40&md5=4ad114fb52c557d36cc8a0ec1ab8bb7e), 2003.

945 Kharol, S. K., Shephard, M. W., Mclinden, C. A., Zhang, L., Sioris, C. E., O'Brien, J. M., Vet, R., Cady-Pereira, K. E., Hare,  
946 E., Siemons, J. and Krotkov, N. A.: Dry Deposition of Reactive Nitrogen From Satellite Observations of Ammonia and  
947 Nitrogen Dioxide Over North America, *Geophys. Res. Lett.*, doi:10.1002/2017GL075832, 2018.

948 Kurpius, M. R., McKay, M. and Goldstein, A. H.: Annual ozone deposition to a Sierra Nevada ponderosa pine plantation,  
949 *Atmos. Environ.*, doi:10.1016/S1352-2310(02)00423-5, 2002.

950 Lamaud, E., Brunet, Y., Labatut, A., Lopez, A., Fontan, J. and Druilhet, A.: The Landes experiment: Biosphere-atmosphere  
951 exchanges of ozone and aerosol particles above a pine forest, *J. Geophys. Res.*, doi:10.1029/94JD00668, 1994.

952 Lamaud, E., Carrara, A., Brunet, Y., Lopez, A. and Druilhet, A.: Ozone fluxes above and within a pine forest canopy in dry  
953 and wet conditions, *Atmos. Environ.*, 36(1), 77–88, doi:10.1016/S1352-2310(01)00468-X, 2002.

954 Lawrence, P. J. and Chase, T. N.: Representing a new MODIS consistent land surface in the Community Land Model (CLM  
955 3.0), *J. Geophys. Res. Biogeosciences*, 112(1), doi:10.1029/2006JG000168, 2007.

956 Li, D., Bou-Zeid, E., Barlage, M., Chen, F. and Smith, J. A.: Development and evaluation of a mosaic approach in the WRF-  
957 Noah framework, *J. Geophys. Res. Atmos.*, 118(21), 11918–11935, doi:10.1002/2013JD020657, 2013.

958 Lin, Y., Medlyn, B. and Duursma, R.: Optimal stomatal behaviour around the world, *Nat. Clim. ...*, (March), 1–6,

959 doi:10.1038/NCLIMATE2550, 2015.

960 Lombardozzi, D., Sparks, J. P., Bonan, G. and Levis, S.: Ozone exposure causes a decoupling of conductance and  
961 photosynthesis: Implications for the Ball-Berry stomatal conductance model, *Oecologia*, 169(3), 651–659,  
962 doi:10.1007/s00442-011-2242-3, 2012.

963 Lombardozzi, D., Levis, S., Bonan, G., Hess, P. G. and Sparks, J. P.: The influence of chronic ozone exposure on global carbon  
964 and water cycles, *J. Clim.*, 28(1), 292–305, doi:10.1175/JCLI-D-14-00223.1, 2015.

965 Malhi, Y., Roberts, J. T., Betts, R. A., Killeen, T. J., Li, W. and Nobre, C. A.: Climate change, deforestation, and the fate of  
966 the Amazon, *Science* (80-. ), doi:10.1126/science.1146961, 2008.

967 Mao, J., Paulot, F., Jacob, D. J., Cohen, R. C., Crounse, J. D., Wennberg, P. O., Keller, C. A., Hudman, R. C., Barkley, M. P.  
968 and Horowitz, L. W.: Ozone and organic nitrates over the eastern United States: Sensitivity to isoprene chemistry, *J. Geophys.*  
969 *Res. Atmos.*, 118(19), 11256–11268, doi:10.1002/jgrd.50817, 2013.

970 Matsuda, K., Watanabe, I., Wingpud, V., Theramongkol, P., Khummongkol, P., Wangwongwatana, S. and Totsuka, T.: Ozone  
971 dry deposition above a tropical forest in the dry season in northern Thailand, *Atmos. Environ.*, 39(14), 2571–2577,  
972 doi:10.1016/j.atmosenv.2005.01.011, 2005.

973 McGrath, J. M., Betzelberger, A. M., Wang, S., Shook, E., Zhu, X.-G., Long, S. P. and Ainsworth, E. A.: An analysis of ozone  
974 damage to historical maize and soybean yields in the United States, *Proc. Natl. Acad. Sci.*, 112(46), 14390–14395,  
975 doi:10.1073/pnas.1509777112, 2015.

976 Mészáros, R., Horváth, L., Weidinger, T., Neftel, A., Nemitz, E., Dammgen, U., Cellier, P. and Loubet, B.: Measurement and  
977 modelling ozone fluxes over a cut and fertilized grassland, *Biogeosciences*, doi:10.1029/2002GL016785

978 Meyers, T. P., Finkelstein, P., Clarke, J., Ellestad, T. G. and Sims, P. F.: A multilayer model for inferring dry deposition using  
979 standard meteorological measurements, *J. Geophys. Res.*, 103(98), 22645, doi:10.1029/98JD01564, 1998.

980 Mikkelsen, T. N., Ro-Poulsen, H., Hovmand, M. F., Jensen, N. O., Pilegaard, K. and Egeløv, A. H.: Five-year measurements  
981 of ozone fluxes to a Danish Norway spruce canopy, in *Atmospheric Environment.*, 2004.

982 Muller, J. B. A., Percival, C. J., Gallagher, M. W., Fowler, D., Coyle, M. and Nemitz, E.: Sources of uncertainty in eddy  
983 covariance ozone flux measurements made by dry chemiluminescence fast response analysers, *Atmos. Meas. Tech.*,  
984 doi:10.5194/amt-3-163-2010, 2010.

985 Munger, J. W., Wofsy, S. C., Bakwin, P. S., Fan, S.-M., Goulden, M. L., Daube, B. C., Goldstein, A. H., Moore, K. E. and  
986 Fitzjarrald, D. R.: Atmospheric deposition of reactive nitrogen oxides and ozone in a temperate deciduous forest and a subarctic  
987 woodland 1. Measurements and mechanisms, *J. Geophys. Res.*, 101657(20), 639–12, doi:10.1029/96JD00230, 1996.

988 Myneni, R. B., Hoffman, S., Knyazikhin, Y., Privette, J. L., Glassy, J., Tian, Y., Wang, Y., Song, X., Zhang, Y., Smith, G. R.,  
989 Lotsch, A., Friedl, M., Morisette, J. T., Votava, P., Nemani, R. R. and Running, S. W.: Global products of vegetation leaf area  
990 and fraction absorbed PAR from year one of MODIS data, *Remote Sens. Environ.*, 83(1–2), 214–231, doi:10.1016/S0034-  
991 4257(02)00074-3, 2002.

992 Norby, R. J. and Zak, D. R.: Ecological Lessons from Free-Air CO<sub>2</sub> Enrichment (FACE) Experiments, *Annu. Rev. Ecol. Evol.*

993 Syst., doi:10.1146/annurev-ecolsys-102209-144647, 2011.

994 Nowlan, C. R., Martin, R. V., Philip, S., Lamsal, L. N., Krotkov, N. A., Marais, E. A., Wang, S. and Zhang, Q.: Global dry  
995 deposition of nitrogen dioxide and sulfur dioxide inferred from space-based measurements, *Global Biogeochem. Cycles*,  
996 doi:10.1002/2014GB004805, 2014.

997 Oleson, K. W., Lawrence, D. M., Bonan, G. B., Drewniak, B., Huang, M., Koven, C. D., Levis, S., Li, F., Riley, J., Subin, Z.  
998 M., Swenson, S. C., Thornton, P. E., Bozbiyik, A., Fisher, R. A., Heald, C. L., Kluzek, E., Lamarque, J.-F., Lawrence, P. J.,  
999 Leung, L. R., Lipscomb, W., Muszala, S., Ricciuto, D. M., Sacks, W. J., Sun, Y., Tang, J. and Yang, Z.-L.: Technical  
1000 Description of version 4.5 of the Community Land Model (CLM)., 2013.

1001 Olson, D. M., Dinerstein, E., Wikramanayake, E. D., Burgess, N. D., Powell, G. V. N., Underwood, E. C., D'amico, J. A.,  
1002 Itoua, I., Strand, H. E., Morrison, J. C., Loucks, C. J., Allnutt, T. F., Ricketts, T. H., Kura, Y., Lamoreux, J. F., Wettengel, W.  
1003 W., Hedao, P. and Kassem, K. R.: Terrestrial Ecoregions of the World: A New Map of Life on Earth, *Bioscience*,  
1004 doi:10.1641/0006-3568(2001)051[0933:TEOTWA]2.0.CO;2, 2001.

1005 Padro, J., den Hartog, G. and Neumann, H. H.: An investigation of the ADOM dry deposition module using summertime  
1006 O<sub>3</sub>measurements above a deciduous forest, *Atmos. Environ. Part A, Gen. Top.*, doi:10.1016/0960-1686(91)90027-5, 1991.

1007 Padro, J., Massman, W. J., Shaw, R. H., Delany, A. and Oncley, S. P.: A comparison of some aerodynamic resistance methods  
1008 using measurements over cotton and grass from the 1991 California ozone deposition experiment, *Boundary-Layer Meteorol.*,  
1009 doi:10.1007/BF00712174, 1994.

1010 Paulson, C. A.: The Mathematical Representation of Wind Speed and Temperature Profiles in the Unstable Atmospheric  
1011 Surface Layer, *J. Appl. Meteorol.*, doi:10.1175/1520-0450(1970)009<0857:tmrows>2.0.co;2, 2002.

1012 Pilegaard, K., Hummelshøj, P. and Jensen, N. O.: Fluxes of ozone and nitrogen dioxide measured by eddy correlation over a  
1013 harvested wheat field, *Atmos. Environ.*, doi:10.1016/S1352-2310(97)00194-5, 1998.

1014 Pio, C. ., Feliciano, M. ., Vermeulen, A. . and Sousa, E. .: Seasonal variability of ozone dry deposition under southern European  
1015 climate conditions, in Portugal, *Atmos. Environ.*, doi:10.1016/S1352-2310(99)00276-9, 2000.

1016 Pleim, J. and Ran, L.: Surface flux modeling for air quality applications, *Atmosphere (Basel)*, 2(3), 271–302,  
1017 doi:10.3390/atmos2030271, 2011.

1018 Potier, E., Ogée, J., Jouanguy, J., Lamaud, E., Stella, P., Personne, E., Durand, B., Mascher, N. and Loubet, B.: Multilayer  
1019 modelling of ozone fluxes on winter wheat reveals large deposition on wet senescing leaves, *Agric. For. Meteorol.*, 211–212,  
1020 58–71, doi:10.1016/j.agrformet.2015.05.006, 2015.

1021 Potier, E., Loubet, B., Durand, B., Flura, D., Bourdat-Deschamps, M., Ciuraru, R. and Ogée, J.: Chemical reaction rates of  
1022 ozone in water infusions of wheat, beech, oak and pine leaves of different ages, *Atmos. Environ.*, 151, 176–187,  
1023 doi:10.1016/j.atmosenv.2016.11.069, 2017.

1024 R core team: R: A language and environment for statistical computing., R Found. Stat. Comput. Vienna, Austria.,  
1025 doi:http://www.R-project.org/, 2017.

1026 Ran, L., Pleim, J., Song, C., Band, L., Walker, J. T. and Binkowski, F. S.: A photosynthesis-based two-leaf canopy stomatal

1027 conductance model for meteorology and air quality modeling with WRF/CMAQ PX LSM, *J. Geophys. Res.*, 122(3), 1930–  
1028 1952, doi:10.1002/2016JD025583, 2017a.

1029 Ran, L., Pleim, J., Song, C., Band, L., Walker, J. T. and Binkowski, F. S.: A photosynthesis-based two-leaf canopy stomatal  
1030 conductance model for meteorology and air quality modeling with WRF/CMAQ PX LSM, *J. Geophys. Res.*, 122(3), 1930–  
1031 1952, doi:10.1002/2016JD025583, 2017b.

1032 Rannik, Ü., Altimir, N., Mammarella, I., Bäck, J., Rinne, J., Ruuskanen, T. M., Hari, P., Vesala, T. and Kulmala, M.: Ozone  
1033 deposition into a boreal forest over a decade of observations: Evaluating deposition partitioning and driving variables, *Atmos.*  
1034 *Chem. Phys.*, 12(24), 12165–12182, doi:10.5194/acp-12-12165-2012, 2012.

1035 Reich, P. B.: Quantifying plant response to ozone: a unifying theory, *Tree Physiol.*, 3(0), 63–91, doi:10.1093/treephys/3.1.63,  
1036 1987.

1037 Rienecker, M. M. and Coauthors: The GEOS-5 Data Assimilation System—Documentation of versions 5.0.1 and 5.1.0, and  
1038 5.2.0, NASA Tech. Rep. Ser. Glob. Model. Data Assim. NASA/TM-2008-104606, doi:10.2759/32049, 2008.

1039 Rigden, A. J. and Salvucci, G. D.: Stomatal response to humidity and CO<sub>2</sub> implicated in recent decline in US evaporation,  
1040 *Glob. Chang. Biol.*, doi:10.1111/gcb.13439, 2017.

1041 Rummel, U., Ammann, C., Kirkman, G. A., Moura, M. A. L., Foken, T., Andreae, M. O. and Meixner, F. X.: Seasonal variation  
1042 of ozone deposition to a tropical rain forest in southwest Amazonia, *Atmos. Chem. Phys.*, doi:10.5194/acp-7-5415-2007, 2007.

1043 Sadiq, M., Tai, A. P. K., Lombardozzi, D. and Val Martin, M.: Effects of ozone-vegetation coupling on surface ozone air  
1044 quality via biogeochemical and meteorological feedbacks, *Atmos. Chem. Phys.*, 17(4), 3055–3066, doi:10.5194/acp-17-3055-  
1045 2017, 2017.

1046 Sanderson, M. G., Collins, W. J., Hemming, D. L. and Betts, R. A.: Stomatal conductance changes due to increasing carbon  
1047 dioxide levels: Projected impact on surface ozone levels, *Tellus, Ser. B Chem. Phys. Meteorol.*, 59(3), 404–411,  
1048 doi:10.1111/j.1600-0889.2007.00277.x, 2007.

1049 Sen, P. K.: Estimates of the Regression Coefficient Based on Kendall's Tau, *J. Am. Stat. Assoc.*,  
1050 doi:10.1080/01621459.1968.10480934, 1968.

1051 Silva, S. J. and Heald, C. L.: Investigating Dry Deposition of Ozone to Vegetation, *J. Geophys. Res. Atmos.*, 123(1), 559–573,  
1052 doi:10.1002/2017JD027278, 2018.

1053 Simpson, D., Benedictow, A., Berge, H., Bergström, R., Emberson, L. D., Fagerli, H., Flechard, C. R., Hayman, G. D., Gauss,  
1054 M., Jonson, J. E., Jenkin, M. E., Nyíri, A., Richter, C., Semeena, V. S., Tsyro, S., Tuovinen, J.-P., Valdebenito, A. and Wind,  
1055 P.: The EMEP MSC-W chemical transport model – technical description, *Atmos. Chem. Phys. Atmos. Chem. Phys.*, 12, 7825–  
1056 7865, doi:10.5194/acp-12-7825-2012, 2012.

1057 Sitch, S., Cox, P. M., Collins, W. J. and Huntingford, C.: Indirect radiative forcing of climate change through ozone effects on  
1058 the land-carbon sink, *Nature*, 448(7155), 791–794, doi:10.1038/nature06059, 2007.

1059 Song-Miao, F., Wofsy, S. C., Bakwin, P. S., Jacob, D. J. and Fitzjarrald, D. R.: Atmosphere-biosphere exchange of CO<sub>2</sub> and  
1060 O<sub>3</sub> in the central Amazon forest, *J. Geophys. Res.*, doi:10.1029/JD095iD10p16851, 1990.

1061 Stella, P., Personne, E., Loubet, B., Lamaud, E., Ceschia, E., B??ziat, P., Bonnefond, J. M., Irvine, M., Keravec, P., Mascher,  
1062 N. and Cellier, P.: Predicting and partitioning ozone fluxes to maize crops from sowing to harvest: The Surf atm-O<sub>3</sub> model,  
1063 Biogeosciences, 8(10), 2869–2886, doi:10.5194/bg-8-2869-2011, 2011.

1064 Stocker, D. W., Stedman, D. H., Zeller, K. F., Massman, W. J. and Fox, D. G.: Fluxes of nitrogen oxides and ozone measured  
1065 by eddy correlation over a shortgrass prairie, *J. Geophys. Res.*, doi:10.1029/93JD00871, 1993.

1066 Sun, S., Moravek, A., Trebs, I., Kesselmeier, J. and Sörgel, M.: Investigation of the influence of liquid surface films on O<sub>3</sub>  
1067 and PAN deposition to plant leaves coated with organic/inorganic solution, *J. Geophys. Res. Atmos.*, 121(23), 14,239-14,256,  
1068 doi:10.1002/2016JD025519, 2016.

1069 Sun, Y., Gu, L. and Dickinson, R. E.: A numerical issue in calculating the coupled carbon and water fluxes in a climate model,  
1070 *J. Geophys. Res. Atmos.*, doi:10.1029/2012JD018059, 2012.

1071 Tai, A. P. K., Martin, M. V. and Heald, C. L.: Threat to future global food security from climate change and ozone air pollution,  
1072 *Nat. Clim. Chang.*, 4(9), 817–821, doi:10.1038/nclimate2317, 2014.

1073 Travis, K. R., Jacob, D. J., Fisher, J. A., Kim, P. S., Marais, E. A., Zhu, L., Yu, K., Miller, C. C., Yantosca, R. M., Sulprizio,  
1074 M. P., Thompson, A. M., Wennberg, P. O., Crounse, J. D., St Clair, J. M., Cohen, R. C., Laughner, J. L., Dibb, J. E., Hall, S.  
1075 R., Ullmann, K., Wolfe, G. M., Pollack, I. B., Peischl, J., Neuman, J. A. and Zhou, X.: Why do models overestimate surface  
1076 ozone in the Southeast United States?, *Atmos. Chem. Phys.*, 16(21), 13561–13577, doi:10.5194/acp-16-13561-2016, 2016.

1077 Turnipseed, A. A., Burns, S. P., Moore, D. J. P., Hu, J., Guenther, A. B. and Monson, R. K.: Controls over ozone deposition  
1078 to a high elevation subalpine forest, *Agric. For. Meteorol.*, doi:10.1016/j.agrformet.2009.04.001, 2009.

1079 Val Martin, M., Heald, C. L. and Arnold, S. R.: Coupling dry deposition to vegetation phenology in the {Community} {Earth}  
1080 {System} {Model}: {Implications} for the simulation of surface {O} <sub>3</sub>, *Geophys. Res. Lett.*, 41(8), 2988–2996,  
1081 doi:10.1002/2014GL059651, 2014.

1082 Wang, Y., Jacob, D. J. and Logan, J. A.: Global simulation of tropospheric O<sub>3</sub>-NO<sub>x</sub>-hydrocarbon chemistry: 1. Model  
1083 formulation, *J. Geophys. Res. Atmos.*, 103(D9), 10713–10725, doi:10.1029/98JD00158, 1998.

1084 Wesely, M. L.: Parameterization of surface resistances to gaseous dry deposition in regional-scale numerical models, *Atmos.*  
1085 *Environ.*, 41(SUPPL.), 52–63, doi:10.1016/j.atmosenv.2007.10.058, 1989.

1086 Wesely, M. L. and Hicks, B. B.: Some Factors that Affect the Deposition Rates of Sulfur Dioxide and Similar Gases on  
1087 Vegetation, *J. Air Pollut. Control Assoc.*, 27(11), 1110–1116, doi:10.1080/00022470.1977.10470534, 1977.

1088 Wesely, M. L. and Hicks, B. B.: A review of the current status of knowledge on dry deposition, *Atmos. Environ.*, 34(12–14),  
1089 2261–2282, doi:10.1016/S1352-2310(99)00467-7, 2000.

1090 Wild, O.: Modelling the global tropospheric ozone budget: exploring the variability in current models, *Atmos. Chem. Phys.*,  
1091 7(10), 2643–2660, doi:10.5194/acp-7-2643-2007, 2007.

1092 Wittig, V. E., Ainsworth, E. A. and Long, S. P.: To what extent do current and projected increases in surface ozone affect  
1093 photosynthesis and stomatal conductance of trees? A meta-analytic review of the last 3 decades of experiments, *Plant, Cell*  
1094 *Environ.*, 30(9), 1150–1162, doi:10.1111/j.1365-3040.2007.01717.x, 2007.

1095 Wolfe, G. M., Thornton, J. A., McKay, M. and Goldstein, A. H.: Forest-atmosphere exchange of ozone: Sensitivity to very  
1096 reactive biogenic VOC emissions and implications for in-canopy photochemistry, *Atmos. Chem. Phys.*, doi:10.5194/acp-11-  
1097 7875-2011, 2011.

1098 Wong, A. Y. H., Tai, A. P. K. and Ip, Y.-Y.: Attribution and Statistical Parameterization of the Sensitivity of Surface Ozone  
1099 to Changes in Leaf Area Index Based On a Chemical Transport Model, *J. Geophys. Res. Atmos.*, 1–16,  
1100 doi:10.1002/2017JD027311, 2018.

1101 Wu, S., Mickley, L. J., Kaplan, J. O. and Jacob, D. J.: Impacts of changes in land use and land cover on atmospheric chemistry  
1102 and air quality over the 21st century, *Atmos. Chem. Phys.*, 12(3), 1597–1609, doi:10.5194/acp-12-1597-2012, 2012.

1103 Wu, Z., Wang, X., Chen, F., Turnipseed, A. A., Guenther, A. B., Niyogi, D., Charusombat, U., Xia, B., William Munger, J.  
1104 and Alapaty, K.: Evaluating the calculated dry deposition velocities of reactive nitrogen oxides and ozone from two community  
1105 models over a temperate deciduous forest, *Atmos. Environ.*, 45(16), 2663–2674, doi:10.1016/j.atmosenv.2011.02.063, 2011.

1106 Wu, Z., Staebler, R., Vet, R. and Zhang, L.: Dry deposition of O<sub>3</sub> and SO<sub>2</sub> estimated from gradient measurements above a  
1107 temperate mixed forest, *Environ. Pollut.*, 210, 202–210, doi:10.1016/j.envpol.2015.11.052, 2016.

1108 Wu, Z., Schwede, D. B., Vet, R., Walker, J. T., Shaw, M., Staebler, R. and Zhang, L.: Evaluation and intercomparison of five  
1109 North American dry deposition algorithms at a mixed forest site, *J. Adv. Model. Earth Syst.*, 1–16,  
1110 doi:10.1029/2017MS001231, 2018.

1111 Wu, Z. Y., Zhang, L., Wang, X. M. and Munger, J. W.: A modified micrometeorological gradient method for estimating  
1112 O<sub>3</sub> dry depositions over a forest canopy, *Atmos. Chem. Phys.*, 15(13), 7487–7496, doi:10.5194/acp-  
1113 15-7487-2015, 2015.

1114 Young, P. J., Archibald, A. T., Bowman, K. W., Lamarque, J.-F., Naik, V., Stevenson, D. S., Tilmes, S., Voulgarakis, A.,  
1115 Wild, O., Bergmann, D., Cameron-Smith, P., Cionni, I., Collins, W. J., Dalsøren, S. B., Doherty, R. M., Eyring, V., Faluvegi,  
1116 G., Horowitz, L. W., Josse, B., Lee, Y. H., MacKenzie, I. A., Nagashima, T., Plummer, D. A., Righi, M., Rumbold, S. T.,  
1117 Skeie, R. B., Shindell, D. T., Strode, S. A., Sudo, K., Szopa, S. and Zeng, G.: Pre-industrial to end 21st century projections of  
1118 tropospheric ozone from the Atmospheric Chemistry and Climate Model Intercomparison Project (ACCMIP), *Atmos. Chem.*  
1119 *Phys.*, doi:10.5194/acp-13-2063-2013, 2013.

1120 Yu, S., Eder, B., Dennis, R., Chu, S.-H. and Schwartz, S. E.: New unbiased symmetric metrics for evaluation of air quality  
1121 models, *Atmos. Sci. Lett.*, doi:10.1002/asl.125, 2006.

1122 Zhang, L., Moran, M. D. and Brook, J. R.: A comparison of models to estimate in-canopy photosynthetically active radiation  
1123 and their influence on canopy stomatal resistance, *Atmos. Environ.*, doi:10.1016/S1352-2310(01)00225-4, 2001.

1124 Zhang, L., Brook, J. R. and Vet, R.: On ozone dry deposition - With emphasis on non-stomatal uptake and wet canopies,  
1125 *Atmos. Environ.*, 36(30), 4787–4799, doi:10.1016/S1352-2310(02)00567-8, 2002.

1126 Zhang, L., Brook, J. R. and Vet, R.: A revised parameterization for gaseous dry deposition in air-quality models, *Atmos. Chem.*  
1127 *Phys. Discuss.*, 3(2), 1777–1804, doi:10.5194/acpd-3-1777-2003, 2003.

1128 Zhang, L., Vet, R., O'Brien, J. M., Mihele, C., Liang, Z. and Wiebe, A.: Dry deposition of individual nitrogen species at eight



1129 Canadian rural sites, *J. Geophys. Res. Atmos.*, doi:10.1029/2008JD010640, 2009.

1130 Zhang, L., Jacob, D. J., Liu, X., Logan, J. A., Chance, K., Eldering, A. and Bojkov, B. R.: Intercomparison methods for satellite  
1131 measurements of atmospheric composition: Application to tropospheric ozone from TES and OMI, *Atmos. Chem. Phys.*,  
1132 10(10), 4725–4739, doi:10.5194/acp-10-4725-2010, 2010.

1133 Zhang, L., Jacob, D. J., Knipping, E. M., Kumar, N., Munger, J. W., Carouge, C. C., Van Donkelaar, A., Wang, Y. X. and  
1134 Chen, D.: Nitrogen deposition to the United States: Distribution, sources, and processes, *Atmos. Chem. Phys.*,  
1135 doi:10.5194/acp-12-4539-2012, 2012.

1136 Zhou, P., Ganzeveld, L., Rannik, U., Zhou, L., Gierens, R., Taipale, D., Mammarella, I. and Boy, M.: Simulating ozone dry  
1137 deposition at a boreal forest with a multi-layer canopy deposition model, *Atmos. Chem. Phys.*, 17(2), 1361–1379,  
1138 doi:10.5194/acp-17-1361-2017, 2017.

1139 Zhou, S. S., Tai, A. P. K., Sun, S., Sadiq, M., Heald, C. L. and Geddes, J. A.: Coupling between surface ozone and leaf area  
1140 index in a chemical transport model: Strength of feedback and implications for ozone air quality and vegetation health, *Atmos.*  
1141 *Chem. Phys.*, doi:10.5194/acp-18-14133-2018, 2018.

1142 Zhu, Z., Bi, J., Pan, Y., Ganguly, S., Anav, A., Xu, L., Samanta, A., Piao, S., Nemani, R. R. and Myneni, R. B.: Global data  
1143 sets of vegetation leaf area index (LAI)<sub>3g</sub> and fraction of photosynthetically active radiation (FPAR)<sub>3g</sub> derived from global  
1144 inventory modeling and mapping studies (GIMMS) normalized difference vegetation index (NDVI<sub>3G</sub>) for the period 1981 to  
1145 2, *Remote Sens.*, doi:10.3390/rs5020927, 2013.

1146 Zhu, Z., Piao, S., Myneni, R. B., Huang, M., Zeng, Z., Canadell, J. G., Ciais, P., Sitch, S., Friedlingstein, P., Arneeth, A., Cao,  
1147 C., Cheng, L., Kato, E., Koven, C., Li, Y., Lian, X., Liu, Y., Liu, R., Mao, J., Pan, Y., Peng, S., Peñuelas, J., Poulter, B., Pugh,  
1148 T. A. M., Stocker, B. D., Viovy, N., Wang, X., Wang, Y., Xiao, Z., Yang, H., Zaehle, S. and Zeng, N.: Greening of the Earth  
1149 and its drivers, *Nat. Clim. Chang.*, 6(8), 791–795, doi:10.1038/nclimate3004, 2016.

1150

# Importance of Dry Deposition Parameterization Choice in Global Simulations of Surface Ozone

Anthony Y.H. Wong<sup>1</sup>, Jeffrey A. Geddes<sup>1</sup>, Amos P.K. Tai<sup>2,3</sup>, Sam J. Silva<sup>4</sup>

<sup>1</sup>Department of Earth and Environment, Boston University, Boston, MA, USA

<sup>2</sup>Earth System Science Programme, Faculty of Science, The Chinese University of Hong Kong, Hong Kong

<sup>3</sup>Institute of Energy, Environment and Sustainability, and State Key Laboratory of Agrobiotechnology, The Chinese University of Hong Kong, Hong Kong

<sup>4</sup>Department of Civil and Environmental Engineering, Massachusetts Institute of Technology, Cambridge, MA, USA

*Correspondence to:* Jeffrey A. Geddes (jgeddes@bu.edu)

## Supplemental Material

### Contents:

1. Mathematical analysis for the sensitivity of  $O_3$  to  $\Delta v_d/v_d$
2. A brief description of photosynthesis-stomatal conductance module in TEMIR
3. Table A1 to Table A3
4. References

## 1. Mathematical analysis for sensitivity of $O_3$ to $\Delta v_d/v_d$ :

Assume that  $\Delta O_3$  is due to changes in dry deposition flux (with proportionality constant  $k_d$ ) and other first-order processes (e.g. NO titration, loss to  $HO_2$  and OH, having total reaction rate  $k_c$ ):

$$dO_3 = d(-k_c O_3 - k_d v_d O_3) \quad (S1)$$

Here,  $k_c$  and  $k_d$  (which are related to meteorology and concentration of other relevant chemical species), are assumed to be relatively constant, so that that the perturbation in  $v_d$  does not trigger significant non-linearity. Expanding the differential and rearranging the terms yields:

$$\frac{dO_3}{O_3} = \frac{-k_d dv_d}{1 + k_c + k_d} \quad (S2)$$

Integrating S2 between perturbed ( $O_3 + \Delta O_3$ ,  $v + \Delta v_d$ ) and unperturbed ( $O_3$  and  $v_d$ ) values yields:

$$\ln\left(1 + \frac{\Delta O_3}{O_3}\right) = -\ln\left(1 + \frac{k_d \Delta v_d}{1 + k_c + k_d v_d}\right) \quad (S3)$$

Since  $\Delta O_3$  is small compared to  $O_{3,0}$ , first-order expansion is valid. When  $\Delta v_d$  is small enough relative to  $v_d$  for first-order approximation, Taylor's expansion of S4 yield:

$$\frac{\Delta O_3}{O_3} = -\frac{k_d}{1 + k_c + k_d v_d} \Delta v_d \quad (S4)$$

S5 can be rearranged to yield:

$$\Delta O_3 = -\frac{k_d v_d O_3}{1 + k_c + k_d v_d} \frac{\Delta v_d}{v_d} = \beta \frac{\Delta v_d}{v_d}, \text{ where } \beta = -\frac{k_d v_d O_3}{1 + k_c + k_d v_d} < 0 \quad (S5)$$

This shows that when the  $\Delta v_d/v_d$  is small enough ( $\ln(1+x) \approx x$ ) and does not cause non-linearity ( $k_c$  and  $k_d$  = constant) in chemistry,  $\Delta O_3$  is linearly proportional to  $\Delta v_d/v_d$ . The error of linearizing the natural logarithms equals to the difference between  $\ln(1+x)$  and  $x$ . This analysis gives the conditions for when the first-order approximation is reasonable, and allowing us to estimate the error when deviating from these condition. Assuming  $\beta$  is correctly estimated by chemical transport model, the error of linearization at  $\Delta v_d/v_d = \pm 50\%$  (the upper bound of  $\Delta v_d/v_d$  consistent with our analysis), is on the order of 25%. For more typical value of  $\Delta v_d/v_d$  (20%), the error is around 10%.

As  $\Delta v_d/v_d$  gets larger, we can expand R.H.S of S3 to the second order and investigate sensitivity of  $\Delta O_3$  to  $\Delta v_d/v_d$ :

$$\Delta O_3 = \beta \frac{\Delta v_d}{v_d} - \frac{\beta^2}{2O_3} \left(\frac{\Delta v_d}{v_d}\right)^2 = \left(\beta - \frac{\beta^2}{2O_3} \frac{\Delta v_d}{v_d}\right) \left(\frac{\Delta v_d}{v_d}\right) = \beta' \frac{\Delta v_d}{v_d} \quad (S6)$$

Where  $\beta'$  is the "corrected  $\beta$ ", which is a function of  $\Delta v_d/v_d$ .

To illustrate the potential impact of such non-linearity on  $\Delta O_3$ , we compare July  $\Delta O_{3,Z03\_BB}$  estimated using first-order estimation with  $\beta$  derived from  $\Delta v_d/v_d = +15\%$  (fig. S1b) and  $+30\%$  (fig. S1a), and second-order approximation (fig. S1c), and the result is shown in figure S1. The three different methods produce very similar  $\Delta O_3$ , and their differences have little impact on our conclusion. For simplicity, we only show the result using  $\beta$  derived from  $\Delta v_d/v_d = +30\%$  in the main manuscript.

As noted above and in the main manuscript, our approach is limited by the assumption that chemistry and transport do not introduce non-linear terms which may not be realistic. Rather, our approach is intended to identify hotspots of impact, and quantify these potential impacts to a first order. More rigorous modeling efforts could then be targeted in future work.

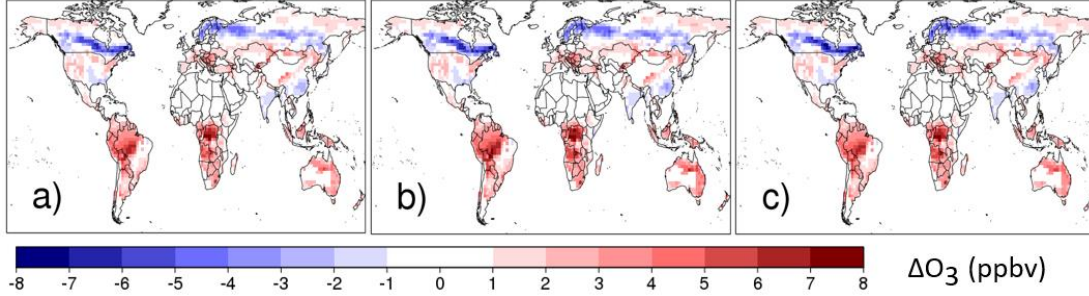


**Figure S1.** July  $\Delta O_{3,203\_BB}$  calculated using a) first-order method where  $\beta$  is derived from  $\Delta v_d/v_d = +30\%$  GC sensitivity run, b) first order method where  $\beta$  is derived from  $\Delta v_d/v_d = +15\%$  GC sensitivity run, and c) second-order method with  $\beta$  derived from  $\Delta v_d/v_d = +15\%$ .

## 2. A brief description of photosynthesis-stomatal conductance ( $A_n$ - $g_s$ ) module in TEMIR (a manuscript is in prep)

TEMIR largely follows Oleson et al. (2013), where net photosynthetic rate ( $A_n$ ,  $\mu\text{mol CO}_2 \text{ m}^{-2} \text{ s}^{-1}$ ), stomatal conductance for water ( $g_{sw}$ ,  $\mu\text{mol m}^{-2} \text{ s}^{-1}$ ) and  $\text{CO}_2$  concentration in leaf mesophyll ( $c_i$ ,  $\text{mol mol}^{-1}$ ) are solved simultaneously by the following coupled set of equations:

$$A_n = \frac{g_{sw}}{1.6} (c_a - c_i) \quad (S7)$$

$$g_{sw} = \beta_t g_0 + g_1 \frac{A_n}{c_s} RH_s \quad (S8)$$

$$A_n = A - R_d \quad (S9)$$

Here,  $c_a$  is  $\text{CO}_2$  concentration ( $\text{mol mol}^{-1}$ ),  $\beta_t$  is soil moisture stress factor (unitless),  $g_0$  is minimum stomatal conductance ( $\mu\text{mol m}^{-2} \text{ s}^{-1}$ ),  $A_n$  is net photosynthetic rate ( $\mu\text{mol CO}_2 \text{ m}^{-2} \text{ s}^{-1}$ ),  $A$  is gross photosynthetic rate ( $\mu\text{mol CO}_2 \text{ m}^{-2} \text{ s}^{-1}$ ) and  $R_d$  is dark respiration rate ( $\mu\text{mol CO}_2 \text{ m}^{-2} \text{ s}^{-1}$ ). Furthermore,  $c_s$  and  $RH_s$  are the  $\text{CO}_2$  concentration ( $\text{mol mol}^{-1}$ ) and relative humidity (unitless) at leaf surface.  $A$  is calculated following Bonan et al. (2011), which is based on Farquhar et al. (1980) and Collatz et al. (1992):

$$\Theta_{cj} A_i^2 - (A_c + A_j) A_i + A_c A_j = 0 \quad (S10)$$

$$\Theta_{ip} A^2 - (A_i + A_p) A + A_i A_p = 0 \quad (S11)$$

For C3 plants,  $\Theta_{cj} = 0.98$  and  $\Theta_{ip} = 0.95$ . For C4 plants,  $\Theta_{cj} = 0.80$  and  $\Theta_{ip} = 0.95$ . Rubisco-limited rate ( $A_c$ ,  $\mu\text{mol CO}_2 \text{ m}^{-2} \text{ s}^{-1}$ ), light-limited rate ( $A_j$ ,  $\mu\text{mol CO}_2 \text{ m}^{-2} \text{ s}^{-1}$ ), product-limited rate ( $A_p$ ,  $\mu\text{mol CO}_2 \text{ m}^{-2} \text{ s}^{-1}$ ) and  $R_d$  are calculated as:

$$A_c = \begin{cases} \frac{V_{c\ max}(c_i - \Gamma_*)}{c_i + K_c(1 + \frac{0.21P_{atm}}{K_o})} & \text{for } C_3 \text{ plants} \\ V_{c\ max} & \text{for } C_4 \text{ plants} \end{cases} \quad (S12)$$

$$A_j = \begin{cases} \frac{J(c_i - \Gamma_*)}{4c_i + 8\Gamma_*} & \text{for } C_3 \text{ plants} \\ 0.23\phi & \text{for } C_4 \text{ plants} \end{cases} \quad (S13)$$

$$A_c = \begin{cases} 3T_p & \text{for } C_3 \text{ plants} \\ k_p \frac{c_i}{P_{atm}} & \text{for } C_4 \text{ plants} \end{cases} \quad (S14)$$

$$R_d = \begin{cases} 0.015V_{c\ max} & \text{for } C_3 \text{ plants} \\ 0.025V_{c\ max} & \text{for } C_4 \text{ plants} \end{cases} \quad (S15)$$

Here,  $V_{c\ max}$ ,  $\Gamma_*$ ,  $P_{atm}$ ,  $J$ ,  $\phi$ ,  $T_p$  and  $k_p$  are the maximum rate of carboxylation ( $\mu\text{mol m}^{-2} \text{s}^{-1}$ ),  $\text{CO}_2$  compensation point ( $\text{mol mol}^{-1}$ ), atmospheric pressure (Pa), electron transport rate ( $\mu\text{mol m}^{-2} \text{s}^{-1}$ ), absorbed photosynthetically active radiation (PAR) ( $\text{W m}^{-2}$ ), triose phosphate utilization rate ( $\mu\text{mol m}^{-2} \text{s}^{-1}$ ) and initial slope of  $C_4$   $\text{CO}_2$  response curve ( $\mu\text{mol Pa}^{-1} \text{m}^{-2} \text{s}^{-1}$ ).  $K_c$  and  $K_o$  are the Michaelis-Menten constants for  $\text{CO}_2$  and  $\text{O}_2$  (Pa). Furthermore,  $J$  is calculated as the smaller root of the following equation:

$$0.7J^2 + (1.955\phi + J_{max})J + 1.955\phi = 0 \quad (S16)$$

Where  $J_{max}$  is the maximum potential rate of electron transport ( $\mu\text{mol m}^{-2} \text{s}^{-1}$ ). As  $J_{max}$ ,  $\phi$ ,  $V_{c\ max}$  and the variables related to  $V_{c\ max}$  ( $\Gamma_*$ ,  $J_{max}$ ,  $T_p$ ,  $R_d$ ) differ between sunlit and shaded leaves, the above set of equations are solved separately for sunlit and shaded leaves.

The parameters ( $V_{c\ max}$ ,  $\Gamma_*$ ,  $K_c$ ,  $K_o$ ,  $J_{max}$ ,  $T_p$ ,  $R_d$ ) are functions of vegetation temperature ( $T_v$ ), and the temperature scaling formulae are given at eq. 8.9 to eq. 8.14, while the effect of temperature acclimation (Kattge and Knorr, 2007) on  $J_{max}$  and  $V_{c\ max}$  are given at eq. 8.15 and 8.16 in Oleson et al. (2013). Other details of the model formalism (e.g. canopy scaling and effect of  $\beta_t$  on  $V_{c\ max}$ ) also follow Chapter 8 in Oleson et al. (2013), therefore we will focus on describing the main differences between CLM 4.5 and TEMIR.

First, TEMIR is driven entirely by assimilated meteorology. Instead of solving the whole surface energy balance equation, TEMIR consistently calculates  $T_v$  from 2-meter air temperature ( $T_2$ , K) and sensible heat flux ( $H$ ,  $\text{W m}^{-2}$ ) using Monin-Obukhov similarity theory (Monin and Obukhov, 1954):

$$T_v = T_2 + \frac{H}{\rho c_p} (r_{a,h} + r_{b,h}) \quad (S16)$$

Where  $\rho$ ,  $c_p$ ,  $r_{a,h}$  and  $r_{b,h}$  are air density ( $\text{kg m}^{-3}$ ), specific heat of air at constant pressure ( $\text{J kg}^{-1} \text{K}^{-1}$ ), aerodynamic and laminar boundary-layer resistance ( $\text{s m}^{-1}$ ) of heat, respectively.

Secondly, MERRA-2 only provides soil moisture output at two levels (surface and root zone), which is not compatible with the multi-layer soil module in CLM. Therefore, instead of aggregating  $\beta_t$  from multiple soil layers, TEMIR calculates  $\beta_t$  from the root-zone soil wetness of MERRA-2. Soil wetness ( $s$ ) is first converted into soil matric potential ( $\psi$ , mm) using the following equation:

$$\psi = \psi_{sat} s^{-B} \quad (S17)$$

Where  $\psi_{sat}$  and  $B$  are the soil matric potential (mm) at saturation and Clapp-Hornberger exponent (Clapp and Hornberger, 1978), which are related to soil property. Then  $\beta_t$  is calculated as:

$$\beta_t = \frac{\psi_c - \psi}{\psi_c - \psi_0} \left( \frac{\theta_{sat} - \theta_{ice}}{\theta_{sat}} \right), 0 \leq \beta_t \leq 1 \quad (S18)$$

Where  $\psi_c$  and  $\psi_0$  are the soil matric potential (mm) at which stomata are full close or fully open, and the term in the bracket account for the fact that frozen water are not available for plants.

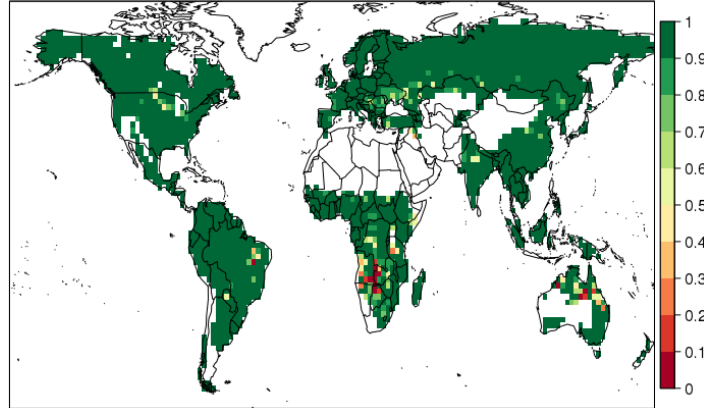


**Figure S2. July average soil moisture stress factor ( $\beta_t$ ).  $\beta_t = 1$  represents no soil moisture stress, while smaller  $\beta_t$  means stronger soil moisture stress and more stomatal closure.  $\beta_t = 0$  signifies that soil moisture stress is so strong that it completely shuts down stomatal activity.**

### 3. Table A1 to Table A3

|   | W98  | Z03   | W98_BB   | Z03_BB  |
|---|--|---|--|---|
| $R_a$   | $R_a = \frac{1}{\kappa u_*} \left[ \ln\left(\frac{z}{z_0}\right) - \Psi\left(\frac{z}{L}\right) + \Psi\left(\frac{z_0}{L}\right) \right]$ <p>When <math>\zeta \geq 0</math>, <math>\Psi(\zeta) = -5\zeta</math><br/> When <math>\zeta &lt; 0</math>, <math>\Psi(\zeta) = 2 \ln\left(\frac{1+\sqrt{1-16\zeta}}{2}\right)</math></p> |   |  |   |
| $R_b$   | $R_b = \frac{2}{\kappa u_*} \left(\frac{Sc}{Pr}\right)^{2/3}$  |   |  |   |
| $R_s$   | $R_s = r_s(PAR, LAI) f_T \frac{D_{H_2O}}{D_{O_3}}$   | $R_s = \frac{r_s(PAR, LAI)}{(1 - w_{st}) f_T f_{vpd} f_\psi} \frac{D_{H_2O}}{D_{O_3}}$  | $g_s = g_0 + m \frac{A_n}{C_s} h_s$ $R_s = \frac{1}{g_s} \frac{D_{H_2O}}{D_{O_3}}$ | $g_s = g_0 + m \frac{A_n}{C_s} h_s$ $R_s = \frac{1}{(1 - w_{st}) g_s} \frac{D_{H_2O}}{D_{O_3}}$ |
| Cuticular Resistance ( $R_{cut}$ )                | $R_{cut} = \frac{R_{cut0}}{LAI}$   | <p>For dry surface,<br/> <math display="block">R_{cut} = \frac{R_{cutd0}}{e^{0.03RH} LAI^{0.25} u_*}</math></p> <p>For wet surface,<br/> <math display="block">R_{cut} = \frac{R_{cutw0}}{LAI^{0.5} u_*}</math></p> | Same as W98  | Same as Z03   |
| In-canopy aerodynamic resistance ( $R_{ac}$ )     | Prescribed   | $R_{ac} = R_{ac0} \frac{LAI^{0.25}}{u_*}$   |  |   |
| Ground Resistance ( $R_g$ )                       | Prescribed   |   |  |   |
| Lower-canopy aerodynamic resistance ( $R_{alc}$ ) | $R_{alc} = 100 \left(1 + \frac{1000}{R + 10}\right)$   | -   |  |   |
| Lower-canopy surface resistance ( $R_{clc}$ )     | Prescribed   | -   |  |   |

**Table A1:** Brief description of the four dry deposition parameterizations.  $\kappa$  = von Karman constant,  $u_*$  = friction velocity,  $z$  = reference height,  $z_0$  = roughness length,  $L$  = Obukhov length,  $Sc$  = Schmidt's number,  $Pr$  = Prandtl number for air,  $LAI$  = leaf area index,  $PAR$  = photosynthetically active radiation,  $D_x$  = Diffusivity of species  $x$  in air,  $f_T$  = temperature ( $T$ ) stress function,  $f_{vpd}$  = vapour pressure deficit ( $VPD$ ) stress function,  $f_\psi$  = leaf water potential ( $\psi$ ) stress function,  $w_{st}$  = stomatal blocking fraction,  $A_n$  = Net photosynthetic rate,  $g_0$  = minimum stomatal conductance,  $m$  = Ball-Berry slope,  $C_s$  =  $CO_2$  concentration on leaf surface,  $h_s$  = relative humidity on leaf surface,  $RH$  = relative humidity,  $h$  = canopy height,  $R$  = downward shortwave radiation

| CLM PFT                               | Z03 surface type           |
|---------------------------------------|----------------------------|
| Needleleaf evergreen tree - temperate | Evergreen needleleaf trees |
| Needleleaf evergreen tree - boreal    |                            |
| Needleleaf deciduous tree - boreal    | Deciduous needleleaf trees |
| Broadleaf evergreen tree - tropical   | Tropical broadleaf trees   |
| Broadleaf deciduous tree - tropical   | Deciduous broadleaf trees  |
| Broadleaf deciduous tree - temperate  |                            |
| Broadleaf deciduous tree - boreal     |                            |
| Broadleaf evergreen shrub - temperate | Thorn shrubs               |
| Broadleaf deciduous shrub - temperate | Deciduous shrubs           |
| Broadleaf deciduous shrub - boreal    |                            |
| C <sub>3</sub> arctic grass           | Tundra                     |
| C <sub>3</sub> grass                  | Short grass                |
| C <sub>4</sub> grass                  | Corn*                      |
| C <sub>3</sub> crop                   | Crops                      |

**Table A2:** Mapping between CLM PFT and Z03 surface type.

\*C<sub>4</sub> grasses are mapped to corn due to the similarity in photosynthetic pathway, and hence stomatal control

| Land Type           | Longitude | Latitude | Season | Mean daytime $v_d$ (cm s <sup>-1</sup> ) | Citation                         |
|---------------------|-----------|----------|--------|--|----------------------------------|
| Deciduous Forest    | -80.9°    | 44.3°    | Summer | 0.92                                     | Padro et al., 1991               |
|                     |           |          | Winter | 0.28                                     |                                  |
|                     | 99.7°     | 18.3°    | Spring | 0.38                                     | Matsuda et al., 2005             |
|                     |           |          | Summer | 0.65                                     |                                  |
|                     | -72.2°    | 42.7°    | Summer | 0.61                                     | Munger et al., 1996              |
|                     |           |          | Winter | 0.28                                     |                                  |
| -78.8°              | 41.6°     | Summer   | 0.83   | Finkelstein et al., 2000                 |                                  |
| -75.2°              | 43.6°     | Summer   | 0.82   |  |                                  |
| Coniferous Forest   | -3.4°     | 55.3°    | Spring | 0.58                                     | Coe et al., 1995                 |
|                     | -79.1°    | 36.0°    | Spring | 0.79                                     | Finkelstein et al., 2000         |
|                     |           |          | Summer | 0.59                                     |                                  |
|                     | -120.6°   | 38.9°    | Spring | 0.58                                     | Kurpius et al., 2002             |
|                     |           |          | Summer | 0.59                                     |                                  |
|                     |           |          | Autumn | 0.43                                     |                                  |
|                     | -120.6°   | 38.9°    | Winter | 0.45                                     | Kurpius et al., 2002             |
|                     |           |          | Spring | 0.58                                     |                                  |
|                     |           |          | Summer | 0.59                                     |                                  |
|                     | -0.7°     | 44.2°    | Summer | 0.48                                     | Lamaud et al., 1994              |
|                     | 105.5°    | 40.0°    | Summer | 0.39                                     | Turnipseed et al., 2009          |
|                     | -66.7°    | 54.8°    | Summer | 0.26                                     | Munger et al., 1996              |
|                     | 11.1°     | 60.4°    | Spring | 0.31                                     | Hole et al., 2004                |
| Summer              |           |          | 0.48   |  |                                  |
| Autumn              |           |          | 0.20   |  |                                  |
| Winter              |           |          | 0.074  |  |                                  |
| 8.4°                | 56.3°     | Spring   | 0.68   | Mikkelsen et al., 2004                   |                                  |
|                     |           | Summer   | 0.80   |  |                                  |
|                     |           | Autumn   | 0.83   |  |                                  |
| Tropical Rainforest | 117.9°    | 4.9°     | Wet    | 0.5                                      | Fowler et al., 2011 <sup>#</sup> |
|                     |           |          | Wet    | 1.0                                      |                                  |
|                     | -61.8°    | -10.1°   | Wet    | 1.1                                      | Rummel et al., 2007              |
|                     |           |          | Dry    | 0.5                                      |                                  |
| -60.0°              | 3.0°      | Wet      | 1.8    | Song-Miao et al., 1990                   |                                  |
| Grass               | -88.2°    | 40.0°    | Summer | 0.56                                     | Droppo, 1985                     |



|        |         |        |                 |                       |                        |
|--------|---------|--------|-----------------|-----------------------|------------------------|
|        | -3.2°   | 57.8°  | Spring          | 0.59                  | Fowler et al., 2001    |
|        |         |        | Summer          | 0.56                  |                        |
|        |         |        | Autumn          | 0.42                  |                        |
|        | -119.8° | 37.0°  | Summer          | 0.15                  | Padro et al., 1994     |
|        | -8.6°   | 40.7°  | Summer          | 0.22                  | Pio et al., 2000       |
|        |         |        | Winter          | 0.38                  |                        |
|        | -104.8° | 40.5°  | Spring          | 0.22                  | Stocker et al., 1993   |
| 10.5°  | 52.4°   | Spring | 0.44            | Meszaros et al., 2009 |                        |
| -96.4° | 39.5°   | Summer | 0.62            | Gao and Wesely, 1995  |                        |
| Crops  | -2.8°   | 55.9°  | Not applicable* | 0.69                  | Coyle et al., 2009     |
|        | -88.4°  | 40.1°  |                 | 0.53                  | Meyers et al., 1998    |
|        |         |        |                 | 0.12                  |                        |
|        |         |        |                 | 0.85                  |                        |
|        | -87.0°  | 36.7°  |                 | 0.39                  |                        |
|        | -86.0°  | 34.3°  |                 | 0.40                  |                        |
|        | -120.7° | 36.8°  |                 | 0.76                  | Padro et al., 1994     |
|        | 8.0°    | 48.7°  |                 | 0.41                  | Pilegaard et al., 1998 |
|        | 2.0°    | 48.9°  |                 | 0.60                  | Stella et al., 2011    |
|        | 0.6°    | 44.4°  |                 | 0.47                  |                        |
| 1.4°   | 43.8°   | 0.37   |                 |                       |                        |

**Table A3:** Information on all the measurement sites included in model evaluation

\*Crops are heavily influenced by management practices rather than natural seasonality. Thus, two data sets in the same location generally represent before and after certain a crop phenology or human management event.

#The two measurements are taken at a rainforest and an oil palm plantation nearby.

#### 4. References

- Bonan, G. B., Lawrence, P. J., Oleson, K. W., Levis, S., Jung, M., Reichstein, M., Lawrence, D. M. and Swenson, S. C.: Improving canopy processes in the Community Land Model version 4 (CLM4) using global flux fields empirically inferred from FLUXNET data, *J. Geophys. Res.*, 116(G2), G02014, doi:10.1029/2010JG001593, 2011.
- Clapp, R. B. and Hornberger, G. M.: Empirical equations for some soil hydraulic properties, *Water Resour. Res.*, doi:10.1029/WR014i004p00601, 1978.
- Coe, H., Gallagher, M. W., Choularton, T. W. and Dore, C.: Canopy scale measurements of stomatal and cuticular O<sub>3</sub> uptake by sitka spruce, *Atmos. Environ.*, doi:10.1016/1352-2310(95)00034-V, 1995.
- Collatz, G., Ribas-Carbo, M. and Berry, J.: Coupled Photosynthesis-Stomatal Conductance Model for Leaves of C<sub>4</sub> Plants, *Aust. J. Plant Physiol.*, 19(5), 519, doi:10.1071/PP9920519, 1992.
- Coyle, M., Nemitz, E., Storeton-West, R., Fowler, D. and Cape, J. N.: Measurements of ozone deposition to a potato canopy, *Agric. For. Meteorol.*, doi:10.1016/j.agrformet.2008.10.020, 2009.
- Droppo, J. G.: Concurrent measurements of ozone dry deposition using eddy correlation and profile flux methods., *J. Geophys. Res.*, doi:10.1029/JD090iD01p02111, 1985.

- Farquhar, G. D., Von Caemmerer, S. and Berry, J. A.: A Biochemical Model of Photosynthetic CO<sub>2</sub> Assimilation in Leaves of C<sub>3</sub> Species, *Planta*, 149, 78–90, doi:10.1007/BF00386231, 1980.
- Finkelstein, P. L., Ellestad, T. G., Clarke, J. F., Meyers, T. P., Schwede, D. B., Hebert, E. O. and Neal, J. A.: Ozone and sulfur dioxide dry deposition to forests: Observations and model evaluation, *J. Geophys. Res. Atmos.*, doi:10.1029/2000JD900185, 2000.
- Fowler, D., Flechard, C., Cape, J. N., Storeton-West, R. L. and Coyle, M.: Measurements of ozone deposition to vegetation quantifying the flux, the stomatal and non-stomatal components, *Water. Air. Soil Pollut.*, doi:10.1023/A:1012243317471, 2001.
- Fowler, D., Nemitz, E., Misztal, P., di Marco, C., Skiba, U., Ryder, J., Helfter, C., Neil Cape, J., Owen, S., Dorsey, J., Gallagher, M. W., Coyle, M., Phillips, G., Davison, B., Langford, B., MacKenzie, R., Muller, J., Siong, J., Dari-Salisburgo, C., di Carlo, P., Aruffo, E., Giammaria, F., Pyle, J. A. and Nicholas Hewitt, C.: Effects of land use on surface-atmosphere exchanges of trace gases and energy in Borneo: Comparing fluxes over oil palm plantations and a rainforest, *Philos. Trans. R. Soc. B Biol. Sci.*, doi:10.1098/rstb.2011.0055, 2011.
- Gao, W. and Wesely, M. L.: Modeling gaseous dry deposition over regional scales with satellite observations-I. Model development, *Atmos. Environ.*, 29(6), 727–737, doi:10.1016/1352-2310(94)00284-R, 1995.
- Hole, L. R., Semb, A. and Tørseth, K.: Ozone deposition to a temperate coniferous forest in Norway; gradient method measurements and comparison with the EMEP deposition module, in *Atmospheric Environment.*, 2004.
- Kattge, J. and Knorr, W.: Temperature acclimation in a biochemical model of photosynthesis: A reanalysis of data from 36 species, *Plant, Cell Environ.*, 30(9), 1176–1190, doi:10.1111/j.1365-3040.2007.01690.x, 2007.
- Kurpius, M. R., McKay, M. and Goldstein, A. H.: Annual ozone deposition to a Sierra Nevada ponderosa pine plantation, *Atmos. Environ.*, doi:10.1016/S1352-2310(02)00423-5, 2002.
- Lamaud, E., Brunet, Y., Labatut, A., Lopez, A., Fontan, J. and Druilhet, A.: The Landes experiment: Biosphere-atmosphere exchanges of ozone and aerosol particles above a pine forest, *J. Geophys. Res.*, doi:10.1029/94JD00668, 1994.
- Matsuda, K., Watanabe, I., Wingpud, V., Theramongkol, P., Khummongkol, P., Wangwongwatana, S. and Totsuka, T.: Ozone dry deposition above a tropical forest in the dry season in northern Thailand, *Atmos. Environ.*, 39(14), 2571–2577, doi:10.1016/j.atmosenv.2005.01.011, 2005.
- Mészáros, R., Horváth, L., Weidinger, T., Neftel, A., Nemitz, E., Dämmgen, U., Cellier, P. and Loubet, B.: Measurement and modelling ozone fluxes over a cut and fertilized grassland, *Biogeosciences*, doi:10.1029/2002GL016785; Leuning, R., Source/sink distributions in plant canopies using Lagrangian dispersion analysis: corrections for atmospheric stability and comparison with a canopy model (2000) *Bound.-Lay. Meteorol.*, 96 (1-2), pp. 293-314; Massman, W.J., A simple method for estimating frequency response corrections for eddy covariance systems (2000) *Agr. Forest Meteorol.*, 104, pp. 185-198; Massman, W.J., Toward an ozone standard to protect vegetation based on effective dose: a review of depos, 2009.
- Meyers, T. P., Finkelstein, P., Clarke, J., Ellestad, T. G. and Sims, P. F.: A multilayer model for inferring dry deposition using standard meteorological measurements, *J. Geophys. Res.*, 103(98), 22645, doi:10.1029/98JD01564, 1998.
- Mikkelsen, T. N., Ro-Poulsen, H., Hovmand, M. F., Jensen, N. O., Pilegaard, K. and Egeløv, A. H.: Five-

year measurements of ozone fluxes to a Danish Norway spruce canopy, in *Atmospheric Environment*, 2004.

Monin, A. S. and Obukhov, A. M.: Basic laws of turbulent mixing in the surface layer of the atmosphere, Tr. Akad. Nauk SSSR Geophys. Inst., 1954.

Munger, J. W., Wofsy, S. C., Bakwin, P. S., Fan, S.-M., Goulden, M. L., Daube, B. C., Goldstein, A. H., Moore, K. E. and Fitzjarrald, D. R.: Atmospheric deposition of reactive nitrogen oxides and ozone in a temperate deciduous forest and a subarctic woodland 1. Measurements and mechanisms, *J. Geophys. Res.*, 101657(20), 639–12, doi:10.1029/96JD00230, 1996.

Oleson, K. W., Lawrence, D. M., Bonan, G. B., Drewniak, B., Huang, M., Koven, C. D., Levis, S., Li, F., Riley, J., Subin, Z. M., Swenson, S. C., Thornton, P. E., Bozbiyik, A., Fisher, R. A., Heald, C. L., Kluzek, E., Lamarque, J.-F., Lawrence, P. J., Leung, L. R., Lipscomb, W., Muszala, S., Ricciuto, D. M., Sacks, W. J., Sun, Y., Tang, J. and Yang, Z.-L.: Technical Description of version 4.5 of the Community Land Model (CLM), 2013.

Padro, J., den Hartog, G. and Neumann, H. H.: An investigation of the ADOM dry deposition module using summertime O<sub>3</sub> measurements above a deciduous forest, *Atmos. Environ. Part A, Gen. Top.*, doi:10.1016/0960-1686(91)90027-5, 1991.

Padro, J., Massman, W. J., Shaw, R. H., Delany, A. and Oncley, S. P.: A comparison of some aerodynamic resistance methods using measurements over cotton and grass from the 1991 California ozone deposition experiment, *Boundary-Layer Meteorol.*, doi:10.1007/BF00712174, 1994.

Pilegaard, K., Hummelshøj, P. and Jensen, N. O.: Fluxes of ozone and nitrogen dioxide measured by eddy correlation over a harvested wheat field, *Atmos. Environ.*, doi:10.1016/S1352-2310(97)00194-5, 1998.

Pio, C. ., Feliciano, M. ., Vermeulen, A. . and Sousa, E. .: Seasonal variability of ozone dry deposition under southern European climate conditions, in Portugal, *Atmos. Environ.*, doi:10.1016/S1352-2310(99)00276-9, 2000.

Rummel, U., Ammann, C., Kirkman, G. A., Moura, M. A. L., Foken, T., Andreae, M. O. and Meixner, F. X.: Seasonal variation of ozone deposition to a tropical rain forest in southwest Amazonia, *Atmos. Chem. Phys.*, doi:10.5194/acp-7-5415-2007, 2007.

Song-Miao, F., Wofsy, S. C., Bakwin, P. S., Jacob, D. J. and Fitzjarrald, D. R.: Atmosphere-biosphere exchange of CO<sub>2</sub> and O<sub>3</sub> in the central Amazon forest, *J. Geophys. Res.*, doi:10.1029/JD095iD10p16851, 1990.

Stella, P., Personne, E., Loubet, B., Lamaud, E., Ceschia, E., B<sup>??</sup>ziat, P., Bonnefond, J. M., Irvine, M., Keravec, P., Mascher, N. and Cellier, P.: Predicting and partitioning ozone fluxes to maize crops from sowing to harvest: The Surf<sub>atm</sub>-O<sub>3</sub> model, *Biogeosciences*, 8(10), 2869–2886, doi:10.5194/bg-8-2869-2011, 2011.

Stocker, D. W., Stedman, D. H., Zeller, K. F., Massman, W. J. and Fox, D. G.: Fluxes of nitrogen oxides and ozone measured by eddy correlation over a shortgrass prairie, *J. Geophys. Res.*, doi:10.1029/93JD00871, 1993.

Turnipseed, A. A., Burns, S. P., Moore, D. J. P., Hu, J., Guenther, A. B. and Monson, R. K.: Controls over ozone deposition to a high elevation subalpine forest, *Agric. For. Meteorol.*, doi:10.1016/j.agrformet.2009.04.001, 2009.